Rock-Structure Interaction: Improving the Consistency in the Finite Element Modelling of Rock Foundations for Bridges

by

Dylan Andrew Fourie

Thesis presented in fulfilment of the requirements for the degree of Master of Engineering in Civil Engineering in the faculty of Engineering at Stellenbosch University

Supervisor: Mrs Nanine Fouché

Co-supervisor: Mr Frans van der Merwe

March 2020

Declaration

By submitting this thesis electronically, I declare that the entirety of the work contained therein is my own, original work, that I am the sole author thereof (unless to the extent explicitly otherwise stated), that reproduction and publication thereof by Stellenbosch University will not infringe any third party rights and that I have not previously in its entirety or in part submitted it for obtaining any qualification.

Signature:……....

Date:…….....

Abstract

The design and modelling of foundations crosses two civil engineering disciplines, namely structural- and geotechnical engineering. The structural engineer goes into great detail when sizing foundations to ensure effective load transfer from the superstructure to the underlying geomaterials. This is usually accomplished by deriving the load and moment taken down from the superstructure onto the foundation. This load takedown is normally established as a first estimate based on either a fixed-base or an assumed springs stiffness model in structural finite element (FE). The loads transferred from the superstructure to the various piers and foundations will vary depending on the fixity assumed by the structural engineer and could result in large discrepancies when modelled with the same stiffness when certain foundations are stiffer than others. This becomes more critical in large bridge structures with tall piers where even the slightest differentials in displacement at the base of subsequent piers of the structure could lead to significant differential tilt and settlement at the top of the piers – resulting in significant load re-distribution between softer and stiffer foundations. It is therefore proposed that the analysis process is and should be an iterative process between the structural- and geotechnical engineer as settlement and distortion is best estimated by the geotechnical engineer whilst load take-down, due to these varying foundation stiffnesses, are best estimated by the structural engineer. This iteration should continue until convergence is reached between the two models.

This study aims to compile a guideline to optimize the iteration process between the geotechnical- and structural engineer, and to assist the geotechnical engineer in improving the consistency in the finite element modelling (FEM) of the interaction between the structure and the rock. This was achieved by modelling a bridge footing on rock using a 3D geotechnical FE software package; obtaining the footing's settlement and rotation; deriving structural springs and inserting these revised springs back into a structural FE software package to determine the revised load

takedown. This allows for more realistic modelling by the bridge engineer. A simplified method was proposed of applying an eccentric loading, which provided accurate results when the footing was assumed to be fully rigid. The settlement values from the geotechnical model differed with less than 10% from the structural model. The derived springs, thus, model the rock-structure interaction more accurately and can be used for rigid and flexible foundations.

Opsomming

Die ontwerp en modellering van fondasies oorskry twee siviele ingenieurswese dissiplines, naamlik strukturele- en geotegniese ingenieurswese. Die strukturele ingenieur gaan in diepte om die grootte van die fondasies te bepaal om te verseker dat die vrag van die bobou korrek en effektief oorgeplaas word na die onderliggende geomateriale. Dit word gewoonlik gedoen deur die vrag en moment te bepaal wat af geneem word van die bobou en geplaas word op die fondasie. Hierdie vrag wat afgeneem word, word gebruik as ‘n eerste skatting gebasseer op ‘n vasgestelde of aanvaarde veer-styfheid model in strukturele eindige element - ”finite element” (FE). Die vragte wat oorgeplaas word van die bobou na die verskeie steunpilare en fondasies sal verskil afhangende van die vastheid aangeneem deur die strukturele ingenieur en kan lei tot groot teenstrydighede wanneer die modellering dieselfde styfheid waarde gebruik terwyl sekere fondasies stywer is as ander. Dit is nog meer noodsaaklik by groot brug strukture met hoë steunpilare waar die kleinste verskil in verplasing by die basis van die struktuur se steunpilare kan lei tot ‘n beduidende kantel en besinking bo die steunpilare, wat lei tot betekenisvolle vrag her-verspreiding tussen die sagter en stywer fondasies. Dit word dus voorgestel dat die analise ‘n iteratiewe proses is en behoort te wees tussen die strukturele- en geotegniese ingenieur aangesien die geotegniese ingenieur die besinking en verdraaing meer akkuraat kan bepaal, terwyl die strukturele ingenieur beter is met die bepaling van die vrag afname, weens verskeie fondasie styfhede. Hierdie iteratiewe proses behoort aan te hou totdat konvergensie tussen die twee modelle bereik is.

Hierdie studie beoog om ‘n riglyn bymekaar te stel om die iteratiewe proses tussen die geotegniese- en strukturele ingenieur te optimaliseer, asook om die geotegniese ingenieur te help om die konsekwentheid in die eindige element modellering – “finite element modelling” (FEM) – van die interaksie tussen die struktuur en die rots te verbeter. Dit was bereik deur die modellering van ‘n brug voetstuk op rots

(deur gebruik te maak van ‘n 3D geotegniese FE sagteware paket); die verkryging van die voetstuk se besinking en rotasie; die afleiding van strukturele vere en deur die aangepaste waardes by die strukturele FE sagteware paket in te voeg om die nuwe vrag afname te bepaal. Dit maak dit moontlik vir die brug ingenieur om meer akkurate modellering te doen. ‘n Vereenvoudigde metode is aanbeveel wat ‘n eksentrieke vrag uitoefen en akkurate resultate verskaf het toe die voetstuk aanvaar was as heeltemal rigied. Die waardes van besinking wat deur die geotegniese ingenieur bepaal is, verskil met minder as 10% van die strukturele model. Die afgeleide vere modelleer dus die rots struktuur interaksie meer akkuraat en kan gebruik word vir rigiede asook buigsame fondasies.

Acknowledgements

First and foremost I want to that the Lord Jesus Christ. Thank you for leading me in Your perfect will, thank you for Your favour upon my life, thank you for Your unending grace and for Your fellowship in the times of adversities over these two years.

I want to thank my parents for your loving support and encouragement when circumstances seemed to have gotten the best of me. I also want to thank you for funding my entire academic career, I want to thank you and honour you.

I want to thank my girlfriend Chené Mostert for your love and selflessness. You are truly a blessing. Thank you for sitting with me late at night while I worked just to support me, I could not have done it without you.

A big thank you to Frans van der Merwe for your patience day in and day out. Thank you for always being willing to help me and meet with me late at night and early in the mornings. Your support is sincerely appreciated.

Thank you to Mrs Nanine Fouche for always being willing to help me and give me advice.

Thank you to the Transportation and Geotechnical department at Stellenbosch University for funding the RS3 software and for allowing me to use the computer required to run my models.

A huge thank you to The Bay CFC for teaching me the uncompromised Word of God and teaching me how to apply my faith in every area of my life, especially my studies.

Table of contents

List of figures

Page

List of tables

Page

List of Abbreviations

DoFs	Degrees of Freedom
FE	Finite Element
FEA	Finite Element Analysis
FEM	Finite Element Modelling
GHB	Generalized Hoek-Brown
GSI	Geological Strength Index
kN	Kilonewton
kPa	Kilopascal
MPa	Megapascal
GPa	Gigapascal
MR	Modulus Ratio
RMR	Rock Mass Rating
RQD	Rock Quality Designation
RS	Rock Soil two-dimensional
RS3	Rock Soil three-dimensional
SLS	Serviceability Limit State
UCS	Unconfined Compressive Strength
UDL	Uniformly Distributed Load

List of Symbols

E	Modulus of elasticity (Young's modulus)
E_i	Intact rock modulus
E_{rm}	Rock mass modulus/ deformation modulus
E_b	Young's modulus of footing
E_s	Modulus of elasticity of the soil or rock
σ	Applied stress
σ'_1	Major/maximum principle effective stress
σ'_3	Minor/minimum principle effective stress
σ_c	Uniaxial compressive stress
σ_{ci}	Unconfined compressive strength
D	Disturbance factor
m_i	Hoek-Brown constant
m_r	Residual m Hoek-Brown constant
m_b	Peak Hoek-Brown constant
s	Hoek-Brown constant
a	Hoek-Brown constant
s_r	Residual Hoek-Brown constant
a_r	Residual Hoek-Brown constant
ϕ	Angle of internal friction / rotation
z	Length over which rotation occurs
c	Cohesion
σ_t	Tensile strength
d	Depth
t	Thickness
B	Breadth/ width
L	Length
l	Column dimension along the footing length
h	Height
N	Vertical load

Q	Lateral load
M	Moment
R	Resultant
α	Angle of rotation
e	Eccentricity
FS	Factor of safety
δ	Deflection / settlement
k_S	Modulus of subgrade reaction
k_v	Vertical spring
k_ϕ	Rotational spring
K_s	System stiffness
K_r	Relative stiffness
I_b	Moment of inertia of the structure per unit length at right angles to B
ν	Poisson's ratio

Chapter 1: Introduction

1.1 Background

Throughout history the growth of civilization has always perceived the topography of the earth as a challenge, such as separating water from crops, natural resources from developments, transportation of food and supplies to the needy etc. The answer to these challenges were to build bridges to provide a way across and to level out the landscape. For centuries bridges have become the icons of certain cities due to their aesthetic design and colossal size. The longest of them being the Danyang–Kunshan Grand Bridge in China, spanning over 165 kilometres in length, and the tallest being the Millau Viaduct in France, spanning 343m above the ground level. Such colossal structures need to be sufficiently supported by the ground beneath their foundations in order to withstand the natural and manmade forces applied to them.

Intuition will tell you that a rock mass can withstand more load than a soil mass, and that building foundations of large structures on rock will be more practical because of their immense strength gained from cementation. While rock may have a higher stiffness than most soil masses, rock is highly unpredictable. This is due to most rock bodies containing discontinuity surfaces such as joints or fractures. A joint is a discontinuity in the rock mass that generally has a very low shear strength and can fail easier than the rock mass itself. Since these joints have poorer strength characteristics than the intact rock mass, the failure modes of the rock mass as a whole will mainly be controlled by those of the joints. These joints can be orientated in any direction and at any angle within the rock mass, thus the rock mass is seen as having non-linear behaviour. However, rock masses do exist where, while discontinuities are present, they do not attribute to the rock failure as it is not the weakest link in the rock mass. In such cases, the joint infill would have a high strength or a high roughness while the rock material would contain the weakest

element. However, for the purposes of this research, the rock will be modelled as a continuous medium of fractured rock using appropriate constitutive models.

A rock mass cannot only undergo in-situ testing, such as core drilling, in order to determine if the rock is suitable to be used as a support for massive structural loadings as there is rarely a rock specimen that is dependable enough to fully represent the entire rock mass from which the results were extracted. Thus, numerical modelling techniques are able to simulate the possible conditions of the rock mass with the information obtained from field investigations and laboratory testing. There are many numerical modelling techniques being developed and are being used in many fields of engineering today with Finite Element Modelling (FEM) being one of the most widely used techniques. Finite Element Method modelling is a numerical modelling procedure used to determine the stresses and strains within a complex engineering problem that can combine civil infrastructure, soils and structures. It is so widely used because it encapsulates techniques that can be applied to many different geometries in either one-, two- or three-dimensional models.

The designing and modelling of foundations cross two engineering disciplines, structural- and geotechnical engineering. The structural engineer designs the structure and the geotechnical engineer determines the bearing capacity, stiffness and settlement of the rock mass when subjected to the structural loads. The structural engineer normally derives the loads and moments applied to the foundation based on assumed spring values at the bottom of the structural model. These transferred loads will vary depending on the assumed springs chosen. This process is therefore iterative, with the geotechnical engineer modelling the displacements and rotations based on the first load set provided, whilst providing feedback to the structural engineer in terms of springs to be used in his simpler model. This will continue until convergence between the structural and geotechnical models is reached.

1.2 Problem Statement

Many projects are encountered in which there is an interaction between the ground and the structure, and thus requires the understanding and experience from both engineering disciplines involved. In the design process of massive structures such as bridges and their foundations, there is an interaction between the structural engineer and the geotechnical engineer.

The interaction between the structural engineer and the geotechnical engineer tends to be an iterative process, and because of this process a considerable amount of time and money is spent which consequently delays construction. The interaction between the modelling processes have not been documented. Improved consistency in the finite element modelling of shallow bridge foundations on rock is needed, which this study will address. An effective way is needed to guide the geotechnical engineer through the iterative process with the structural engineer, and will be able to save time and money for the companies involved in the design of the structure.

1.3 My unique contribution

The findings of this report will assist structural and geotechnical engineers when modelling bridge foundations on rock. The study will shed light on various factors involved in modelling, such as the influence of foundation stiffness on the behaviour of foundations, the use of solid and plate structural elements in the three-dimensional finite element computation of footings, and the derivation of springs to ultimately create consistency in the iterative modelling process. All of these factors will contribute to the understanding the geotechnical engineer will have in the decision-making process about how to model footings on rock using three-dimensional FEM. The geotechnical engineer will then be able to derive springs from the geotechnical model to give to the structural engineer to use in the structural model.

1.4 Research Aims

The aims of this research are:

i. To compile a guideline to optimize the iteration process between the geotechnical and structural engineer, for the geotechnical engineer to improve the consistency in the modelling of the interaction between the structure and the rock.

ii. To provide insight into the determination of spring input parameters for modelling the interaction between bridge structures and shallow rock foundations.

1.5 Research objectives

The following are the research objectives of the thesis in order to achieve the proposed research aims:

i. Determine what parameters are required and constitutive models are applicable for rock foundations to be modelled.

ii. Perform sensitivity analyses on the effects of foundation stiffness and the use of solid and plate structural elements on footing deflection.

iii. Analyse the same loads in Prokon Frame structural FE software with the springs that are derived from Rocscience's RS3 geotechnical FE software, and determine whether or not the same deflections and settlements are obtained. This shows how linear and rotational springs can be derived from three-dimensional geotechnical FEM for rock foundations.

1.6 Research challenges and limitations

The following factors proved to limit the outcome of the research:

- The RS3 software is a relatively new software and is not commonly used in South Africa yet and thus finding assistance with the software application was limited.
- The modelling of joints was not user friendly and limited as joint patterns could not be modelled, nor could statistical methods be used as is applied in RS2 (Rocscience's two-dimensional FE software).
- Data on the rock material was limited and thus average values were used for the Geological Strength Index (*GSI*), the Hoek-Brown constant m_i and the modulus ratio *MR* used to calculate the intact rock modulus E_i.
- Applying point loads to the footing is not possible unless an additional element is created within the footing to provide a surface to apply the load.

1.7 Overview of thesis

This research thesis consists of six chapters. The content is briefly discussed below:

Chapter 1 contains the introduction to bridge foundations on rock, along with an introduction to numerical modelling and the interaction between the structural and geotechnical engineer. The problem statement, aims and objectives, the unique contribution this research brings to the industry, the research challenges encountered and the thesis overview are also included.

Chapter 2 is the literature review on rock mass properties and classification systems, constitutive models used for rock, types of rock foundations, the considerations when modelling foundations, background into spring theory and spring derivation
.

Chapter 3 gives guidelines to the setup of the models, input parameters used and the comparison of geotechnical FE and structural FE models. The testing procedures used to obtain the results from Chapter 4 are also outlined.

Chapter 4 provides the results and discussion of the foundation models. This includes foundation stiffness models, solid versus plate elements models and the results of spring models using structural FE software. The results obtained from the models will be discussed. Comparisons are made between the settlement of the foundations in RS3 and in Prokon Frame to verify if the same deflections and settlements are obtained to achieve convergence in the models. A guideline to optimize the iteration process between the geotechnical and structural engineer is given.

Chapter 5 provides the conclusions of the research and recommendations to further the research.

Chapter 2: Literature Review

2.1 Introduction

This chapter presents an overview of the literature on the relevant topics that are associated with Finite Element (FE) modelling of bridge spread foundations on rock. The iteration process between the structural and geotechnical engineer constitutes several topics of consideration, thus the literature will not be focussed on one topic, but of the numerous topics involved in the process. The first part of the literature review includes a definition and background of rock masses and how rock behaves as a formation. This will also include residual behaviour of rock once it has undergone failure. Well known and effective rock classification systems will be presented along with relevant failure criterions used to obtain rock strength parameters for inputs into numerical software packages.

The second part of the literature includes definitions and types of foundations used for bridges on rock specifically. Additionally, numerical modelling considerations will be discussed such as footing element types, foundational spring models, rigid versus flexible footing behaviour, with the influence of columns and a brief illustration of passive rock dowels and how they can be used to reduce uplift of spread footings. Although many aspects could have been expanded to greater lengths, the scope of this research is limited to the main design considerations of spread footings on rock using three-dimensional geotechnical FE software and the process of connecting the settlement results to spring constants in order for the structural engineer to use in the structural FE software.

2.2 Rock Masses

2.2.1 What is rock

Rock is one of the most abundant materials on earth, covering the entire earth's surface. Rock is "any solid mass that consists of a conglomerate of several smaller crystals called minerals or mineral-like matter that occurs naturally on earth" (Tarbuck & Lutgens, 2005). Minerals (chemical compounds with unique composition and physical properties) determine the physical properties of the rock of which they form aggregates. This can be seen in Figure 2.1 below. It is the crystalline structure and chemical composition of mineral aggregates that determine the properties of a rock (Tarbuck & Lutgens, 2014). As previously mentioned, rock can also consist of non-mineral matter such as coal, which comprises of solid organic debris. According to Wyllie (1999), the compressive strength of a rock mass can reach 200+ MPa, which can accommodate substantial loads and be used as structural foundations. This is due to the cementation process of the minerals that rocks experience.

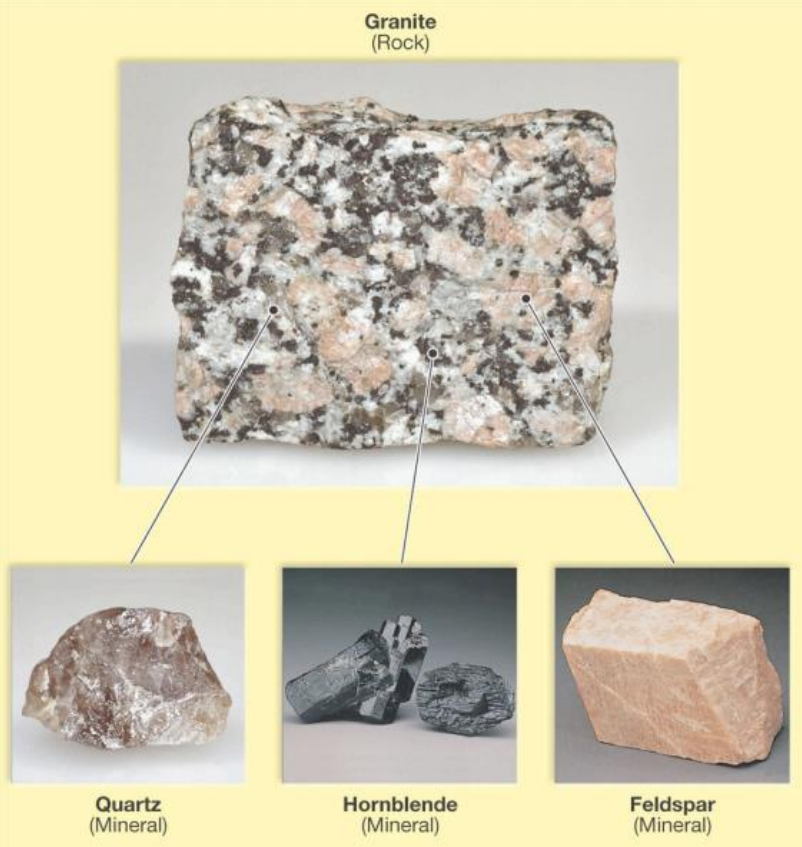

FIgure 2.1: Schematic of rock aggregates (Tarbuck & Lutgens, 2005)

2.2.2 Rock mass behaviour

Due to the ability of rock to withstand immense shear and tensile loading, structures such as bridge piers and dams are more frequently founded on rock as an alternative to soil. However, caution must be exercised as a single low strength discontinuity in the rock mass at a certain orientation may cause total failure of the rock. These discontinuities can range from joints with rough surfaces that have substantial shear strengths to massive faults that contain various kinds of clays with relatively low shear strengths, and most rocks contain them (Wyllie, 1999). Due to these discontinuities being found in the majority of rock masses, the behaviour of rock is seen to be non-linear as the normal and shear stress of these discontinuities are non-linear. However, there are rock masses that while discontinuities are present, do not attribute to the failure as it is not the weakest link in the rock mass. For example, in

particular friable sandstones, the sand particles may be so poorly bonded that failure through the rock material itself would be more likely to occur than by sliding in joints or bedding planes (Goodman, 1976). A rock mass constitutes two main components, the rock material itself and jointing, as shown in Figure 2.2 below:

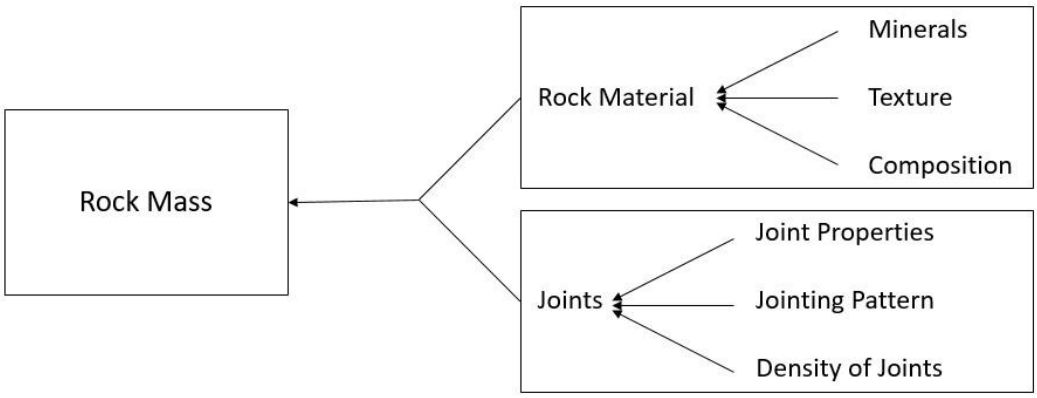

Figure 2.2: Rock mass constituents (Palmstrom, 1995)

Rock mass properties are greatly affected by lithological changes, but structural features such as jointing, folding and faulting affect the properties of a rock mass (Budavari, 1983). Singh and Goel (2011) agree with Budavari (1983) by also explaining that the properties of a rock mass are governed by the discontinuities within the rock mass as well as the properties of the intact rock materials.

2.2.3 Rock classification

Rock properties cannot be allocated to a design calculation with the same certainty as other engineering materials. This is due to the fact that there is rarely a rock specimen that can fully represent the entire rock mass from which the results were extracted. Most of the rock volume that is of concern is usually unseen and inaccessible and, therefore, cannot represent the entire mass. However, if rock is to be used for engineering purposes, certain properties such as rock quality first need to be identified by using rock classification systems.

2.2.3.1 Complications of rock as a construction material

Designers cannot use and assign rock properties with as much confidence as other types of structural and hydraulic computations, as is rarely amendable to idealistic assumptions (Goodman, 1976). Firstly, the majority of rock formations are highly directional due to bedding planes in sedimentary rocks (Fig. 2.3a), foliation in metamorphic rocks (Fig 2.3b) and flow banding in igneous rocks (Fig 2.3c) – rock is, thus, a moderately to highly anisotropic material. Secondly, rock responds differently to excavations according to their initial stress state, which is dependent on the stress history of the rock (that is not always available). Thirdly, many rock masses are semi-discontinuous on a specimen scale due to a network of fractures within, whereas the majority of all rock masses on a formation scale are penetrated by surfaces of potential or real discontinuity and thus, discontinuous. Finally, some rocks are chemically changeable due to chemical weathering. Moreover, some rock shows a variability vertically and horizontally due to the different degrees of weathering (Goodman, 1976).

Figure 2. 3: a) Sedimentary bedding planes, b) Metamorphic foliation, c) Igneous flow bands

In its ideal form, a rock mass consists of a network of rock blocks and fragments, which are separated by discontinuities or fractures that form a material in which all elements behave as a unit in mutual dependence (Matula & Holzer, 1978). As a result, this complicated structure cause challenges and complications in engineering and construction, with its defects and heterogeneities.

2.2.3.2 Rock Mass Rating (RMR)

During the initial stages of any engineering project that incorporates rock masses, it is difficult to access detailed data regarding strength properties, in-situ stresses, deformation modulus, and hydrological properties for instance. The only data that

is usually easily accessible is borehole cores since they are easy to obtain. Due to a lack of detailed data, empirical methods such as rock mass classification systems are used for solving engineering problems. Empirical methods are necessary to determine rock quality in order to define input parameters in the designing of any underground engineering structure; the recommendation of support systems; and the determination of numerical modelling input parameters.

The RMR system, first developed by Bieniawski in 1973, are used to classify rock masses for design purposes. It has been proved over time and has been accepted by many authors because of the ease of application and versatility in engineering practice involving tunnels, mines, slopes and foundations (Bieniawski, 1989). Bieniawski suggested in the 1989 version (RMR89), that instead of using discrete values for the RMR, the user could incorporate the RMR values between different classes using tables.

Chen and Yin (2019) conducted data analyses with the goal of determining if the rock quality designation *RQD* (presented below) along with the RMR89 was outdated and whether the *RQD* should be abandoned in the RMR or if the new and updated 2013 version (RMR13) should be adopted. This discussion sparked much controversy amongst researchers worldwide. Until then, no study fully compared the older RMR89 and the newer RMR13 from the perspective of data analysis. Chen and Yin's study compared the two systems using a variety of data sets to improve accuracy. They concluded that even though the RMR89 and the RMR13 are very similar, the RMR89 was found to be superior to the RMR13 in terms of the (187 actual) case studies assessed in the analysis. The RMR89 could better capture the differences between rock masses of various qualities. In addition, it was highlighted that the RQD and RMR89 have been time tested over the past 40 to 50 years and therefore shall be used with confidence. While the application potential of the RMR13 cannot be denied, additional time and results are required before it is widely accepted throughout industry.

In 1964, D. U. Deere introduced an index called the rock quality designation *RQ,* which is used to assess the quality of rock quantitatively. The *RQD* represents a core recovery percentage that is a result of the number of fractures observed within a rock core. The *RQD* only considers intact rock pieces that are longer than 100mm in the formulation. The amount of rock pieces (100mm or greater) are summed and divided by the total core length as demonstrated in Equation 1 (Deere & Deere, 1988):

$$RQD = \frac{\sum Length\ of\ core\ pieces > 100mm}{Total\ core\ length} \times 100\ (\%) \qquad (1)$$

The *RQD* is to be considered as an index of rock quality where problematic rock is counted in compliment to rock mass (Deere & Deere, 1988). In other words, the *RQD* is the measurement of the percentage of 'good' rock recovered from an interval of a borehole (Edelbro, 2004). This procedure is illustrated in Figure 2.4.

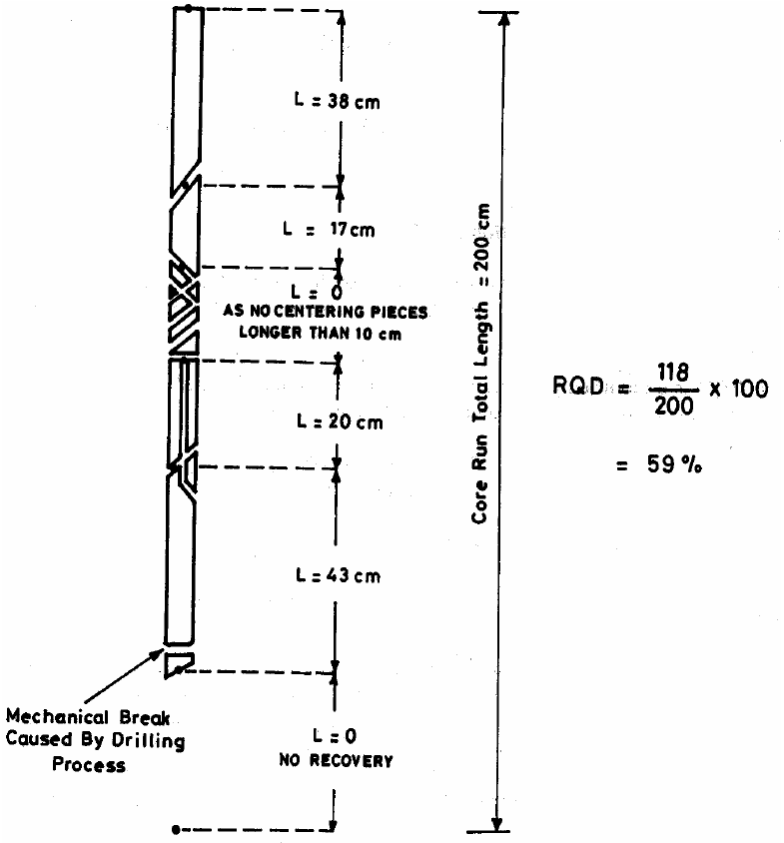

Figure 2.4: Procedure for measurement and calculation of RQD (Deere & Deere, 1988)

Deere suggested in 1968 the relationship between the RQD value and the engineering quality of the rock mass as shown in Table 2.1:

Table 2.1: Relationship between RQD and rock mass quality (Bieniawski, 1989, cited in Deere, 1968)

RQD (%)	Quality of rock
< 25	Very poor
25 - 50	Poor
50 - 75	Fair
75 - 90	Good
90 - 100	Very Good

When applying the RMR89 system, the rock mass is divided into various structural regions and each region is classified independently. Bieniawski (1989) mentions six parameters that are used to classify rock masses: Rock quality designation

(*RQD*); uniaxial compressive strength of intact rock material; discontinuity spacing; condition of discontinuities; groundwater conditions; and orientation of discontinuities. The ratings are then added to detrmine the total RMR value.

The first five parameters represent the basic parameters (RMR_{basic}), while the sixth parameter is treated separately because the discontinuity orientations are dependent on engineering applications. Each parameter is given an importance rating that describes the rock quality. The ratings of the parameters of the RMR89 system are shown in Appendix A. All of the RMR_{basic} parameter ratings are summed and can be adjusted depending on the joint orientation parameter as shown in Equations 2 and 3:

$$RMR = RMR_{basic} + discontinuity\ orientation\ adjustment \qquad (2)$$

$$RMR_{basic} = \sum parameters(1 + 2 + 3 + 4 + 5) \qquad (3)$$

The final RMR value is used to classify the rock mass as shown in Table 2.2. The higher the RMR, the better the rock mass quality.

Table 2.2: Rock Mass Rating classes (Bieniawski, 1989)

Rock mass properties	Rock Mass Rating class				
Ratings	81-100	61-81	41-60	21-40	<20
Class Number	I	II	III	IV	V
Classification of rock mass	Very Good	Good	Fair	Poor	Very Poor
Average stand-up time	20 yr for 15m span	1 yr for 10m span	1 week for 5m span	10h for 2.5m span	30 mins for 1m span
Cohesion of rock mass (kPa)	> 400	300 - 400	200 - 300	100 - 200	< 100
Friction angle of rock mass (deg)	> 45	35 - 45	25 - 35	15 - 25	< 15

2.2.3.3 Geological Strength Index and joint properties

After the use of the Rock Mass Rating over numerous years and improvements made to the Hoek-Brown failure criterion, it was also recognised that the RMR was

no longer adequate as a procedure for relating the failure criterion to geological observations in the field, specifically for very weak rock masses. This led to the conception of the Geological Strength Index (*GSI*) produced by Hoek, Wood and Shah (1992); Hoek (1994); and Hoek, Kaiser and Bawden (1995). This index was thereafter extended for weak rock masses in a series of papers by Hoek, Marinos and Benissi (1998); Hoek and Marinos (2000); and Marinos and Hoek (2001).

The strength of a jointed rock mass is dependent on the properties of the intact rock pieces as well as their freedom of movement under stress. This freedom of movement is controlled by the shape of the rock pieces as well as the condition of the joint infill surfaces separating the pieces. Due to this uncertainty with the RMR, the *GSI* was developed to provide a system for estimating the adjustment in rock mass strength for different geological conditions. The GSI system for blocky rock masses and for schistose metamorphic rocks is presented in Appendix B in Table B.1 and Table B.2 respectively. Once the GSI has been estimated for the rock mass, the GHB strength parameters presented in Equations 6 to 8 in Section 2.2.4.2, can be determined.

2.2.4 Non-linear failure criterion of rock types and constitutive models

A rock mass can never be accurately imitated as it is highly variable, never the same as another of the same type due to fractures, weathering and mineralogy differences in the rock mass. Therefore, reliable estimates of strength and deformation characteristics are required for any analysis of rock masses used for design purposes. In order to accurately simulate the behaviour of rock masses, constitutive models are used. Constitutive models describe a material's response to different loading conditions such as mechanical loads, which in turn provide the stress-strain relations of the material to formulate governing equations (Zhang, Chen & Liu, 2017). This section presents the most prominent constitutive models used to model rock masses.

2.2.4.1 Hoek-Brown Failure Criterion

The Hoek-Brown failure criterion is used for estimating the strength of a rock mass. Hoek and Brown (1988) state that this criterion was originally derived for the applications in underground excavation design and was thus expressed in terms of the major and minor principle effective stresses, σ'_1 and σ'_3 respectively, acting upon a specified element of the rock mass. However, the criterion has been altered to be used in many aspects of civil engineering, primarily in the design of slopes in heavily jointed rock masses (Hoek & Brown, 1988). The original equation defining the criterion is shown in Equation 4:

$$\sigma'_1 = \sigma'_3 + \sqrt{m\sigma_c\sigma'_3 + s\sigma_c{}^2} \tag{4}$$

Where:

σ'_1 is the major principle effective stress at failure, in MPa

σ'_3 is the minor principal effective stress (confining pressure), in MPa

m and *s* are material constants, dimensionless

σ_c is the uniaxial compressive stress of the intact rock, in MPa

The constant *s* varies as a function of how fractured the rock mass is from the defined maximum value. Fully intact rock will have an *s* value of $s = 1$, and a completely granulated rock specimen will have an *s* value of $s = 0$. Likewise, the material constant *m* depends on the extent of prior fracturing of the rock, where the value of *m* decreases as the degree of prior fracturing increases (Hoek & Brown, 1980).

Throughout the last 20 years there have been a few revisions made on the criterion mainly due to the original being based on experiments done on hard rock. The results were thus bias when other users of the criterion were applying it to problems that were not considered when the criterion was first established. The criterion was based upon the assumption that failure of the rock mass was only controlled by the movements of the pieces of rock that were separated by joint surfaces (Hoek &

Brown, 1980). As time progressed the criterion had to be made applicable for the technological advances that were occurring with numerical software. Advances such as creating a relationship between the non-linear *m* and *s* parameters from the Hoek-Brown criterion and the linear *c* and ϕ parameters from the Mohr-Coulomb criterion (Hoek, 1983). The application of the criterion to poor quality rock masses was not yet accurate, thus more changes needed to be made and from this arose the development of the *GSI* as a replacement for Bieniawski's RMR which could not take poor quality rock into consideration. The GSI was introduced and presented in Section 2.2.3.3 which is used in the more recent GHB Failure Criterion (Hoek, Carranza & Corkum, 2002).

The GHB criterion is a revised form of the original criterion that has been found practical in the field. It appears to provide the most reliable set of results for use as input for methods of analysis currently used in rock engineering (Hoek, 2001).

2.2.4.2 Generalized Hoek-Brown Failure Criterion

The Generalised Hoek-Brown criterion establishes the rock strength in terms of major and minor principle stresses and calculates strength envelopes that concur with laboratory triaxial test values of intact rock, and from observed failures in jointed rock masses. It is expressed as:

$$\sigma'_1 = \sigma'_3 + \sigma_{ci}\left(m_b \frac{\sigma'_3}{\sigma_{ci}} + s\right)^a \qquad (5)$$

Where:

σ'_1 is the maximum effective principle stress at failure, in MPa

σ'_3 is the minimum effective principle stress at failure (confining pressure), in MPa

m_b is the reduced value of the Hoek Brown constant *m* for the rock mass, dimensionless

s and a are constants that depend upon the rock mass characteristics, dimensionless

σ_{ci} is the uniaxial compressive stress of the intact rock pieces, in MPa

The term m_b was introduced to account for broken rock. The original m_i value was revised and found to be dependent on the properties of the intact rock. The material constant m_b is given by Equation 6:

$$m_b = m_i \exp\left(\frac{GSI - 100}{28 - 14D}\right) \tag{6}$$

The newly introduced exponential term a was added to address the equation's bias toward hard rock and additionally, to better account for the poorer quality rock masses. This is done by enabling the curvature of the failure envelope to be adjusted, especially under very low normal stresses (Hoek *et al.*, 1992). The s and a constants are given by the following relationships respectively:

$$s = \exp\left(\frac{GSI - 100}{9 - 3D}\right) \tag{7}$$

$$a = \frac{1}{2} + \frac{1}{6}\left(e^{\frac{-GSI}{15}} - e^{\frac{-20}{3}}\right) \tag{8}$$

Additionally, the uniaxial compressive strength is obtained by setting $\sigma'_3 = 0$ in Equation 9:

$$\sigma_c = \sigma_{ci}\, s^a \tag{9}$$

And the tensile strength is obtained by setting $\sigma'_1 = \sigma'_3 = 0$ and is given as:

$$\sigma_t = \frac{s\,\sigma_{ci}}{m_b} \tag{10}$$

This represents the biaxial tension condition.

The rock mass modulus E_{rm} or also known as the deformation modulus (Young's modulus) of a rock mass is not a well-known or easily measured parameter. However, for many types of numerical analyses, such as FE stress analyses, it is a required input parameter and is therefore important to obtain realistic values for any analysis that involves deformations (Rocscience, 2018). The generalized Hoek and Diederichs equation (2006) is the most widely used form, and utilizes the *GSI*, disturbance factor *D* and the modulus of intact rock:

$$E_{rm}\ (\text{MPa}) = E_i \left(0.02 + \frac{1 - \frac{D}{2}}{1 + e^{\frac{(60+15D-GSI)}{11}}} \right) \tag{11}$$

Where: E_i is the intact rock modulus, in MPa

D is the disturbance factor, dimensionless

However, reliable estimates of the intact rock modulus are not always available. In such a case, Hoek and Diederichs (2006) concluded that the following equation can be used where only the GSI or RMR data is available.

$$E_{rm}\ (\text{MPa}) = 100\,000 \left(\frac{1 - \frac{D}{2}}{1 + e^{\frac{(75+25D-GSI)}{11}}} \right) \tag{12}$$

In order to use the GHB failure criterion for the estimation of strength and deformability of rock masses, three properties have to first be estimated, they include:

1. σ_{ci}: The uniaxial compressive strength of the rock elements, in MPa
2. m_i: the Hoek-Brown constant for intact rock elements, no units
3. GSI: Geological Strength Index for the rock mass

When the rock mass consists of no discontinuities and is thus classified as an intact rock mass, the *GSI* = 100, making $m_b = m_i$, $s = 1$ and $a = 0.5$. This leads to the formulation of the Hoek-Brown criterion for intact rock masses:

$$\sigma'_1 = \sigma'_3 + \sigma_{ci}\left(m_i \frac{\sigma'_3}{\sigma_{ci}} + 1\right)^{0.5} \tag{13}$$

Hoek (2001) states that the relationship between the principle effective stress for a given rock at failure is defined by the uniaxial compressive strength σ_{ci} and the constant m_i. When possible, these constants should be determined by using statistical analyses of the results of a set of triaxial tests on prepared core samples. In cases where laboratory tests are not available, Table C.1 and C.2 in Appendix C can be used to estimate σ_{ci} and m_i.

As a result of the assumption that the rock mass and rock mass behaviour is isotropic in the original Hoek-Brown failure criterion, the criterion should only be applied to rock masses with an appropriate number of closely spaced discontinuities, as well as with similar surface characteristics so that isotropic failure behaviour may be assumed. Hence, in an analysis when the block size is small in comparison to the structure, the rock mass may be treated as a continuum. However, where the block size is of the same size as the structure that is being analysed, or when one of the discontinuity sets is significantly weaker than the others in the rock mass, the Hoek-Brown failure criterion should not be used. In cases such as these, the stability of the structure should be analysed by investigating mechanisms of failure involving rotation or sliding of blocks and wedges that are defined by intersection structural features. Figure 2.5 characterises these concepts.

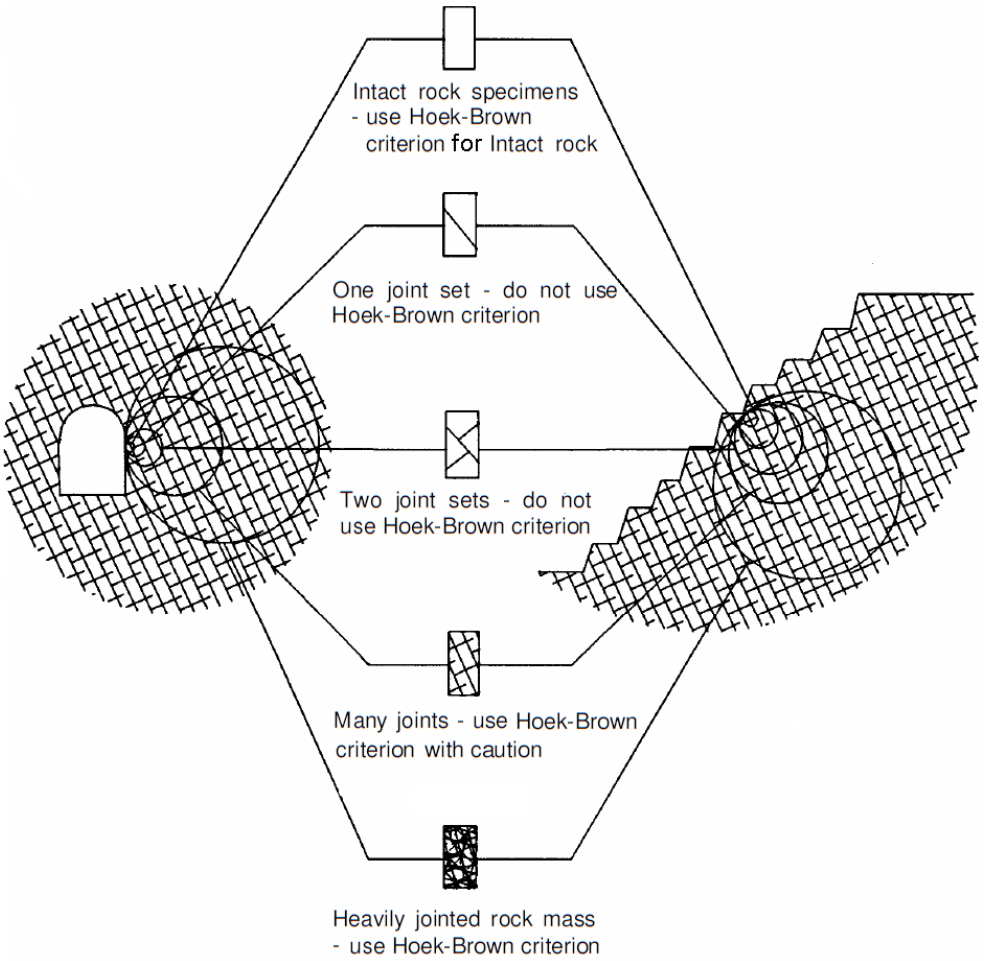

Figure 2.5: Diagram showing the transition from an intact rock mass to a heavily jointed rock mass with increasing sample size (Hoek, 2001)

2.2.4.3 Post-failure Behaviour

Estimates of deformation and strength characteristics of rock masses are required when analysing the stability of rock excavations. The Hoek-Brown failure criterion, presented in Section 2.2.4.1, is one of the most widely accepted failure criterions used to estimate rock strength. However, the Hoek-Brown failure criterion only deals with the stress in the rock mass up to the point of failure, not regarding the residual behaviour thereafter. Crowder and Bawden (2004) published an article in which a discussion between the company Rocscience Inc. and industry leaders in rock mechanics took place. The discussion involved post-peak, or residual, rock parameters. The article was based on the Generalized Hoek-Brown (GHB) failure

criterion, presented in Section 2.2.4.2, as it is the most widely accepted and used form of the Hoek-Brown strength criterion.

The post-peak rock mass properties play a vital role in the support design of excavations. As the rock mass begins to yield, fractures form in the rock and start to expand (dilate). Once this occurs it is important to know what type of support is necessary to prevent failure of the rock mass and thus the post-peak rock mass properties are required. When modelling rock masses in many geotechnical software packages, as a rock mass element exceeds its peak strength, it fails in a brittle manner by simply changing from peak parameters to post-peak parameters with no incorporation of a softening mechanism (Crowder & Bawden, 2004).

During the development of the Rocscience two-dimensional FEM software *Phase*^{2}, now known as *RS2* (a two-dimensional version of *RS3*), Rocscience Inc. asked industry leaders in rock mechanics, who use Rocscience's software, to define what properties establish residual strength in the GHB model. The participants involved included, E. Hoek (Evert Hoek Consulting Engineer Inc.), C. Carranza-Torres (Itasca Consulting Group Inc.), M. Diederichs (Queen's University), J. Carvalho (Golder Associates Ltd.), B. Corkum (Rocscience Inc.) and D. Martin (University of Alberta). Therefore, the results obtained from the discussion that were agreed upon can be considered the most supported values for post-peak behaviour.

According to the GHB model, the industry leaders agreed that the unconfined compressive strength σ_{ci} is a "fixed" parameter that is determined from intact rock specimens, and thus a residual value would not make physical sense.

Similarly, the disturbance factor *D*, denoting the degree to which the rock has been disturbed due to blasting, should not be altered to a residual value as it is used in the calculation of the peak Hoek-Brown constants m_b and *s* rock mass parameters. More specifically, it is based on the existing damage of the rock mass due to blasting and not due to failure of the rock mass. Just like the disturbance factor, the *GSI*

should not be changed to a residual value as it is a basic field observed classification parameter and used to establish the peak Hoek-Brown constants *a*, *s* and m_b.

On the contrary, the m_b parameter (considered to be the equivalent of friction angle in the Mohr-Coulomb criterion), should be allowed to change as the rock mass fails. This is done by decreasing the value as the rock mass is subjected to internal shear. To expand on this concept, for a rock mass that experiences failure in a brittle manner, the m_b parameter should undergo a large reduction. Whereas, a very weak rock mass that experiences plastic failure should undergo a minor reduction to the m_b value, as it is deemed to already be in the residual state (Crowder & Bawden, 2004).

Likewise, the Hoek-Brown *s* parameter, viewed as the "cohesive" component of the GHB criterion, should be allowed to decrease to zero with the intention of decreasing the intact rock strength upon failure. However, for the Hoek-Brown *a* parameter that essentially controls the curvature of the failure envelope, allowing residual values would give geotechnical software users full parametric flexibility. Therefore, having $a = 0.5$ as a fixed value will not allow the confined strength to increase quickly enough for highly fractured rock masses.

Crowder and Bawden (2004) documented general guidelines which Dr Evert Hoek follows in practice. He emphasized that these are his personal choices for residual parameters, and he suggested that they not be adopted by other engineers as a great deal of judgement is required on a job-specific basis. The guidelines are as follows, based on the *GSI* of the rock:

1. Massive Brittle Rocks ($70 < GSI < 90$) as illustrated in Figure 2.6
   - Great stress causing intact rock failure
   - All rock strength is lost at failure
   - $m_r = 1$, $s_r = 0$, and dilation = 0

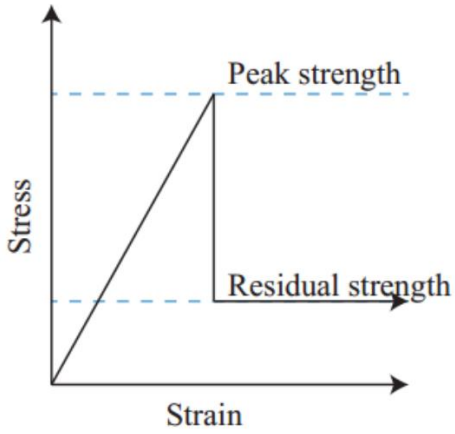

Figure 2.6: Assumed elastic brittle plastic behaviour of massive brittle rock (Hoek *et al.*, 1995)

2. Jointed Strong Rocks ($50 < GSI < 65$)
   - Moderate stress levels causing joint systems to fail
   - Rock fails to a "gravel"
   - $m_r = 15$, $s_r = 0$, and dilation = $0.3*m_r$

3. Jointed Intermediate Rocks ($40 < GSI < 50$) as illustrated in Figure 2.7
   - Weathered sandstone, granite, schist
   - Assumed to experience strain softening, loss of tensile strength, but retains shear strength
   - $m_r = 0.5*m_b$, $s_r = 0$, and dilation is small

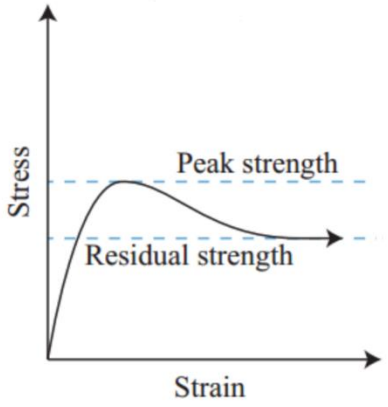

Figure 2.7: Assumed strain softening behaviour for jointed intermediate rock (Hoek et al., 1995)

4. Very Weak Rock (*GSI* < 30) as illustrated in Figure 2.8

   - Extreme tectonic shearing/folding (flysch, phyllite)

   - Experiences elastic-perfectly plastic behaviour, no dilation occurs – i.e. already at residual

   - $m_r = m_b$, s_r = s, and dilation = 0

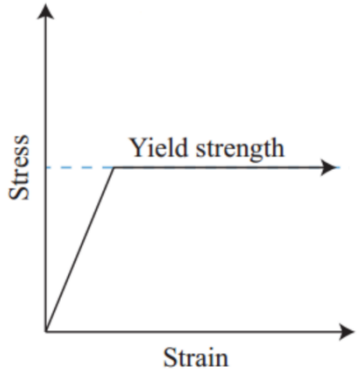

Figure 2.8: Assumed perfectly plastic behaviour for very weak rock(Hoek et al., 1995)

2.2.4.4 Equivalent Mohr-Coulomb parameters

Most geotechnical software is written in terms of the Mohr-Coulomb failure criterion and it is therefore necessary to determine the equivalent cohesive strengths and angles of friction for the rock mass. According to Hoek *et al.* (2002), this is achieved by fitting an average linear relationship to the Hoek-Brown curve generated by solving Equation 5 for a range of minor principal stress values ($\sigma_t < \sigma_3 < \sigma'_{3max}$). Figure 2.9 illustrates the concept. The curve fitting process involves balancing the areas below and above the Mohr-Coulomb plot. As a result of this process, the following equations for friction angle ϕ' (degrees) and cohesion c' (MPa) were derived respectively:

$$\phi' = sin^{-1}\left(\frac{6\,a\,m_b(s + m_b\,\sigma'_{3n})^{a-1}}{2(1+a)(2+a) + 6\,a\,m_b(s + m_b\,\sigma'_{3n})^{a-1}}\right) \qquad (14)$$

$$c = \frac{\sigma_{ci}\,[s(1+2a)+(1-a)\,m_b\,\sigma'_{3n}](s+m_b\,\sigma'_{3n})^{a-1}}{(1+a)(2+a)\sqrt{\dfrac{1+(6\,a\,m_b(s+m_b\,\sigma'_{3n})^{a-1})}{((1+a)(2+a))}}} \qquad (15)$$

Where: $\sigma'_{3n} = \frac{\sigma'_{3max}}{\sigma_{ci}}$

The value σ'_{3max} is the upper limit of the confining stress over the stress range considered, and it must be determined for each individual case. Thereafter, the Mohr-Coulomb normal stress and shear strength can be found using Equation 16.

$$\tau = c' + \sigma tan\phi' \qquad (16)$$

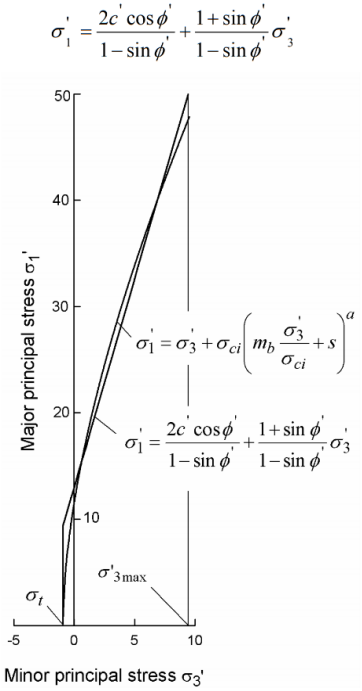

Figure 2.9: Relationship between major and minor principal stresses for Hoek-Brown and equivalent Mohr-Coulomb (Hoek et al., 2002)

2.3 Foundations

2.3.1 Definition

The term foundation is often used to describe the structural component that transmits the weight of, and loads acting upon the entire structure on to the ground. According to Chen & Duan (2014), this is not a fitting description for a foundation but is just one aspect of a foundation, as the foundation incorporates not only the concrete component, but the materials below on which it rests as well. These materials, such as soil and rock are more generally known as geomaterials.

2.3.2 Types of foundations on rock

Foundations can be classified into two types, shallow foundations and deep foundations. A foundation can be classified as a shallow foundation when the depth of the foundation is smaller than two times the breadth (Day, 2018) of the foundation ($d < 2B$) and conversely, a foundation can be classified as a deep foundation when the depth of the foundation is larger than 2 times its breadth ($d > 2B$). Types of shallow foundations firstly include spread footings such as strip foundations and pad foundations, and secondly stiffened and unstiffened raft foundations. On the other hand, types of deep foundations include piled foundations and deep spread footings.

Wyllie (1999) considers rock foundations to be classified into three groups, spread footings, socketed piles and tension foundations. The foundation used depends on the direction and magnitude of loading, and the geotechnical conditions in the bearing area. The basic geotechnical information required for the design of rock foundations consists of the rock strength properties, the structural geology and the ground water conditions.

2.3.2.1 Spread footings

Spread footings are isolated foundations, usually a square, rectangular or circular shape. They are typically concentrically loaded to avoid destabilising moments from the dead weight of the structure above. They can be constructed on any surface that has adequate bearing capacity and settlement characteristics, even on inclined surfaces in which tension anchors or steel dowels would be used to secure the footing to the rock. Figure 2.10 below illustrates a typical bridge spread footing subjected to an eccentric loading and showing the contact stress distribution exerted by the subsoil or rock.

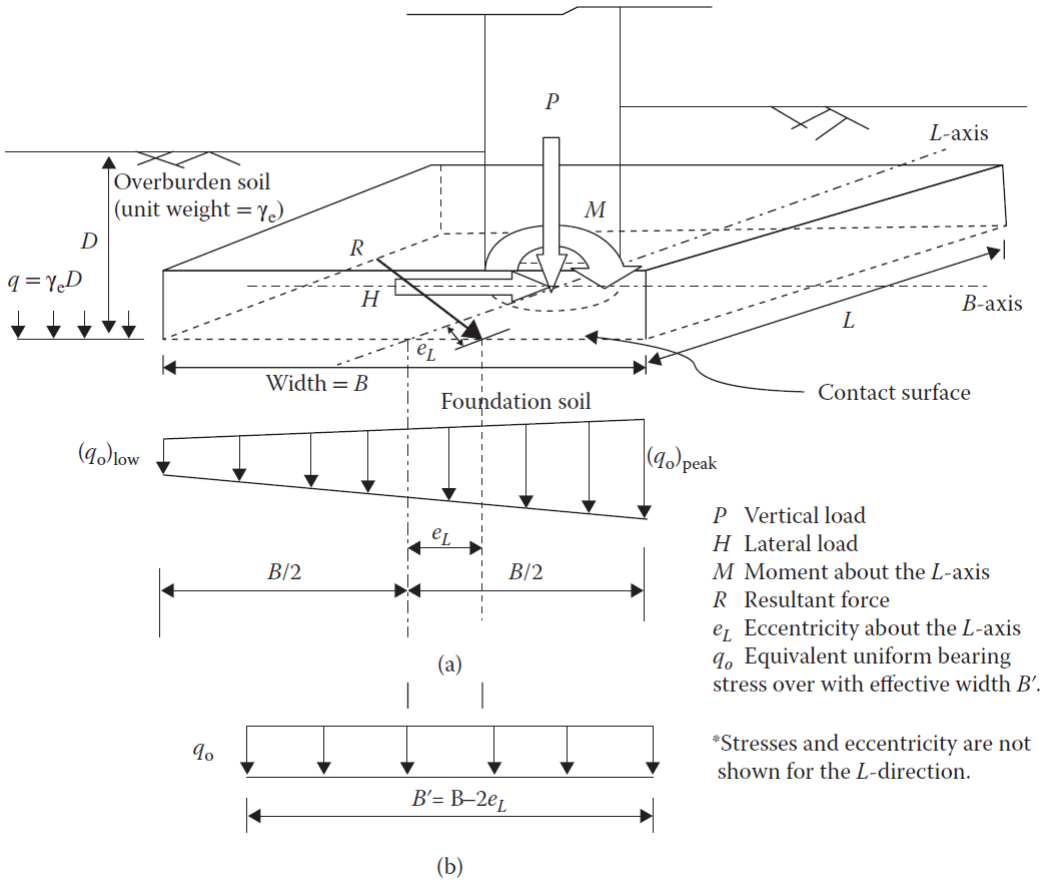

Figure 2.10: Sketch of typical bridge spread footing; (a) Idealised contact stress distribution and (b) stress distribution for geotechnical analysis and design (Chen & Duan, 2014)

2.3.2.2 Rock socketed piles

Rock socked piled foundations are typically used when the ground just below the surface level is weak and a stronger stratum is needed to support the foundation or when a spread footing cannot be constructed at the edge of an existing excavation. The support provided consists of the shear strength around the periphery of the drill hole and the end bearing at the bottom of the pile. Rock socketed piles can be designed to withstand high compressive and tensile axial loads and lateral forces provided minor displacements are experienced. A socketed rock pile is illustrated in Figure 2.11.

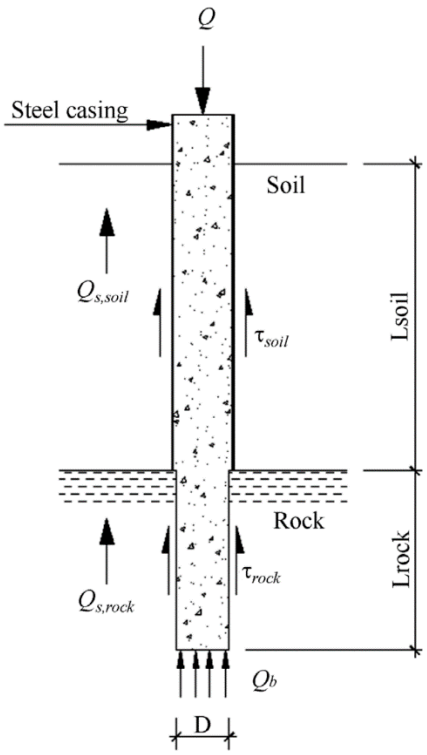

Figure 2.11: Rock socketed pile (Juvencio, Lopes & Nunes, 2017)

2.3.2.3 Tension foundations

Tension foundations are used for structures that produce permanent or temporary uplift loads. Support can be provided by the weight of the structure and tie down anchors or rock dowels into the underlying rock as illustrated in Figure 2.12. The uplift capacity of the anchor is determined by the characteristics of the rock cone

developed by the anchor and the shear strength of the rock-grout bond. As shown in Figure 2.12, the anchor lengths are staggered so that the stress in the rock is not concentrated on a single plane. This type of foundation is also used for structures subjected to high overturning moments that result in uplift of the foundation. Foundations built for structures such as bridges, resist uplift forces generated by horizontal loads such as traffic and wind which result in overturning moments.

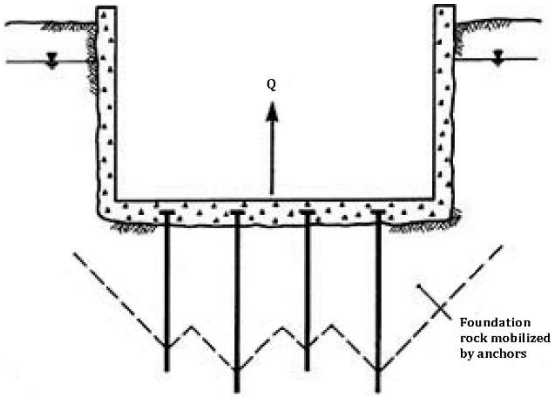

Figure 2.12: Tie down anchors with staggered lengths to prevent uplift (Wyllie, 1999)

2.3.3 Bridge Foundations

Many factors contribute to the selection of bridge foundations such as size and use of the bridge, the nature of subsoil, cost to build, number of piers, abutments and spans etc. According to Ponnuswamy (2008), there are four types of foundations that are mainly used for piers and abutments of bridges. These include open foundations/spread footings and block foundations, which are classified as shallow foundations, and piled foundations and well foundations, which are classified as deep foundations.

In general, when designing shallow foundations for serviceability, geotechnical movements and deformations are evaluated for the following material-foundation response parameters when subjected to the design service load (Chen & Duan, 2014):

- Settlements
- Lateral movements
- Footing deformations
- Rotations (overturning)

The design of shallow foundation for bridges is normally concerned only with settlement (Chen & Duan, 2014) due to the immense vertical force applied by the weight of the pier and deck. However, when designing a shallow foundation on hard rock, the rock is usually stiff enough to withstand settlement, but then overturning becomes a more prominent failure mode. Settlement refers to the downward movement of the foundation which occurs due to the compression of the foundation soils or rock. Limiting the settlement depends on numerous factors such as the types and functions of the structure and the spacing between the two adjacent supports. However, more often than not, the differential settlement between two adjacent supports proves to be more critical than the total settlement of the foundations. While settlement is very important to consider, it is equally critical to also consider the upward movement of the foundation. Uplift foundation movements are usually a result of externally applied upward loads. Foundation uplift can also be a result of an externally applied load to the top of a bridge pier at height h. This creates an eccentric load about the central axis of the foundation, causing a part of the foundation to settle and the other part to lift up. This type of foundation rotation results in the tilting of the supported structure. Tilt is defined as (Chen & Duan, 2014):

$$Tilt(\%) = \frac{\rho}{h} \times 100 \tag{17}$$

Where ρ (units in meters) is the lateral displacement of the structure at height h due to the footing rotation (α). Chen and Duan (2014) state that both the foundation and the superstructure are assumed to be rigid, which means the tilt is constant and that the tilt angle, $i = tan^{-1}\left(\frac{\rho}{h}\right)$, is equal to the angle of rotation of the footing (α). An

eccentrically loaded spread footing subject to overturning is illustrated in Figure 2.13:

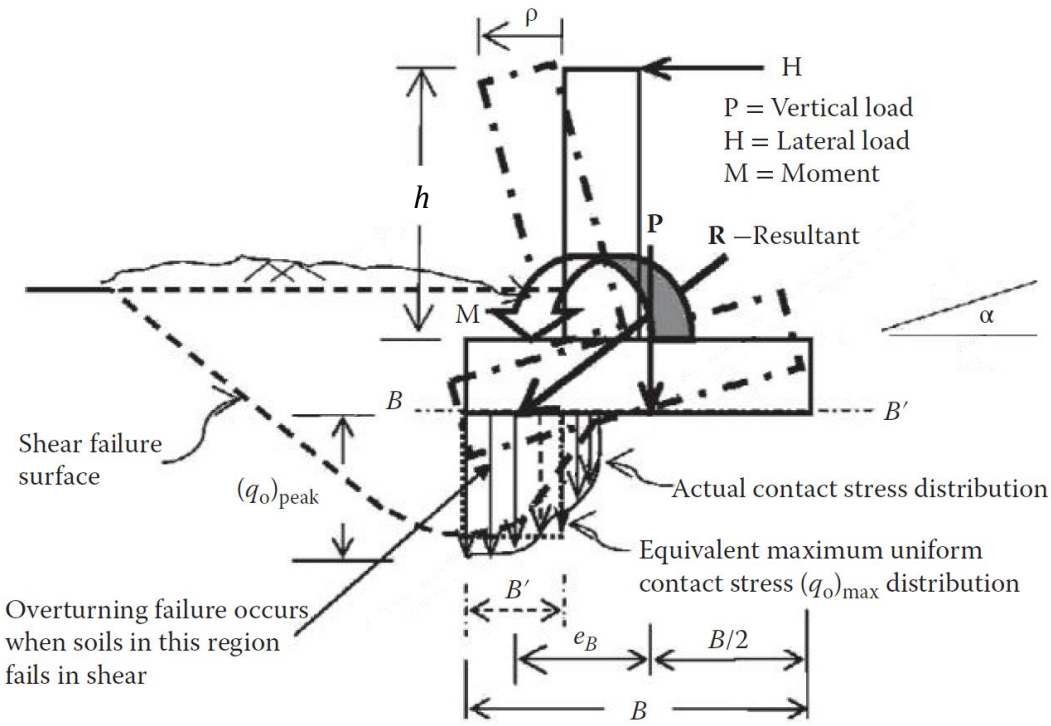

Figure 2.13: Rotation of shallow foundations (Chen & Duan, 2014)

USACE (2005) refers to the pertinent mode of failure as the rotational failures. Rotation of a shallow foundation due to serviceability loads should be limited to a small value as the structure must remain in a state of adequate serviceability. The maximum amount of footing rotation that is allowed as a result of serviceability loads depends on various factors, including the type, use and height of the supported structure. Chen and Duan (2014) suggest that, depending on the height of the bridge, a 0.25% - 0.5% tilt should be allowed for most bridges structures. With regards to the eccentricity of the applied load on the foundation, it is suggested by AASHTO (2002) that $e \leq B/6$ for soils and $e \leq B/4$ for rock to have a $FS \geq 2$ for soils and $FS \geq 1.5$ for rock in order to resist overturning failure.

2.3.4 Settlement and rotation of foundations on rock

Numerous surveys have been conducted to assess allowable settlement values of highway bridges as a result of vertical and horizontal movements (Grover, 1978; Walkinshaw, 1978; Bozozuk, 1978). It was concluded that the settlement can be divided into three categories depending on its effects on the structure:

1. Tolerable movements
2. Intolerable movements, only resulting in poor riding characteristics, and
3. Intolerable movements resulting in structural damage.

Due to the wide variety of bridge designs and subsurface conditions, it was unfeasible to specify limiting settlement values for the categories. Figure 2.14 shows the survey results of bridge piers and abutments on spread footings obtained by Bozozuk (1978). The surveys concluded that the tolerable movements can be as big a 50-100mm and that structural damage may not occur until the movements are greater than 200mm.

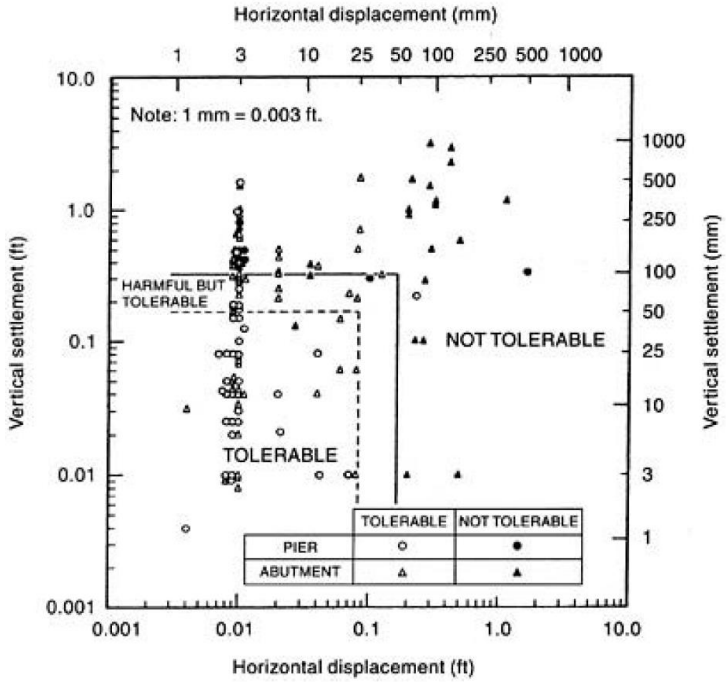

Figure 2.14: Engineering performance of bridge piers and abutments on spread footings (Bozozuk, 1978)

Forces produced by wind and traffic loads on tall structures such as bridge piers induce moments at the foundation level which changes the pressure distribution below the footing. For a square or rectangular footing with applied vertical load *N* and overturning moment *M* the resultant force will be situated at a distance *e* from the axes of the footing. The eccentricity of the loading *e* is given by (Merritt, 1976):

$$e = \frac{M}{N} \tag{18}$$

According to Wyllie (1999), when the moment is applied about the long axis of the footing and the eccentricity falls within the middle third of the base ($e < B/6$), the minimum and maximum pressures in kPa (σ_1 and σ_2 respectively) will be:

$$\sigma_1 = \frac{N}{BL}\left(1 + \frac{6e}{B}\right) \tag{19}$$

$$\sigma_2 = \frac{N}{BL}\left(1 - \frac{6e}{B}\right) \tag{20}$$

Where *B* is the width (m) and *L* is the length (m). Under these conditions the entire base is in compression and it is necessary to check if the bearing capacity has been exceeded. This calculation, however, assumes the footing to be completely rigid. Thus, the flexibility of reinforced concrete footings means that the actual pressures experienced will be lower than those given when assuming the footing to be rigid as the footing bends and won't undergo as much settlement. If the eccentricity falls outside of the middle third ($e > B/6$), the bearing is only in a portion of the footing and tensile forces develop in the remaining portion. For this condition, and with a rectangular footing of length *L* and width *B*, the maximum pressure in kPa is:

$$\sigma = \frac{2N}{3L\left(\frac{B}{2} - e\right)} \tag{21}$$

In the case where the eccentricity falls outside of the middle third, stability can be improved by the installation of tie-down anchors or passive rock dowels around the edges of the footing. The anchors/dowels will provide a stabilizing moment to counteract the overturning moment *M*.

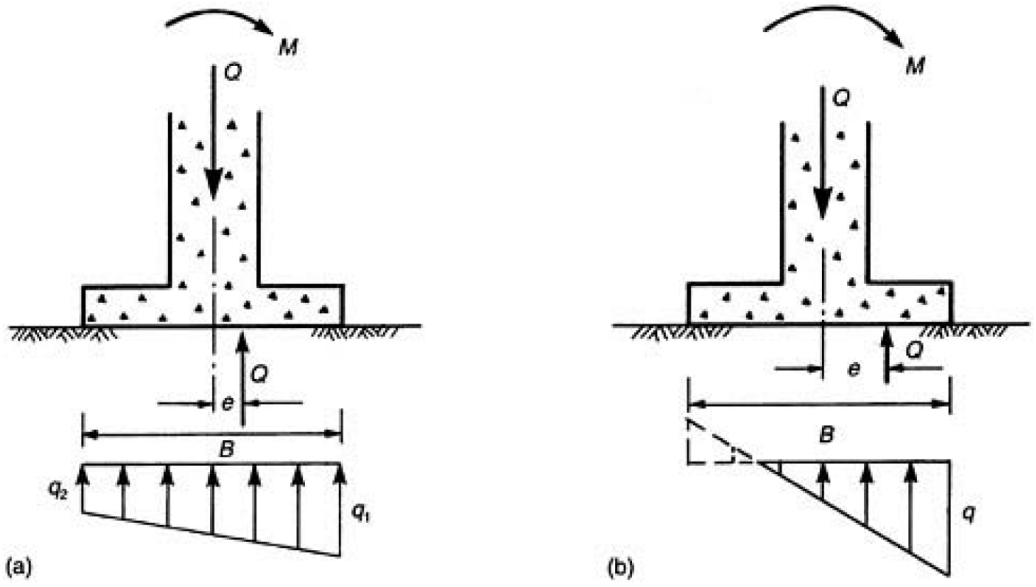

Figure 2.15: Soil pressures produced by footings subjected to overturning (a) e < B/6; (b) e > B/6 (Wyllie, 1999)

2.4 Modelling of foundations

Modelling of rock masses is a complicated task to undertake due to the presence of discontinuities, the non-elastic nature of rock masses, heterogeneity and material anisotropy when using numerical modelling techniques. It comes down to the complex nature and numerous formations of rock masses that make it a complicated material to model.

Empirical methods are used to classify rock masses quantitatively into different classes having similar characteristics for easy understanding and construction of underground engineering structures. Despite its wide range of applications, the empirical methods cannot evaluate deformations, stress redistribution, nor the

performance of support systems. It is important to consider these parameters in the design of foundations, underground structures and support systems. These shortcomings are solved by numerical methods.

Numerical modeling is being more readily used in the field of civil and rock engineering for the prediction of rock mass response to various excavation activities (Hussain *et al.*, 2018). Numerical methods are convenient, less costly, and less time consuming for the computation of stress redistribution and the effects it has on the behavior of rock masses and the designing of structures. Numerical techniques give exact mathematical solutions to problems based on engineering judgment and input parameters such as strength parameters of rock masses (Hussain *et al.*, 2018).

2.4.1 Foundation stiffness in numerical modelling

The material properties of the soil or rock are difficult to determine when designing a foundation system. As previously stated in Section 2.3.1, a foundation system consists of the soil or rock supporting the structure in addition to the foundation used to spread the load of the structure over a sufficient volume of material to withstand the imposed load. On the contrary to the material properties, the properties of the foundation can be determined quite accurately as the strength, and hence stiffness is ultimately up to the designer.

In order to simplify the design of the foundation system, structural engineers tend to use a system of linear springs to model the material behaviour of the soil as a compromise between accuracy and computational simplicity. The use of elastic-interaction-springs produce fairly accurate results for settlement and deflection when the soil-structure systems are associated with minor elastic deformation of the foundations (Conniff & Kiousis, 2007). Although this method may be fairly accurate in a couple of aspects, there are more shortcomings in the broader spectrum. For instance, this system cannot accurately compute inelastic material behaviour in response to loading and is also difficult to apply to foundation system models that approach ultimate bearing capacity. In addition, it cannot take strain

compatibility into account beneath or adjacent to the loaded foundation, as it does not model lateral soil response unless lateral springs are added (Lemmen *et al.*, 2017).

As a first iteration, structural engineers often take it upon themselves to design foundations for their structures and thereafter compare their results with the geotechnical engineers' results. From the structural engineer's point of view the foundation designed is based on two assumptions. Firstly, that the foundation acts as a rigid body and secondly, that the foundation rests on an elastic medium. Thus, it can be assumed that the settlement of the footing will always have a planar distribution because the rigid body cannot bend and thus remains planar when it settles. This planar distribution theory is based on the assumption that the ratio of contact pressure to settlement remains constant under the foundation, and that the stress distribution is always linear (Lemmen *et al.*, 2017). This method is based on the pioneering work of Westergaard (1926) where a mathematical model was presented with the intention of computing the stresses in concrete slabs.

However, the assumptions made by the structural engineer are not necessarily accurate, as experimental studies have revealed that footings generally have a finite stiffness, soil and rock tend to exhibit plastic behaviour, and the distribution of footing pressure within soil and rock vary with time. The pressure distribution of the soil beneath the footing depends on the type of soil as well as the stiffness of the footing and superstructure (Algin, 2007).

2.4.1.1 Elastic spring models

The current design of footings is based on an iterative process where the dimensions of the footing often relies on an estimation by the design engineer. The size of the footing is then checked to see if it complies with serviceability conditions and whether the bearing capacity of the soil has been exceeded or not. Once the footing dimensions have been established as acceptable, the thickness of the footing must be determined to ensure that it has adequate shear, bending and punching shear

strength to tolerate the applied loading (Algin, 2007). This design procedure focuses on the strength of the concrete and the bearing capacity of the soil.

Therefore, the methods such as the Winkler hypothesis is often used to design and analyse the foundations where the soil is modelled as a system of continuous, non-connected discrete linear elastic springs. This is a simplified method of analysing forces of foundations in which the reaction forces of the subsoil are proportional to the deflection of the foundation at each point (Zhan, 2012). The stiffness of these springs relate the applied stress on the foundation (σ) in kN/m^2, to the deflection (δ) in meters, by using the modulus of subgrade reaction with units kN/m^3 presented by Bowles (1996), shown in Equation 22.

$$k_S = \frac{\sigma}{\delta} \tag{22}$$

Elastic theories such as the Winkler method yields accurate results for loading below initial yield, but if the loading increases and continues beyond yielding, the method results become decreasingly accurate (Baumann & Weisgerber, 1983). Figure 2.16(a) and (b) demonstrate how a foundation system is modelled as an elastic spring model.

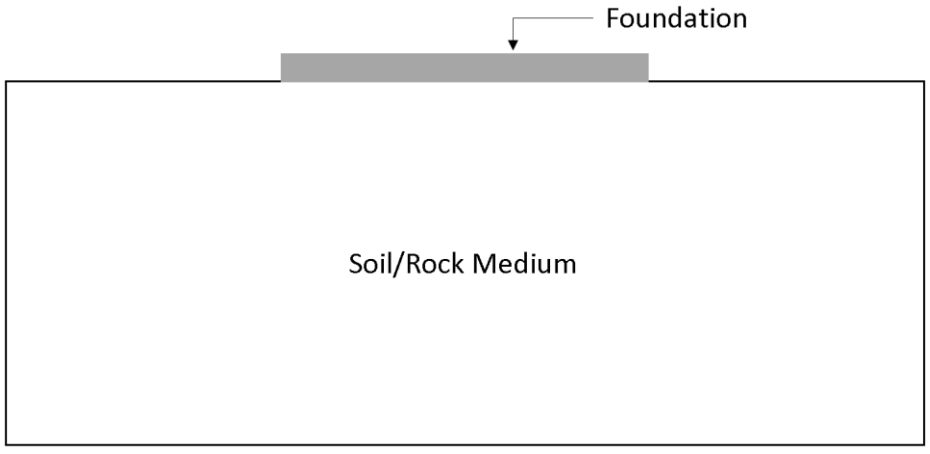

(a)

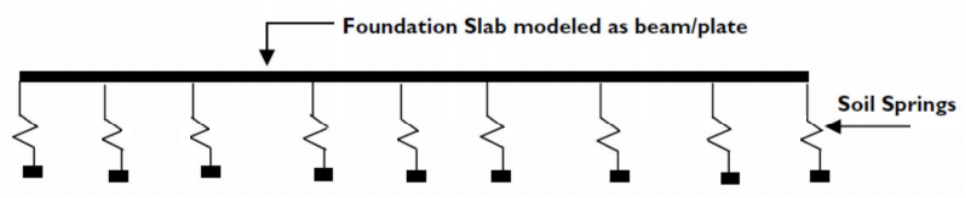

(b)

Figure 2.16: (a) Original foundation system; (b) Equivalent foundation resting on an elastic spring system

Linear elastic models are widely used because of their application in simplifying the behaviour of the soil under loading conditions. However, soil-structure interaction is an inevitable outcome as structures transfer their loads to the foundations, the foundations move or deflect and thus creates changes in the internal forces within the foundation and soil. Due to the interaction between the foundation and the underlying material, idealized linear models are not applicable to a wide range of problems and loads because of the simplifying assumptions that are needed for the use of the model. Figure 2.17 displays why the linear elastic models can be limited in their application because of how they differ from the true behaviour of rock or soil which are highly non-linear. (Conniff & Kiousis, 2007).

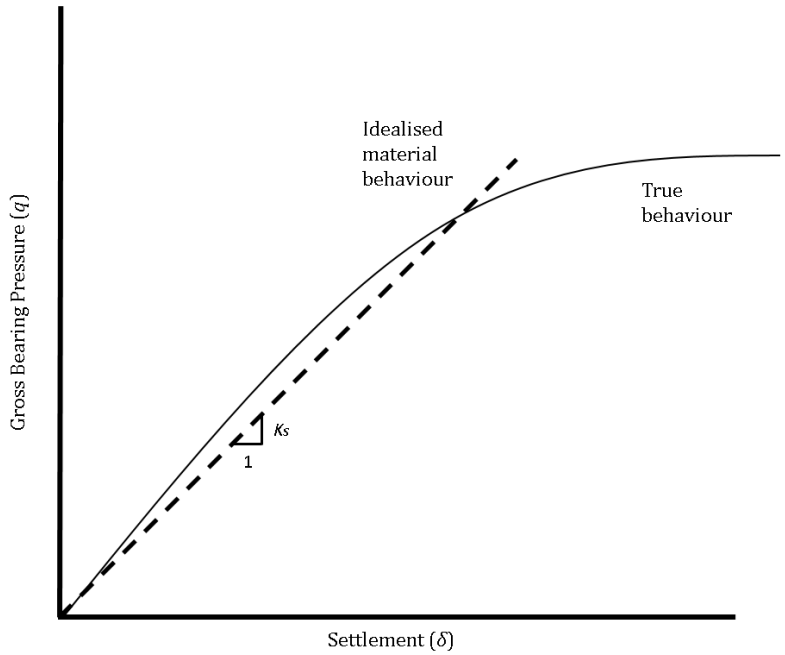

Figure 2.17: Linear behaviour compared to true material behaviour

Tests and experiments conducted in years past have shown that the structural behaviour of footings is dependent on their degree of stiffness. Moreover, it is important to not just take the footing stiffness into account, but the stiffness of the entire system in order to account for the soil-structure interaction (Lemmen *et al.*, 2017). Amongst such tests were centrifuge model experiments conducted by Arnold *et al.* (2010) to determine the effect of system stiffness on the contact stress distribution beneath the footing. The experiments confirmed that the settlement and stress distribution beneath the footing is dependent on the stiffness of the footing. As a result of the interaction that takes place within the foundation system, no element should be considered in isolation but it is vital that the entire system as a whole be considered in the design procedure (Arnold *et al.*, 2010). In order to measure the stiffness of the entire foundation system and thus determine whether the system is rigid or flexible, a dimensionless parameter K_s was developed which incorporates the stiffness of the footing combined with the Winkler spring model (*Canadian Foundation Engineering Manual*, 2006). Equation 23 is used to calculate the system stiffness parameter K_s (Arnold *et al.*, 2010).

$$K_s = \left(\frac{1}{12}\right)\left(\frac{E_b}{E_s}\right)\left(\frac{d}{B}\right)^3 \tag{23}$$

Where: K_s = system stiffness, dimensionless

E_b = Young's modulus of footing, in MPa

E_s = secant stiffness modulus of the soil/rock, in MPa

d = footing depth, in meters

B = footing width, in meters

In order to determine whether the foundation system is rigid or flexible, Arnold *et al.* (2010) proposed a classification criteria based on the K_s value as indicated in Table 2.3.

Table 2.3: Stiffness classification of foundation system

K_s range	System Stiffness
0	Absolutely flexible
0 - 0.01	Semi-flexible
0.01 - 0.1	Semi-stiff
0.1 - infinity	Stiff

While foundation stiffness is an important factor contributing to the stress distribution beneath the foundation, it was also concluded by Arnold *et al.* (2010) that the stress distribution beneath a footing on sand is highly dependent on the magnitude of the applied load on the footing. Following the conclusion presented by Arnold *et al* (2010), as part of the research of this thesis, a sensitivity analysis will be undertaken to determine the important factors contributing to the behaviour of the foundation when constructed on rock.

2.4.1.2 Influence of columns on footing stiffness

Meyerhof (1953) developed a relative stiffness factor K_r to determine whether a footing should be considered as flexible or rigid:

$$K_r = \frac{EI_b}{E_s B^3} \tag{24}$$

Where: K_r = relative stiffness, dimensionless

E = modulus of elasticity of the structure, in kN/m^2

E_s = modulus of elasticity of the soil/rock, in kN/m^2

B = width of the foundation, in meters

I_b = moment of inertia of the structure per unit length at right angles to B

The American Concrete Institute (ACI) Committee 336 recommends that if the K_r value is equal to or larger than 0.5, the foundation can be analysed as rigid.

However, if the K_r is less than 0.5, the footing should be designed as a flexible member on elastic supports. Equation 24 presented by Meyerhof (1953) was widely used in years past but was not without its shortcomings. The formulation firstly doesn't account for the size and stiffness of the column. Secondly, the load is always assumed to be a point load, which is not an accurate representation of reality. Lastly, it only considers one dimension of the footing. Tabsh and Al-shawa (2005) proposed a footing stiffness factor that was based on Meyerhof's formulation with modifications to account for the footing and column dimensions in Equation 25:

$$K_r' = \frac{Et^3}{k(1 - \nu^2)(B - b)^2(L - l)^2} \tag{25}$$

Where: t = uniform thickness of footing, in meters

b = column dimension along the footing breadth, in meters

L = footing length, in meters

l = column dimension along the footing length, in meters

ν = Poisson's ratio of the soil, dimensionless

k = modulus of subgrade reaction, kN/m^2/m

In this formulation the effects of footing width, footing thickness, modulus of subgrade reaction and column size were all investigated. The investigation considered square and rectangular footings, square and rectangular columns, and concentric and eccentric applied loadings.

It was concluded that the K_r' factor equal to or greater than 1.0 indicates that a footing can be safely analysed as a rigid footing. Additionally, if a footing is analysed as rigid, K_r' values below 1.0 lead to underestimates of the maximum vertical displacement and soil pressures. It was also observed that footing flexibility leads to lower load effects; therefore, it will be conservative to assume a footing to be rigid for the sake of determining shear forces and bending moments. Furthermore, it was observed that bending moments are more sensitive to changes

in footing stiffness than shear forces. The only shortcoming to this formulation is that only square and rectangular footings can be considered.

2.4.1.3 Rigid versus flexible behaviour

A rigid footing is assumed to have an infinite stiffness which means that the entire footing will settle as a rigid element. Under no circumstance can the footing undergo any curvature along its length or width and thus the contact pressure distribution beneath the footing remains linear. Rigid footing settlement is nearly uniform for all types of soil, whereas the contact stress beneath the footing is highly dependent on soil type as shown in Figure 2.18.

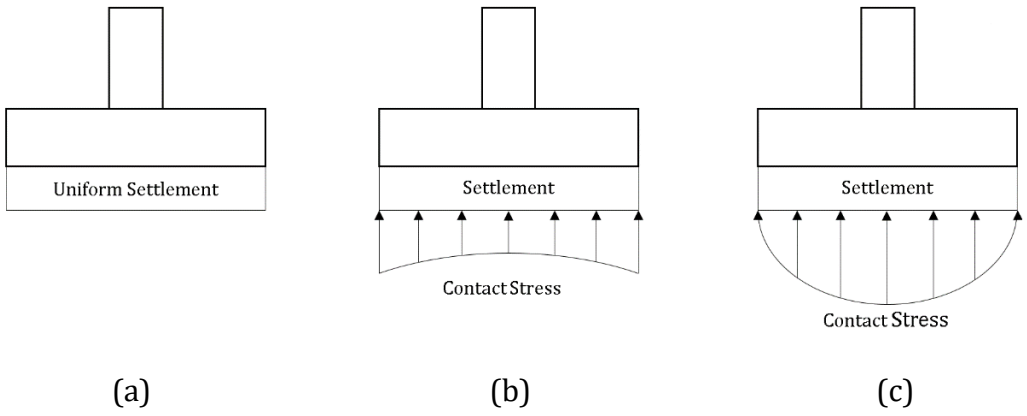

Figure 2.18: (a) Settlement of rigid footing (b) settlement and contact stress of rigid footing on cohesive soil (c) settlement and contact stress of rigid footing on cohesion less soil (Magade & Ingle, 2019)

In the case of a flexible footing, the footing is considered to have some degree of flexibility and thus when a pressure or concentrated load is applied, the footing undergoes bending. As the flexible footing bends, the soil beneath the footing experiences differential settlement and leads to a non-linear pressure distribution. Contact stress beneath a flexible footing is highly dependent on soil type, whereas the settlement is nearly uniform for all types of soil as shown in Figure 2.19.

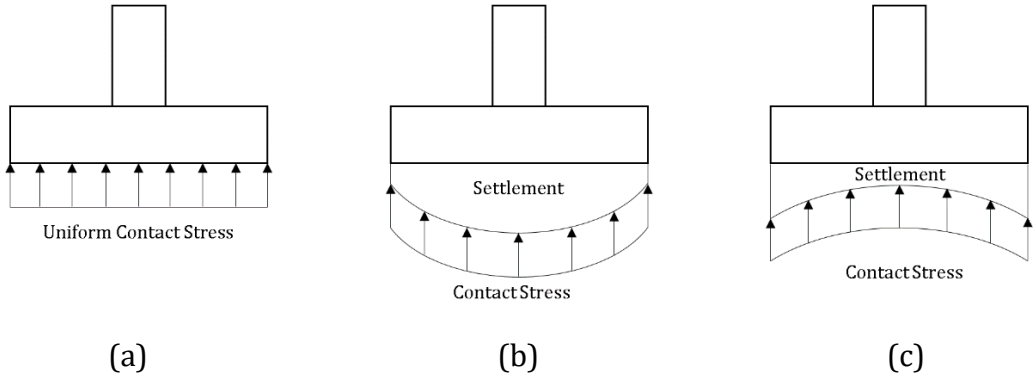

Figure 2.19: (a) Settlement of flexible footing (b) settlement and contact stress of flexible footing on cohesive soil (c) settlement and contact stress of flexible footing on cohesion less soil

The South African Bridge Design Code, the TMH7 Part 3 (1989), states that if the reactions to applied loads and moments are not derived by more accurate methods such as elastic analyses or by applying established soil mechanics principles, it can be assumed that the reactions to ultimate loads may be uniformly distributed over the base area when the base is axially loaded. In addition, when the base is eccentrically loaded, it may be assumed that the reactions vary linearly across the base. Thus, the TMH7 is essentially stating that the base can be assumed to act as a rigid element. This is valid for bases designed as "beam on slab" or "flat slab" when the breadth-to-depth ratio is more than 2 (B/d > 2). However, the same cannot be said about deep bases. The TMH7 Part 3 (1989) considers a deep base as having a breadth-to-depth ratio of 2 or less (B/d < 2), and in such a case, specialist literature would need to be consulted for design.

2.4.2 Footing element selection

An important question that needs to be asked when modelling footings is whether the foundation will be modelled as a plate element or a solid element. Plate elements by definition are plane structural elements possessing relatively small thicknesses compared to planar dimensions, whereas a solid element is a three-dimensional object containing information about the faces, edges and the interior of the object (Chang, 2016). In order to analyse plate models, plate theories are used to calculate stresses and deformations within a plate subjected to loading. Of the numerous plate

theories developed, the Kirchhoff-Love (classical plate theory) and the Mindlin–Reissner (first order shear plate theory) plate theories are the most widely accepted in engineering (Cen & Shang, 2015).

Structural elements are classified as plates when the element thickness is sufficiently smaller than the length and width. This is valid where $t/L << 1$, with t being the thickness and L the length of the element (Steele & Balch, 2009). Consequently, this reduces the three dimensional soil mechanics problem to a two dimensional problem and examined at middle surface. The middle surface is a flat surface equidistant to the plate faces at $t/2$. Thus, the geometry of the middle plane defines the shape of the plate.

2.4.2.1 Classification of plates

Plates are categorised based on the thickness of the plate. Thus, plates can be classified as either thick plates or thin plates. Plates are roughly classified as thin when $0.01 < t/L < 0.1$ and thick plates when $t/L > 0.1$. These ratios provide guidance as to when a particular element type is valid for the analysis. When the t/L is large then shear deformation is at maximum importance and solid elements should be used. Conversely, when the t/L ratio is very small then shear deformation is negligible and thin plate elements would be the most cost effective option (Akin, 2010). Akin (2010) continues to describe that in the intermediary range, thick shell elements would be the most effective option as they are generally able to develop shear forces, flexible moments and twisting moments (Shwetha & Subrahmanya, 2018). These loads always act perpendicular to the surface of the plate. Figure 2.20 presents the classification ranges for the three continuum element types that may be used.

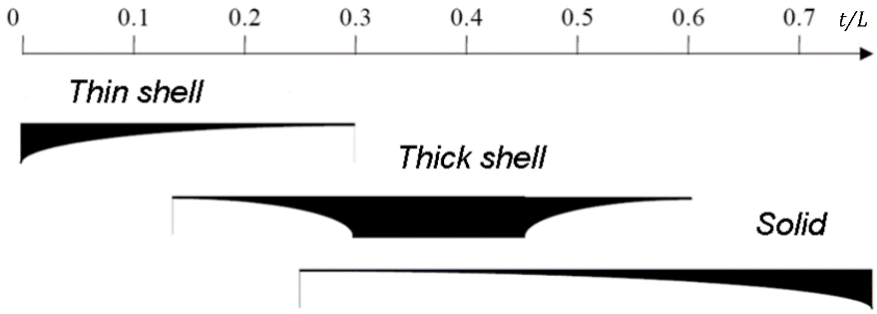

Figure 2.20: Ranges for choice of element types (Akin, 2010)

The main assumption for thin plates is that the straight line normal to the middle plane remains normal after plate deformation. However, the straight line normal to the middle plane does not remain normal after deformation for thick plates. The most used and accepted thin plate theory is the Kirchhoff-Love plate theory and for thick plates is the Mindlin–Reissner plate theory.

2.4.2.2 Kirchhoff-Love thin plate theory

The Kirchhoff-Love plate theory was derived from the one dimensional Euler-Bernoulli beam theory and developed as a two-dimensional equivalent of the Euler-Bernoulli beam theory with the same assumptions. The main assumptions include straight lines normal to the mid surface remain normal and straight after deformation (Steele & Balch, 2009) as shown in Figure 2.21, and the thickness of the plate does not change during plate deformation.

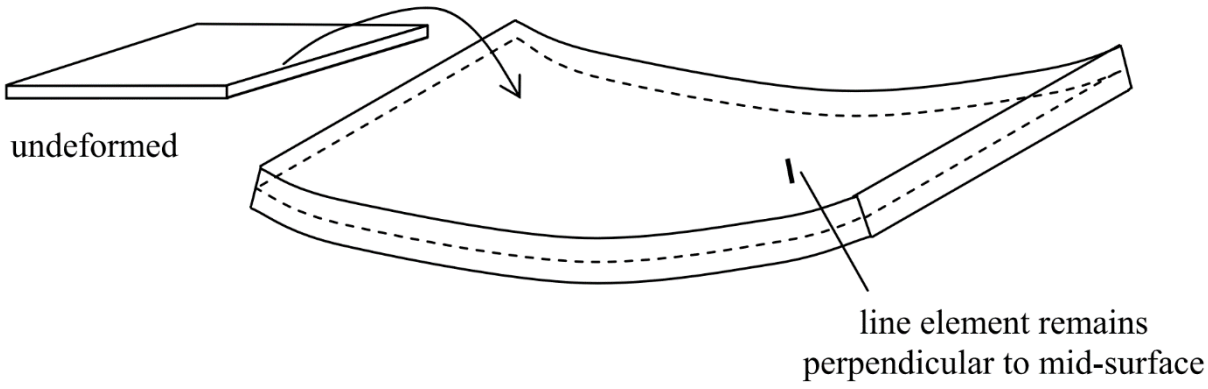

Figure 2.21: Line elements remain normal to middle plane after deformation (Stavridis, 2010)

Thin plates do not consider the stress in the direction perpendicular to the shell surface as transverse shear forces are neglected and thus the theory is only appropriate for modelling problems where the variation of such stresses are expected to be negligible (Cen & Shang, 2015). The forces and moments applied to the thin plates are shown in Figure 2.22(a) and (b).

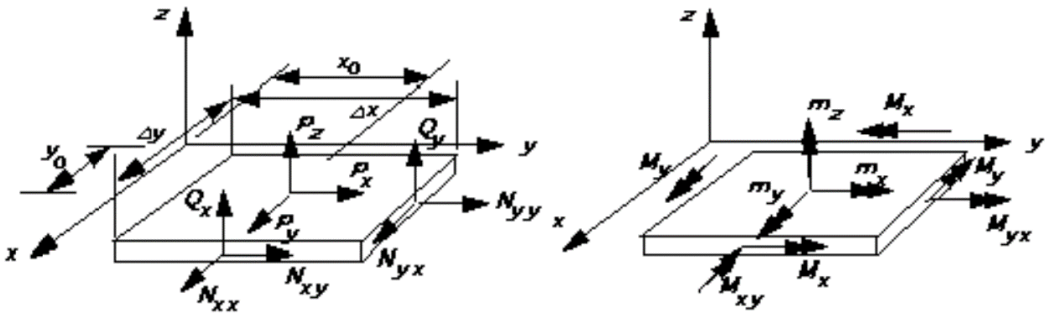

(a) **(b)**

Figure 2.22: (a) Force resultants acting on a two-dimensional plate element (b) Moment resultants acting on a two-dimensional plate element (Steele & Balch, 2009)

2.4.2.3 Mindlin–Reissner thick plate theory

The Mindlin–Reissner theory of plates is a refinement of the Kirchhoff–Love thin plate theory that considers the stresses through the thickness on the shell, in the direction normal to the middle surface by introducing two additional transverse shear measurements (Akin, 2010). Steele and Balch (2009) agree that substantially more accurate results can be obtained for thicker plates by including the effects of transverse shear deformation as seen in Figure 2.23. The main assumption for thick plate theory includes linear variation of displacement across the plate thickness while the plate thickness remaining constant during deformation.

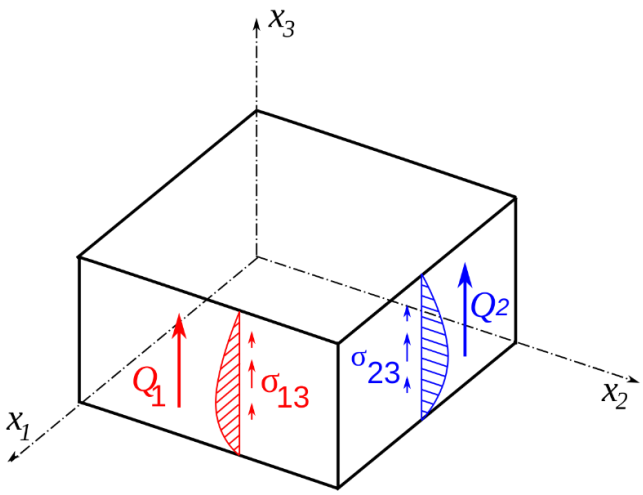

Figure 2.23: Shear stresses across thickness of plate (Reddy, 1999)

2.4.2.4 Solid elements versus plate elements

When analysing a finite element model it is important to know when certain elements are valid in order to get accurate results without the model being computationally strenuous. The main reason for using beam or plate elements in modelling is because it can lead to huge computational time saving as they allow modelling of thin features with fewer mesh elements and because they have less Degrees of freedom (DoFs) than solid elements do. On the other hand, solid finite elements would better resemble the physical problem and offer visualized information about the stress and strain distributions through the thickness of the foundation and in various planes because the material is represented throughout the entire component (Kuusisto, 2017). Solid elements consider the stresses in all directions while shells are mathematical simplifications of solids of different shape. Plates are like two dimensional lines, they do not have physical thickness in order to collide with each other and hence do not allow the three dimensional behaviour of the component to be fully captured. The two elements will be modelled and the results will be compared by the author to assist for future modelling purposes.

2.5 Structural Engineer's first iteration

The information presented in this section was provided during an interview with a South African structural engineer A. van der Merwe (2019). Van der Merwe states that structural engineers go into much detail when sizing foundations to make sure the loads from the superstructure can be effectively transferred to the underlying geomaterials to prevent either a bearing capacity, overturning or sliding failure. The behaviour of the foundation is, however, mainly dependent on the underlying geomaterials, thus, it is left to geotechnical engineers to provide the structural engineer with an allowable bearing capacity (for spread foundation) as a first step to estimate appropriate sizing for the foundation. This process is therefore, iterative between the structural and geotechnical engineer as settlement and distortion will also need to be checked by the geotechnical engineer. The route structural engineers generally follow is to model the soil-structure interaction with a system of springs in their finite element models.

The process of determining viable springs, able to simulate the foundation movements of the underlying material, begins with the structural engineer either using a hand calculation, a "fixed based" analysis or a "constant springs" analysis to derive the first load takedown estimates based on geotechnical information. The footing is then normally sized as a first estimate based on these loads. Thereafter, vertical-, lateral- and rotational springs are normally obtained by the structural engineer using both the loads and foundation sizes derived, and a modulus of subgrade reaction k_s to 'more accurately' model soil-structure interaction below their bridge structures. What is, however, proposed in this thesis is that the first load takedown and proposed sizing is given to the geotechnical engineer to insert into a three-dimensional geotechnical finite element model for each pier, and the settlement and distortions are calculated with rock and soil constitutive models, which will model rock-structure interaction much better. Springs are then derived from these analyses and given to the structural engineer. Thereafter the new springs are used in the structural model to derive new loads and they are given to the

geotechnical engineer. The iteration continues until convergence is reached for the settlement and distortion between the geotechnical and structural models. This will result in a more realistic modelling of the rock-structure interaction, which is explained below.

The structural engineers determine the spring stiffness by using Bowles' modulus of subgrade reaction k_s (in kN/m^3) presented in Equation 22 in Section 2.4.1.1. The structural engineers normally approach the problem as follows, when not following the above recommendations:
The vertical- and lateral spring stiffness (in kN/m) can be calculated using Equation 26 – with B and L representing the width and length of the foundation.

$$Vertical\ spring\ stiffness = k_s\ B\ L \tag{26}$$

According to Bowles (1996), the subgrade reaction values can be estimated using Table 2.4 below:

Table 2.4: Range of modulus of subgrade reaction k_s (Bowles, 1996)

Soil		k_s (kN/m^3)
Loose sand		4800 - 16 000
Medium dense sand		9600 - 80 000
Dense sand		64 000 - 128 000
Clayey medium dense sand		32 000 - 80 000
Silty medium dense sand		24 000 - 48 000
Clayey soil:		
	$q_a \leq 200$ kPa	12 000 - 24 000
200 <	$q_a \leq 800$ kPa	24 000 - 48 000
	$q_a > 800$ kPa	> 48 000

Using force equilibrium, the derivation of the rotational springs due to bending moment (in kN.m/rad) used by structural engineers are summarised in Appendix D. Rotational springs can be calculated using Equation 27.

$$Rotational\ spring\ stiffness = \frac{1}{12}\ k_s\ \phi\ z^3 \qquad (27)$$

With ϕ being the rotation angle in radians and z being the length over which rotation occurs in meters.

However, the above approach using tabulated subgrade moduli, in isolation from the three-dimensional geotechnical FE analysis, is not advised as k_s is a conceptual relationship between deflection and soil pressure that is derived using plate load tests (Bowles, 1996) – with plates generally smaller than 1.0m in diameter. The subgrade modulus is, however, not a constant soil property and will vary depending on the geometry of the foundation and the strain level of the soil – as soil deflection is highly non-linear in nature as previously shown in Figure 2.17 in Section 2.4.1.1. For illustration purposes, a crude hand calculation for settlement was used to compare two footings with the same applied stress and soil stiffness in order to show that the subgrade modulus varies depending on the geometry. The first with a footing width of B = 0.6m, an applied stress of σ = 200kPa and a soil stiffness of E = 10 Mpa; and the second with a footing width of B = 7m.

$$\delta = \frac{0.9\ B\ \sigma}{E}$$

The settlement for the 0.6m wide footing was calculated as:

$$\delta = \frac{0.9 * 0.6 * 200}{10}$$
$$= 10.8\ mm$$

The subgrade reaction is then calculated as:

$$k_s = \frac{200 * 1000}{10.8}$$

$$= 18518 \frac{kN}{m^3}$$

Whereas, the settlement for the 7m wide footing was calculated as δ = 126mm, and the subgrade reaction as k_s = 1587.3 kN/m^3. It can be concluded that the smaller the footing, the stiffer the spring, and Bowles' k_s values will rarely be applicable to larger geometries and could result in erroneous soil-structure interaction properties.

2.6 Synthesis

As previously stated in the introduction to the literature, various relevant topics involve the numerical modelling of bridge spread foundations on rock. Before the modelling can take place, an understanding of rock mass behaviour is required. The rock mass will have to be tested and classified through classification techniques such as the RMR or GSI in order to calculate certain rock parameters, which are used as inputs in constitutive models. A constitutive model is used to model rock behaviour in numerical software programs. Not all geotechnical software uses the same rock parameters as an input, so depending on the software used, equivalent rock strength parameters may have to be calculated to be used in a different constitutive model.

Thereafter, a decision must be made about how to model the concrete foundation – more specifically, what footing stiffness should be used and if a solid- or plate structural element should be used to model footing behaviour. Once the foundation system has been modelled, a rotation serviceability check needs to be carried out to ensure acceptable serviceability conditions are maintained. If uplift exceeds 25% of the footing area, measure should be taken such as inserting passive rock dowels into the model to ensure acceptable uplift. Once the rotational check has been completed, settlement results are obtained from the geotechnical FEM. The loads and settlement results are used to calculate spring constants, which are used in the structural FEM to model the rock. The settlements obtained from the structural

FEM must correlate to the settlements obtained from the geotechnical FEM. This will eliminate the tedious iterative process between the structural and geotechnical engineers.

Chapter 3: Finite Element Model Setup

3.1 Introduction

The majority of this study was undertaken by modelling bridge pier foundations on rock using three-dimensional Finite Element (FE) Analyses to illustrate to the reader how to use a similar methodology for large structures founded on rock. Rocscience RS3 geotechnical FE software was selected to model the bridge foundations on rock for the main reason that RS3 contains built in constitutive models used to accurately model rock behaviour such as the well-known Hoek-Brown and Generalised Hoek-Brown constitutive models. The software RS3, standing for Rock Soil 3D, was designed for three-dimensional analysis of geotechnical structures for civil and mining applications. It is a general-purpose FEA software that can be used for foundation design, support excavations, underground excavations, embankments, consolidation etc. and is thus a viable option to model bridge foundations on rock with applied bending moments on top of the foundation.

In order to achieve consistency in the FEM of bridge foundations on rock, a widely used structural FE software, Prokon Frame, was also used to model the bridge footing from a structural engineer's perspective. This was done by using springs to model the rock-footing interaction behaviour in addition to using geotechnical FE software to model the bridge footing from the geotechnical engineer's perspective. This was undertaken so that the results in the geotechnical FEA could be compared to the results in the typically-used structural FEA.

The following section shows the process that was undertaken to setup the finite element models in geotechnical Rocscience RS3 and the structural Prokon Frame model. This encompasses the geometry, the dimensions, the loading, material inputs, element types, loading, boundary conditions and discretization.

3.2 Project overview

The project overview, as shown in Figure 3.1 for part 1 and Figure 3.2 for part 2, includes flowcharts of the steps that were completed in order to meet the objective stated in Section 1.4.

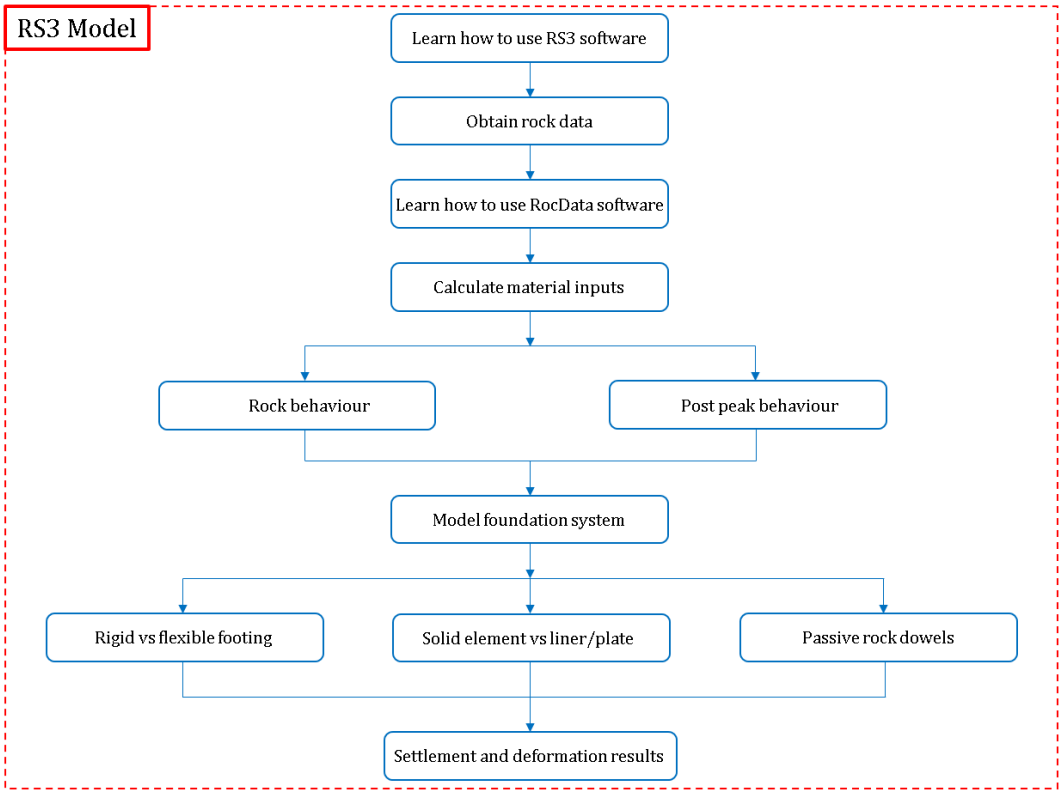

Figure 3.1: Schematic diagram showing part 1 of the project overview

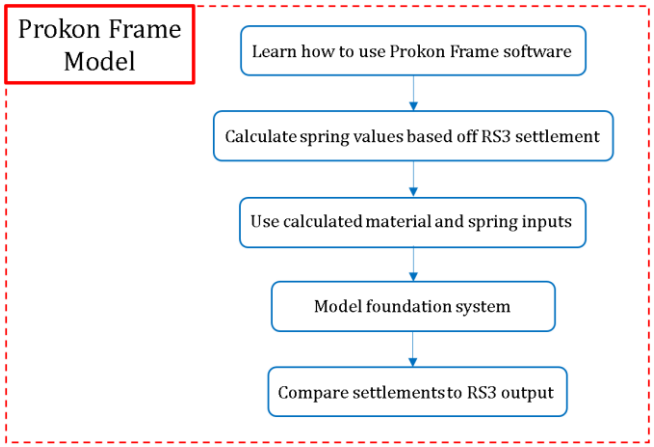

Figure 3.2: Schematic diagram showing part 2 of the project overview

3.3 Case Study

The bridge foundation modelled is an exact representation of an actual bridge that was designed in South Africa with both piled solutions and spread foundations on rock on different piers. It was proposed to be a spread footing with dimensions 9m long, 7m wide and 2m thick. The geometry and dimensions of the bridge footing and bridge pier are shown in Figure 3.3(a) and (b) respectively. The footing is subjected to eccentric loading due to wind forces, launching loads, dynamic forces applied from the moving vehicles on the bridge deck as well as seismic loading. The pier is underlain by very hard rock (Granite-gneiss) at a shallow depth.

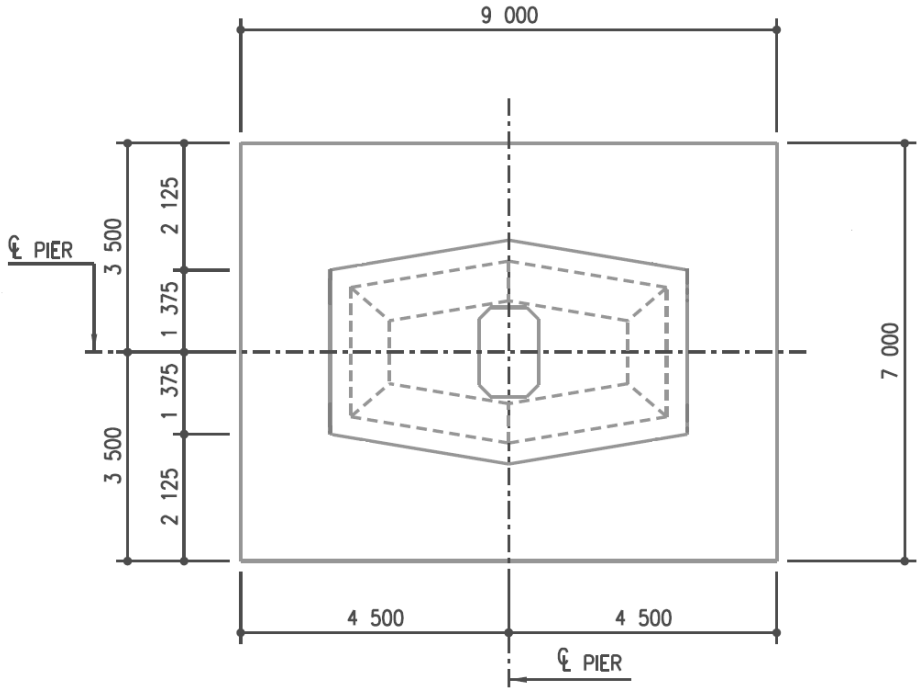

(a)

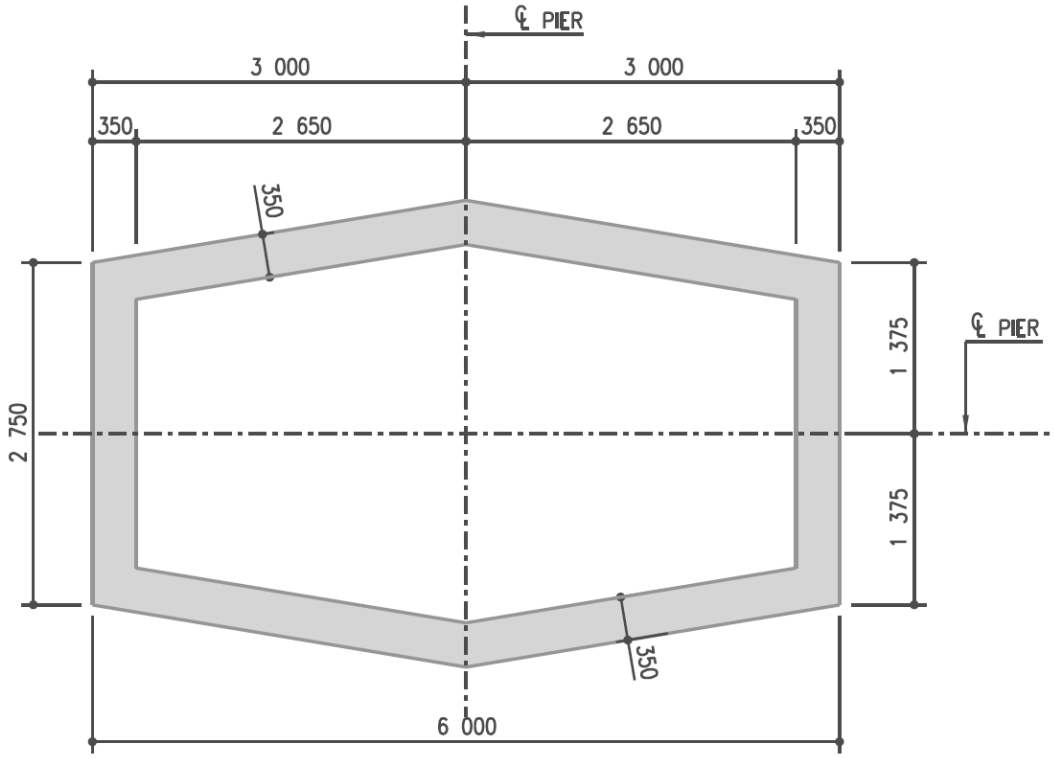

(b)

Figure 3.3: (a) Foundation dimensions, (b) Pier dimensions

The SLS loading applied to the footing was modelled and is summarised in Table 3.1. The foundation axis is represented in Figure 3.4.

Table 3.1: Bridge pier loading conditions

SLS Loading		
Load	Magnitude	Unit
N_x	-20626	kN
M_z	-46223	kNm
M_y	37839	kNm
V_y	925	kN
V_z	-108	kN

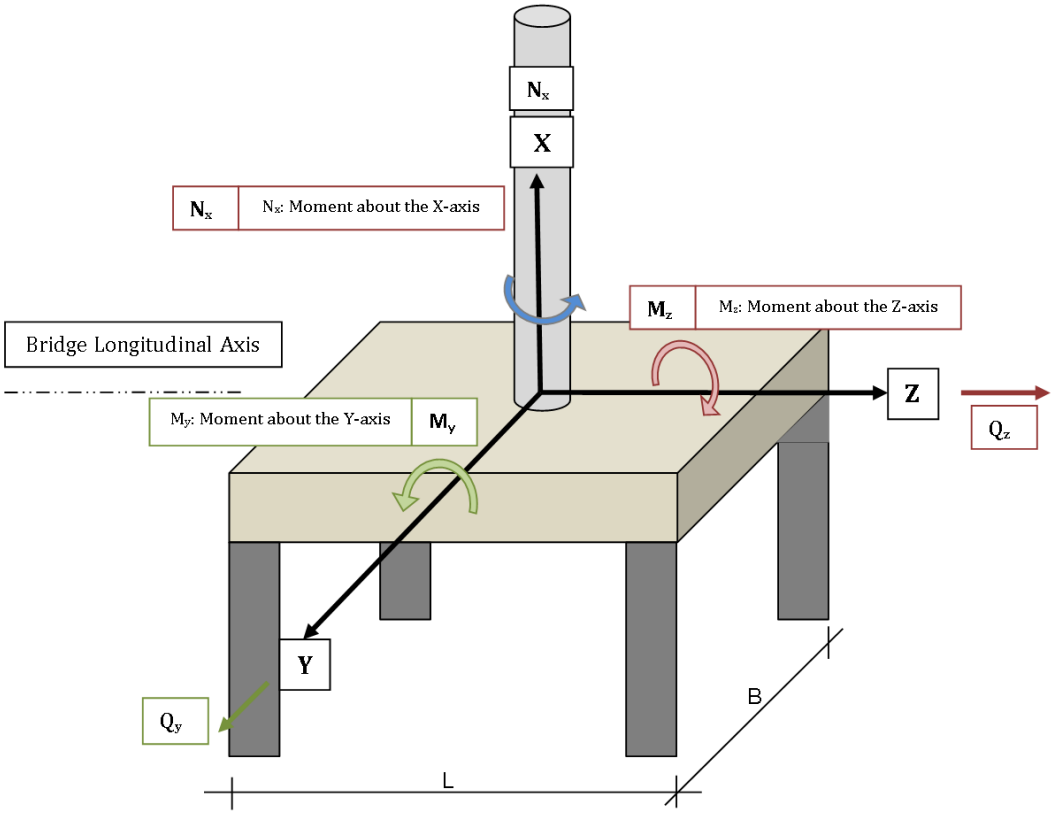

Figure 3.4: Foundation axes

3.4 RS3 Finite Element Model

3.4.1 Geometry

The foundation system is a simple model where a rectangular footing of 9mx7mx2m was constructed upon a homogeneous mass of rock (25mx25mx27m) – as shown in Figure 3.6. It was stated in the design report that the very hard rock was excavated using pneumatic tools or chemical fracturing in order to avoid blasting next to the existing structure. The foundation was then constructed on top of the rock and backfill was added to cover the foundation, hence it was considered that there was minimal sidewall resistance. In order to account for the zero sidewall friction resistance and not disturb rock movement once loaded, a circular excavation of 12m radius surrounding the footing was modelled as shown in Figure 3.5.

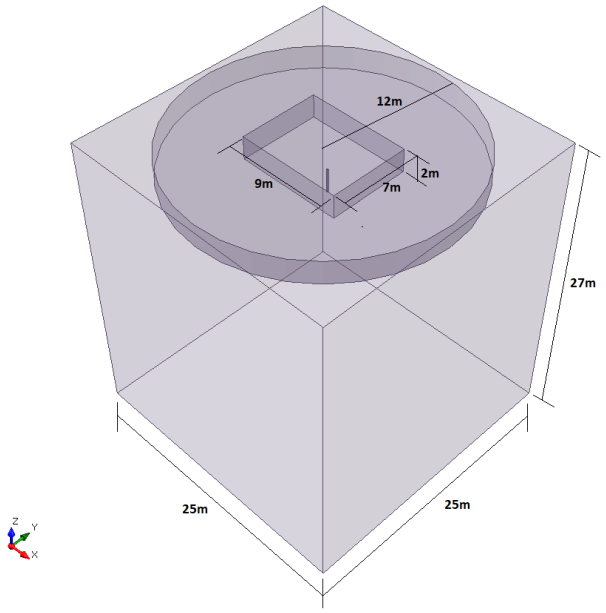

Figure 3.5: RS3 model of the foundation system

RS3 allows the user to create a multi-stage model in order to better simulate the construction process. The full model was defined in 5 stages, namely the first "Initial" stage in which the entire body consists only of rock in order to allow in-situ stresses to be developed without external loading. Secondly, the "Excavate Spread" stage in which the footing volume is removed from the external body of rock. Thirdly, the "Pour Concrete" stage in which the footing volume was filled with concrete. The fourth stage, "Excavate rock", is where the rock surrounding the footing was excavated and the last stage, the "Load Spread" stage, is where the loading was applied to the footing. Due to the rock material having a plastic nature, plastic rock properties were added. This, however, did not make a difference in the analysis as the rock was very hard, but it was added to be used for any rock hardness. A tolerance was used for each load step in RS3 and was set at a default of 0.001. The tolerance value of a FE model is a dimensionless parameter that defines the point at which the finite element solution is considered to have converged. The tolerance value represents the allowable unbalanced 'energy' in the system.

3.4.2 Material parameters

The model consisted of two materials, namely the rock and the concrete. As previously stated, the rock was a very hard Granite-Gneiss. The constitutive model chosen to model the rock material was the GHB failure criterion as it has been found to be practical in the field and provides the most reliable set of results according to Hoek (2001). The material inputs for the rock needed in *RS3* included the intact compressive strength σ_{ci}, the modulus of deformation E_{rm}, Poisson's ratio ν and the Hoek Brown constants m_b, s and a. The values for the Hoek Brown constants m_b, s and a needed to be calculated using Equations 6, 7 and 8 respectively, and the modulus of deformation needed to be calculated using Equation 11. These equations thus needed the inputs of the *GSI*, the Hoek Brown constant m_i, the disturbance factor D and the intact rock modulus E_i as shown in Figure 3.6.

The intact compressive strength σ_{ci} was calculated from the unconfined compressive strength (UCS) data extracted from the site and using the cautious estimate method explained in Appendix E. Thereafter, the intact compressive strength was entered into Rocscience's *RocData* program which was used for the determination of strength envelopes and other physical parameters of the rock. *RocData*, an updated version of the well-known program *RocLab*, was released as an associate program to the 2002 Edition of the Hoek-Brown Failure Criterion (Hoek *et al.*, 2002) and is based on the GHB Failure Criterion. *RocData* was used to calculate the Generalised Hoek-Brown input values used in the model. Due to the lack of rock parameters obtained from in-situ and lab tests, average values from estimation tables in *RocData* were used for the m_i and the modulus ratio *MR* values. The modulus ratio is used when E_i is not known, $E_i = MR \times \sigma_{ci}$. The process used by *RocData* to calculate the material inputs was presented in Section 2.2.4.2. The *RocData* inputs are summarised in Figure 3.6.

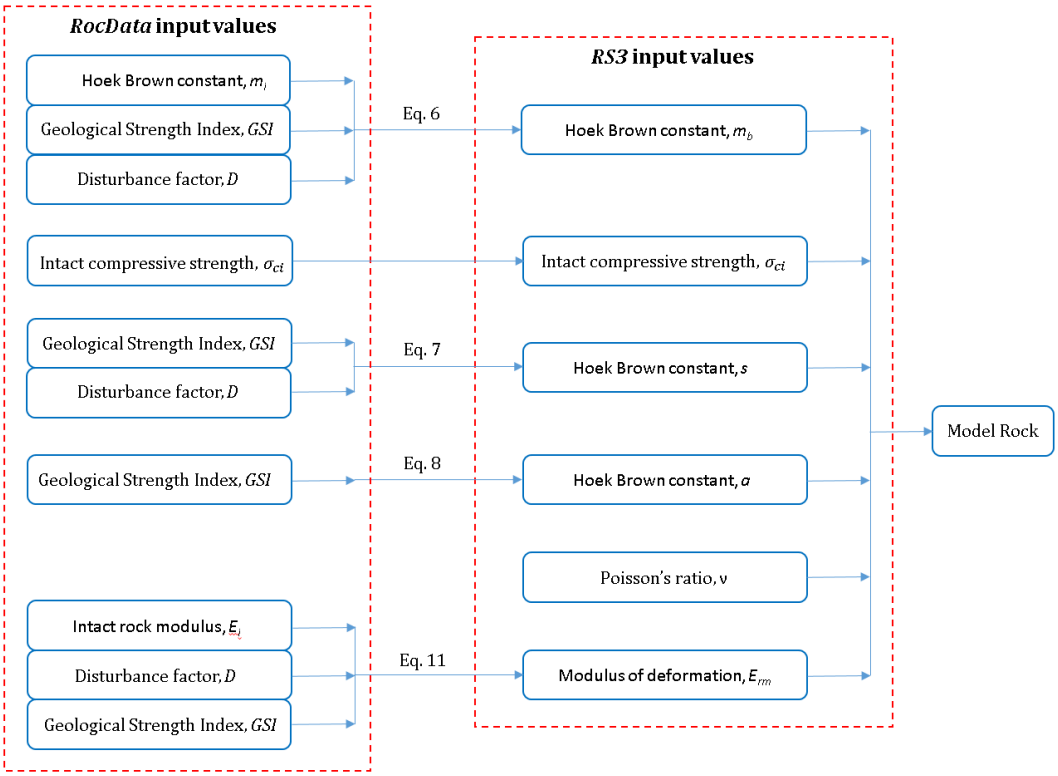

Figure 3.6: Inputs needed to model rock

Due to the rock having a plastic nature, the post peak values needed to be determined and entered into *RS3*. As documented in Section 2.2.4.3, the post peak estimates recommended by the industry leaders were used. For massive brittle rocks with a *GSI* value of 65 and greater, the m_r (residual) value was estimated to be 1.0, the a_r value being a constant of 0.5 and the s_r and dilation parameter β being 0. The rock material inputs are summarized in Table 3.2.

Table 3.2: Rock material inputs

Rock Inputs			
Rock behaviour values			
Parameter	Symbol	Value	Unit
RocData inputs			
Intact compressive strength	σ_{ci}	40.45	MPa
Geological Strength Index	GSI	65	
Disturbance factor	D	0	
Hoek-Brown constant	m_i	32	
Modulus ratio	MR	425	
Intact rock modulus	E_i	17191.25	Mpa
RS3 inputs			
Intact compressive strength	σ_{ci}	40.45	MPa
Hoek Brown constants	m_b	9.168	
	s	0.02	
	a	0.502	
Poisson's ratio	ν	0.3	
Deformation modulus	E_{rm}	10860.05	MPa
RS3 Residual values			
Dilation parameter	β	0	
Residual Hoek Brown constants	m_r	1	
	s_r	0	
	a_r	0.5	

Concrete, like rock and soil, is a complex material. However, since concrete materials are much stiffer and stronger than soils and soft rocks, geo material (rock and soil) characteristics are more prone to govern the material-structure interaction behaviour. Thus, it is usually possible to simplify the concrete constitutive model to a simple, isotropic, homogenous, linear elastic model (Lees, 2016). The concrete foundation was thus modelled as a homogenous Mohr-Coulomb material with a friction angle of ϕ' = 45°, cohesion of c = 2500kPa, Poisson's ratio of ν = 0.2 (simulating concrete in compression) and modulus of elasticity (Young's Modulus) of E = 1x10^6 GPa (Rigid behaviour) and E = 30 GPa obtained from TMH7 Part 3 (1989) for 40MPa concrete based on short term loading as creep and crack widths were not considered in this research. Two Young's Moduli were used to compare results as it is impossible for a concrete footing to have an infinite stiffness in

reality. Due to the bridge foundation being so thick (and will thus not reach yield capacity as it is designed for serviceability) it was modelled as an elastic material.

3.4.3 Footing elements

When modelling the footing element, it is important to determine what output is desired. If high accuracy is needed, then modelling the footing as a solid element would be most advantageous as a solid element is a three-dimensional object calculating stresses and deformations about the faces, edges and the interior of the object, as previously stated in Section 2.4.2. However, if time is a constraint in the process, then a two-dimensional plate element, modelled as a liner in *RS3*, should be used as they are thinner elements consisting of fewer mesh elements and thus take less time to converge.

3.4.3.1 Solid elements

Solid elements are simply modelled using different geometric elements such as a box or cylindrical elements. Solid elements can also be created by drawing the desired shape using a polyline, creating a polygon from the polyline and then extruding the polygon. When analysing the results of a solid element, the entire element is analysed and contour patterns are displayed on the perimeter of the element or when the element is sectioned and contour patterns are displayed on the internal section within the element as shown in Figure 3.7.

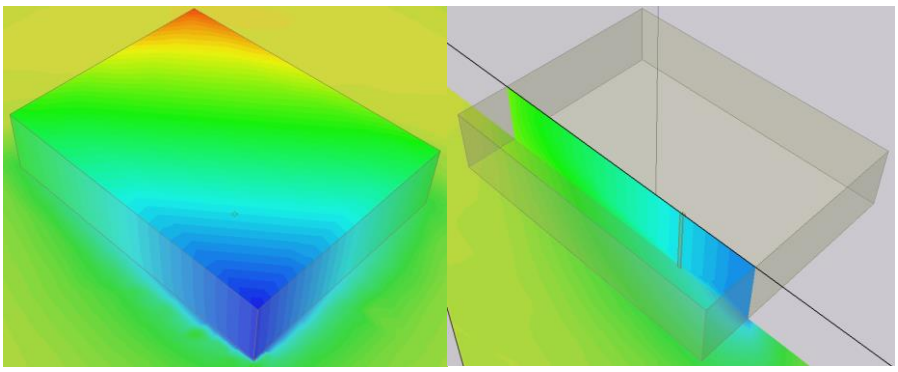

Figure 3.7: Footing as a solid element

3.4.3.2 Plate elements

Liners in RS3 can be likened to a plate structural support element used in numerical models. The Standard liner was used in the analysis to model the footing. This type can be used to model a liner which has flexural rigidity (i.e. resistance to bending), such as a concrete or a shotcrete liner. A Standard liner is made up of two-dimensional plate elements which can respond to axial (tensile or compressive), flexural and transverse shear loads.

Structural elements such as plates and beams are three-dimensional elements that are relatively thin along one of their axes. Plate components in RS3 are two-dimensional elements exhibiting flexural rigidity about their local x and y axes. The only dimension in a plate element that is reduced is its thickness and, therefore, the additional input geometry defined is the thickness of the element. Bending mechanism is formulated based on the Mindlin-Reissner thick plate theory discussed in Section 2.4.2.3. Each node is in the Mindlin-Reissner thick plate theory is associated with one translational (deflection) DoF and two rotational DoF's. However, RS3 plate elements are modified to take into account the membrane stresses and to eliminate shear locking effects on the linear plate element based on Tessler formulation (Tessler, 1991).

The Standard liner used was defined following elastic properties as the liners in RS3 are assumed to have isotropic elastic properties and, thus, only a single Young's Modulus and a single Poisson's ratio are needed for the model. The liner was modelled to simulate concrete and thus the Young's Modulus and Poisson's ratio values were the same as the concrete. Figure 3.8 below shows a plate element in RS3.

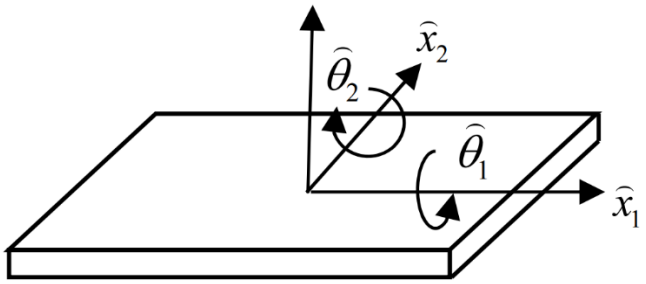

Figure 3.8: Geometric representation of a plate element in RS3

In RS3 formulation, $\hat{\theta}_1$ is defined as the rotation about $\hat{x}_1$ (x) axis, and $\hat{\theta}_2$ represents rotation about $\hat{x}_2$ (y) axis. This notation is different from other references (Owen & Hinton, 1980). When a thick plate element is analysed, it is analysed through the mid-plane of the plate as shown in Figure 3.9.

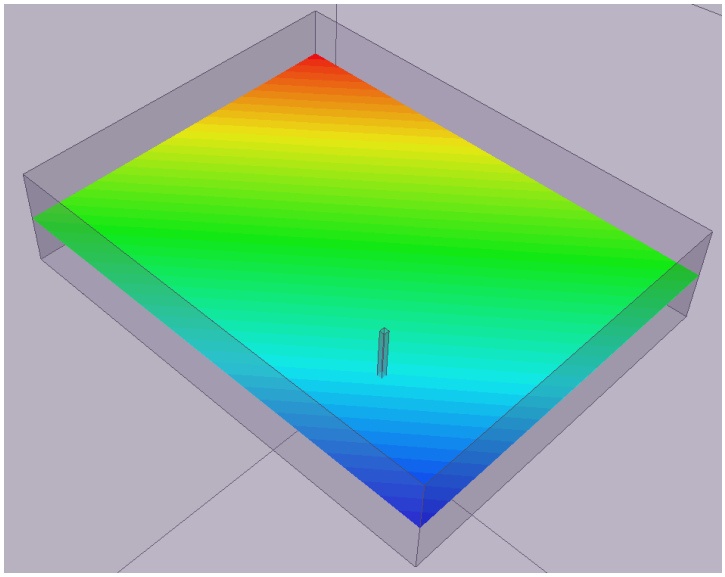

Figure 3.9: Plate element analysed through mid-surface

3.4.4 Loading

Two loading geometries were modelled and their settlements and deflections were compared.

3.4.4.1 Point load at an eccentricity

The top structure of the bridge pier is loaded by horizontal forces and bending moments. Since it is not possible to insert bending moments in the RS3 software, the bending moment is transferred into a vertical force at an eccentricity (lever arm) with respect to the centre of the footing. Thus, the first loading geometry was to apply the resultant load at an eccentricity to the footing as a point load which makes the modelling process simpler. The load eccentricity was calculated using Equation 18 in Section 2.3.4. The eccentricity in the "z" direction was calculated to be 2.24m and the eccentricity in the "y" direction was calculated to be -1.83m for the SLS load case provided in Table 3.1.

As a consequence of the RS3 software only allowing point loads to be applied to a vertex (where two lines or edges of an external body meet), the load could not be added to the eccentric point on the footing surface. In order to apply a load at an eccentricity, a separate solid element was created at the point of eccentricity and a stress applied. To model a point load, the element had a geometry of 0.1x0.1x2m, hence, the vertical applied stress was applied to the surface of 0.1m x 0.1m. This eccentrically placed element can be seen in Figure 3.10 and a three-dimensional view of the element inside the foundation as shown in Figure 3.11. However, when using this method, the footing has to be modelled as a rigid element, with $E = 1*10^6$ GPa, or else stress concentrations would develop at the point of loading and the model would not yield accurate results.

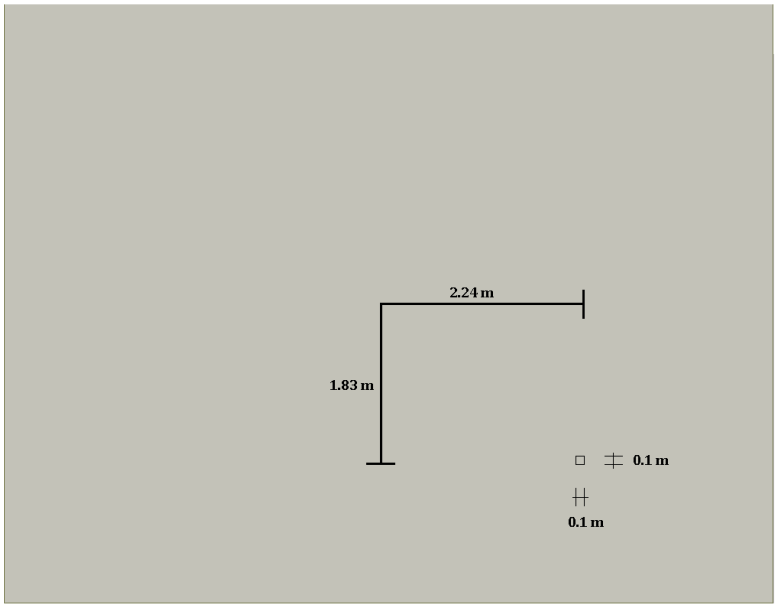

Figure 3.10: Eccentricity of element on foundation

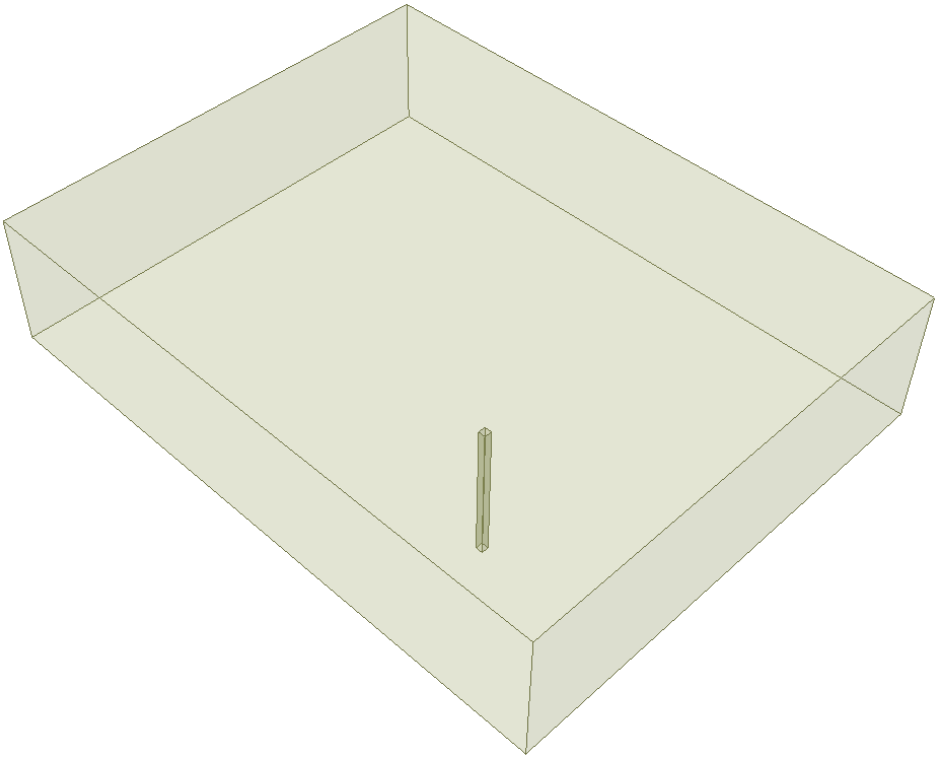

Figure 3.11: Eccentric element used as a surface to apply loading

3.4.4.2 Pier geometry

The second loading geometry was to model the pier and apply the loadings to the top of the pier. The pier was modelled with the same material parameters as the concrete footing with the exception that the stiffness was changed to $E = 1*10^6$ GPa to simulate a rigid material (to account for the straight lever arm of the moment), and the unit weight was changed to zero, as the vertical load had already accounted for the weight of the concrete pier. The model is shown in Figure 3.12.

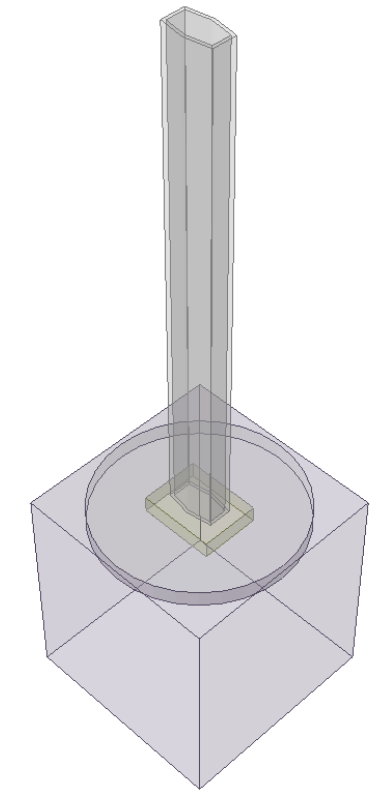

Figure 3.12: Model of loading applied to the top of the pier

3.4.5 Model restraints

The "Auto Restrain (Surface)" was used to automatically apply restraint boundary conditions to the model. With this option, the sides and the bottom of the external boundary were assigned XYZ restraints and the top surface (ground surface in most cases) was free. This means that the bottom and side boundaries of the model were not able to move in or rotate about the "X", "Y" or "Z" axes, but that the top surface

was able to move and rotate about any axis. This option was chosen because the volume of rock material surrounding the foundation was large enough that the effects of the foundation on the rock would not have influenced the boundary elements. Thus, no elements would be restricted to move. The boundary conditions can manually be assigned, but that was not considered necessary if the boundary is far enough from the foundation to prevent interaction.

3.4.6 Discretization

A graded mesh containing ten-noded tetrahedral elements was used to discretize the model. The ten-noded quadratic tetrahedral element has 10 nodes with three degrees of freedom at each node. This yields a total of 30 degrees of freedom (DoF) per element.

3.5 Prokon Frame Finite Element Model

Prokon Frame Analysis was used in this research as the software is widely used in industry, easily available and simple to learn. Prokon Frame Analysis performs frame and finite element analyses of two-dimensional and three-dimensional structures.

The model setup consisted of defining nodes, creating shells within the nodes, specifying footing material properties, adding supports (springs) and applying nodal loads. The first step was to define nodes and create four shell/plate elements with thickness of t = 0.01m within the nodes as shown in Figure 3.13.

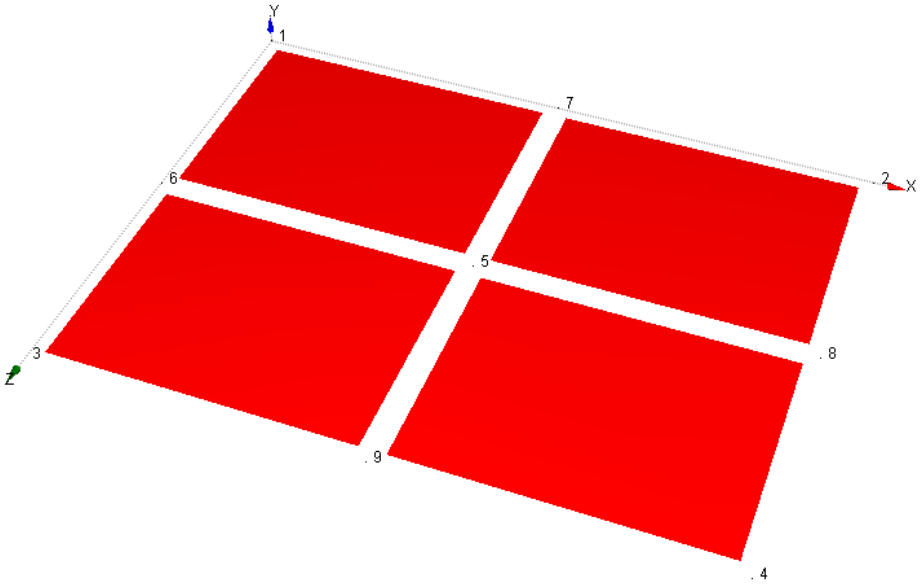

Figure 3.13: Model of footing in Prokon Frame Analysis

Thereafter, 40 MPa concrete material was chosen with a Poisson's ratio of v = 0.2, a unit weight of γ = 25 kN/m^3 and the footing assumed to have a rigid stiffness. Thereafter, nodal supports were inserted at node 5 in the form of springs (discussed in Section 3.8) to model the underlying rock mass. Lastly, the nodal loads in Table were inserted at node 5. Node 5 is shown in Figure 3.14.

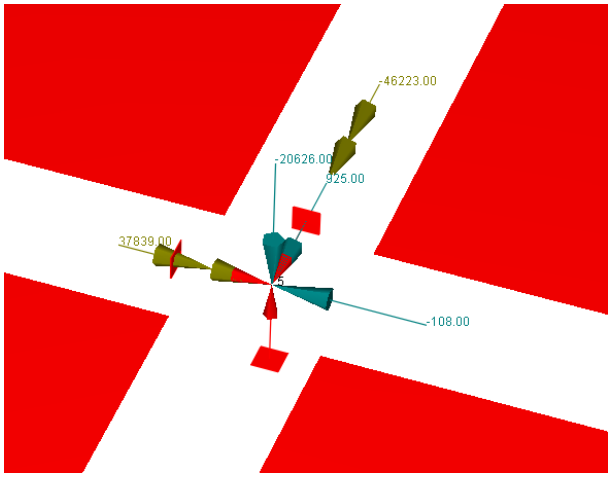

Figure 3. 14: Loads and springs applied to node 5 in Prokon Frame Analysis

Once the foundation system was modelled, the model was computed and the settlements were obtained.

3.6 Testing stiffness

Spread footings are designed for loads supported by individual columns with the leading factor for this design being the soil pressure beneath the footing. Magade and Ingle (2019) concluded that this contact stress distribution is a function of the footing settlement. Experiments carried out by Lemmen, Jacobsz and Kearsley (2017) on the influence of foundation stiffness on the behaviour of surface strip foundations determined that the relative stiffness of the foundation system affects the contact stress distribution and the deflection beneath the foundation. They concluded that the contact stress distribution beneath a concentrically loaded rigid foundation on dense sand is approximately uniform as no deflection occurs. Whereas, a reduction in the foundation stiffness induces bending and thus reduces the contact stress distribution at the edges of the footing. While this is true for dense sands, the outcome is not certain for footings founded on rock.

To determine the effect the footing stiffness has on the deflection, which contributes to the contact stress distribution, two models were created. The models were identical in every way besides the footing stiffness varied from 30 to $1x10^6$ GPa, modelling both the scenarios discussed in 3.4.4.2– one footing was classified as rigid and the other more flexible. The foundation system stiffness parameter K_s was calculated for the two models using Equation 2.23 in Section 2.4.1.1. For the E = 30 GPa footing, the system stiffness was calculated to be:

$$K_s = \left(\frac{1}{12}\right)\left(\frac{30}{10.8}\right)\left(\frac{2}{7}\right)^3 = 0.0054$$

For the E = 1e+06 GPa footing, the system stiffness was calculated to be:

$$K_s = \left(\frac{1}{12}\right)\left(\frac{1e+06}{10.8}\right)\left(\frac{2}{7}\right)^3 = 180$$

Table 2.3 in Section 2.4.1.1 was used to classify the footings system stiffness's. The 30 GPa footing was classified as semi-flexible and the 1e+06 GPa footing was classified as rigid.

Each model's loading conditions included being loaded over the full area of the footing (Figure 3.3a) with only vertical stress to prevent moment distortion and being loaded following the pier geometry (Figure 3.3b). In addition, each model with each geometry was loaded with vertical stress, half of the vertical stress and double the vertical stress. This was done to determine the influence the loading magnitude, the footing stiffness and loading geometry has on the deflection of the footing. This testing procedure is summarised in Table 3.3:

Table 3.3: Foundation stiffness testing procedure

		Loading Geometry	
		UDL over footing area	UDL over pier geometry
System stiffness	Semi-flexible	Half Load	Half Load
		Load	Load
		Double load	Double load
	Rigid	Half Load	Half Load
		Load	Load
		Double load	Double load

Thereafter, the influence of rock stiffness on the deformation of the footing was investigated. This constituted the same load magnitude being applied onto the semi-flexible footing while the stiffness of the rock was changed as presented in Table 3.4. The results are presented in Chapter 4.

Table 3.4: Rock inputs for stiffness test

Rock Inputs					
Parameter	Symbol	Value			Unit
		Strong rock	Weaker rock	Weak rock	
Intact compressive strength	σ_{ci}	40.45	30	15	MPa
Geological Strength Index	GSI	65	52	40	
Intact rock modulus	E_i	17191.25	12750	6375	Mpa
Hoek Brown constants	m_b	9.168	5.763	3.754	
	s	0.02	0.005	0.001	
	a	0.502	0.505	0.511	
Deformation modulus	E_{rm}	10860.046	4408.867	1017.783	MPa
Dilation parameter	β	0	4.5	0	
Residual Hoek Brown constants	m_r	1	15	1.877	
	s_r	0	0	0	
	a_r	0.5	0.5	0.5	

3.7 Comparing solid element to plate element

As previously mentioned in Section 3.4.3.2, the footing was modelled as a solid element and as a standard thick plate element. This was done in order to compare the outputs, as both elements are used for specific outputs. The solid element will imitate the behaviour of the footing more accurately whereas structural forces within the footing can be obtained when using a plate element. The standard liner used had a stiffness E = 1e+12 kPa, a Poisson's ration ν = 0.2, a thickness of 2m and a unit weight of 24.5kN/m^3 (same as rigid concrete footing). According to the element range in Figure 2.20 in Section 2.4.2.1, the plate element used, according to footing dimensions in Section 3.3, would be considered as a thick shell (d/L = 2/9 = 0.22). Hence, shear stresses are developed through the thickness of the element. Each model was computed using two loading geometries, the first being the model with the eccentric element (Figure 3.11), and the second being the model where the pier is taken into consideration (Figure 3.12). The loading conditions summarised in Table 3.1 were applied to these models. Deflections of the models were taken at the points shown in Figure 3.15 and compared with each other.

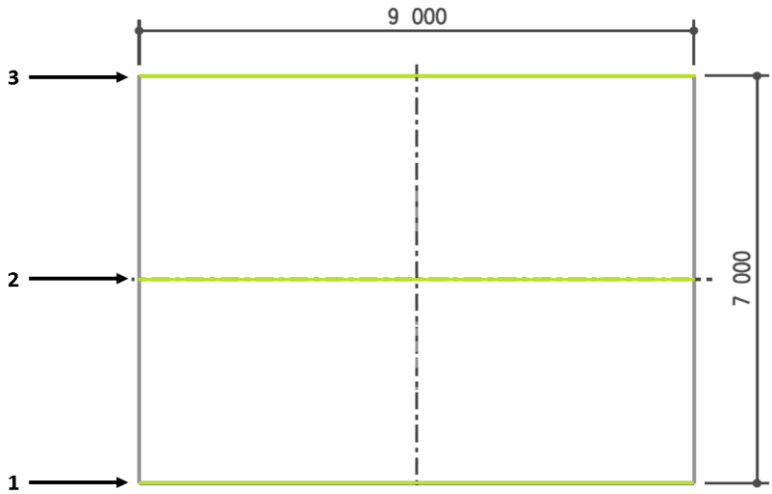

Figure 3.15: Sections where deflection readings were obtained

3.8 Derived springs from RS3

As discussed in Section 2.5, during the iteration process, the structural engineer gives the geotechnical engineer a load set that is inserted into the geotechnical model to determine the settlement whilst the rock properties are used to calculate the allowable bearing capacity. Thereafter, new springs are calculated and given to the structural engineer. This section will show the derivation of the equations used to calculate the new springs.

The loads in Table 3.1 were inserted into the RS3 model. As stated in the TMH7 Part 3 (1989), the footing was assumed to be rigid, with the loading applied to the top of the column as shown in Figure 3.12 in Section 3.4.5. A solid structural element was used for the footing and the rock mass properties used are described in Table 3.2. The model was run and the vertical- and lateral movements were computed. Thereafter, the settlements at the bottom four corners and the middle of the footing (at points A, B, C, D and E), as well as the lateral movements in the middle of the footing, were recorded using query lines as shown in Figure 3.16. The axis system in Figure 3.4 in Section 3.3 was used.

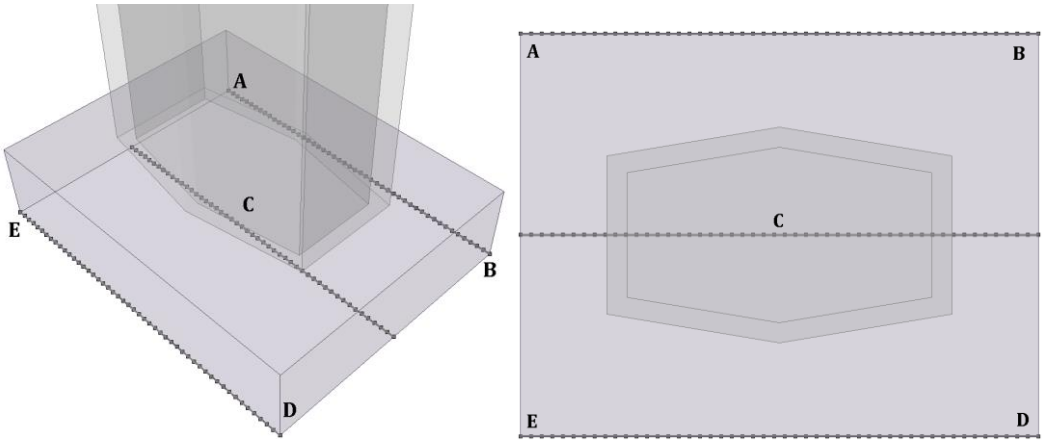

Figure 3.16: Query lines on which movements were taken

Once the settlements were obtained from the RS3 computation, the vertical-, lateral- and rotational springs were derived. The vertical spring k_v (in kN/m) was derived by dividing the vertical load applied to the footing, by the vertical settlement at point C δ_{cv} as shown in Equation 28.

$$k_v = \frac{N_x}{\delta_{cv}} \tag{28}$$

The lateral springs in the z- and y- directions (in kN/m) are similarly derived by dividing the lateral load applied to the footing (in the respective direction) by the lateral movement in the same direction at point C δ_{cz} and δ_{cy} – as shown in Equation 29 and Equation 30 respectively.

$$k_z = \frac{V_z}{\delta_{cz}} \tag{29}$$

$$k_y = \frac{V_y}{\delta_{cy}} \tag{30}$$

Thereafter, the rotational springs around the respective axes are derived. The rotational spring around the z-axis $k_{\phi z}$ (in kN.m/rad) was derived by dividing the

applied moment about the z-axis by the average angle of rotation ϕ_z in the direction of the applied moment (as the moment is causing the rotation). The average angle of rotation about the z-axis ϕ_z (in radians) is derived using Equation 31.

$$\phi_z = tan^{-1}\left[\frac{\left(\frac{(\delta_A - \delta_E) + (\delta_B - \delta_D)}{2}\right)}{B}\right] \tag{31}$$

The rotational spring around the z-axis $k_{\phi z}$ is calculated using Equation 32.

$$k_{\phi z} = \frac{M_z}{\phi_z} \tag{32}$$

The rotational spring around the y-axis $k_{\phi y}$ (in kN.m/rad) was derived in a similar method to that of the z-axis, and was derived by dividing the applied moment about the y-axis by the average angle of rotation ϕ_y in the direction of the applied moment (as the moment is causing the rotation). The average angle of rotation about the y-axis ϕ_y (in radians) is derived in a similar method to that of the z-axis using Equation 33.

$$\phi_y = tan^{-1}\left[\frac{\left(\frac{(\delta_A - \delta_B) + (\delta_E - \delta_D)}{2}\right)}{L}\right] \tag{33}$$

The rotational spring around the y-axis $k_{\phi y}$ is calculated using Equation 34.

$$k_{\phi y} = \frac{M_y}{\phi_y} \tag{34}$$

Once the springs have been derived, they are inserted as the nodal supports at node 5 in the Prokon Frame structural FE model – to confirm that the springs derived

will give accurate results in the structural engineer's model. The Prokon Frame model is then computed and the nodal movements recorded as an output. These vertical settlements and lateral movements at the points A, B, C, D and E are then compared to those obtained from the RS3 geotechnical FE model.

3.9 Synthesis

The methodology section presented the project overview as well as case study that was used in the research, along with an outline of how the RS3 and Prokon Frame finite element model were setup. In addition, the testing procedures used to achieve consistency in the modelling process for the geotechnical engineer were outlined. These testing procedures act as a preparation to determine how the geotechnical models are setup in order for the foundation settlements to yield realistic results. The foundation movements were then used to derive springs to be inserted into the Prokon Frame structural finite element model. The deflection outputs computed from the Prokon Frame model were compared to those of the RS3 geotechnical model to determine if convergence was reached.

Chapter 4: Results and Discussion

4.1 Introduction

This chapter presents the results obtained from the RS3 geotechnical and Prokon Frame structural finite element models of bridge spread foundations on rock, described in Section 3. The objective of the setup of the models is to achieve convergence between the settlement and displacement outputs of the models; to decide on a suitable constitutive model to accurately imitate the rock mass behaviour; and then to determine the rock parameters needed as an input into the RS3 model. The next step was to determine if the footing was to be modelled as a rigid element or a flexible element, and to decide what outputs are needed and accordingly choose a suitable structural element to model the footing. Once these components have been determined, the RS3 settlement outputs were used to derive structural springs, which were then used as supports in the structural model to model the rock. Finally, the models' outputs will be compared with the intention of achieving convergence in the results.

4.2 Rigid footing versus flexible footing

When modelling the footing with the realistic material stiffness of E = 30 GPa using the point load method, stress concentrations occur at the point of loading. Thus, using this simplified method requires the footing to have a rigid stiffness in order for the footing to show accurate settlement values. Figure 4.1 shows how using a semi-flexible (realistic stiffness) footing will not deliver accurate settlement results as a consequence of stress concentrations. The deflections were taken along the footing length beneath the stress application. Figure 4.1 presents the settlements of the semi-flexible and the rigid footings using the simplified point load method described in Section 3.4.4.1.

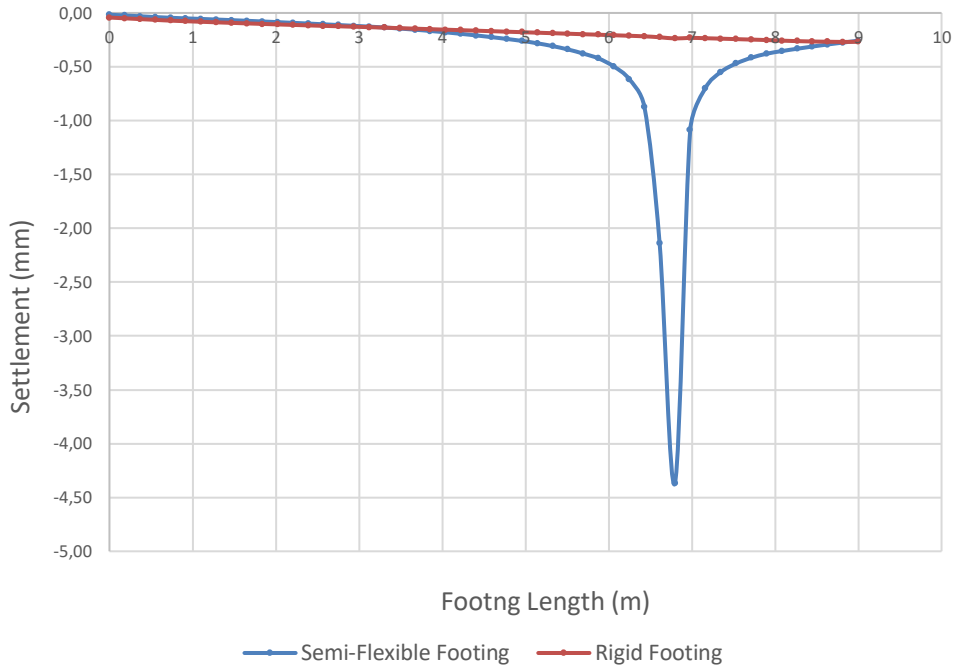

Figure 4.1: Settlements of semi-flexible- and rigid footings using the simplified point load method

Figure 4.1 confirms that when the simplified point load method is used, the footing must be rigid to obtain accurate settlements or else stress concentrations will occur at the point of load application if a flexible foundation is used. Numerical output values are included in Appendix F.1. Figure 4.2 visually shows the stress concentrations by presenting the deflection outputs.

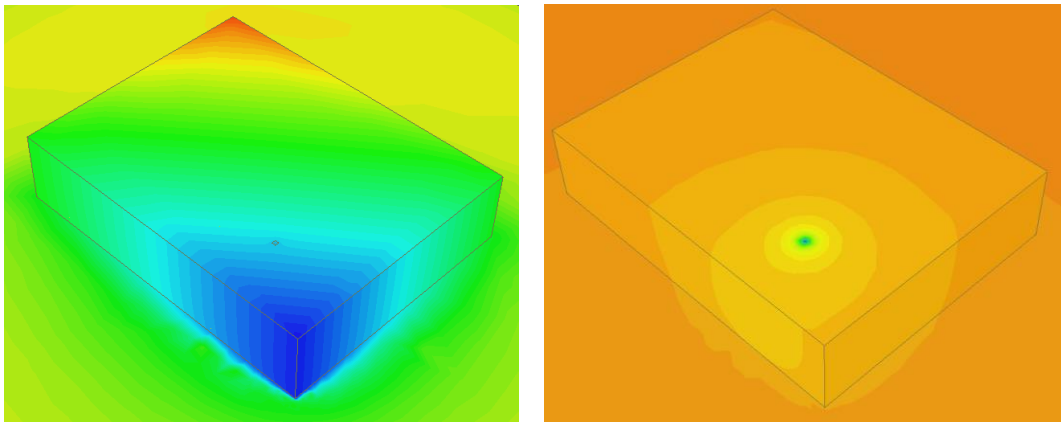

(a) **(b)**

Figure 4.2: Stress concentration visually shown for (a) rigid footing, (b) flexible footing

4.3 Foundation stiffness

The purpose of determining the effects of foundation stiffness, was to determine if the contact stress distribution beneath the spread footing was a function of the properties of the footing and of the underlying rock. Additionally, the deflection of the footing, depending on the system stiffness, can determine where the maximum bending moment occurs and where steel reinforcement should be situated within the footing during construction. The load geometry and magnitude details are presented in Table 4.1 for the pier and the footing respectively.

Table 4.1: Load geometry details

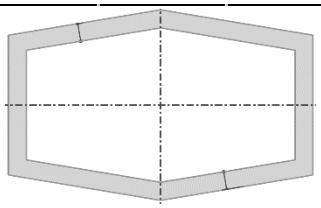	Area	3.4	m^2
	Vertical load	20626	kN
	UDL	6066.5	kPa
	Half UDL	3033.25	kPa
	Double UDL	12133	kPa
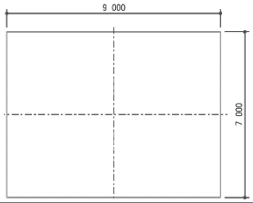	Area	63	m^2
	Vertical load	20626	kN
	UDL	327.4	kPa
	Half UDL	163.7	kPa
	Double UDL	654.8	kPa

The deformation graph presented in Figure 4.3 is a comparison between the loadings on a semi-flexible footing and a rigid footing through the centre of the footing, with the stress applied over the entire footing area.

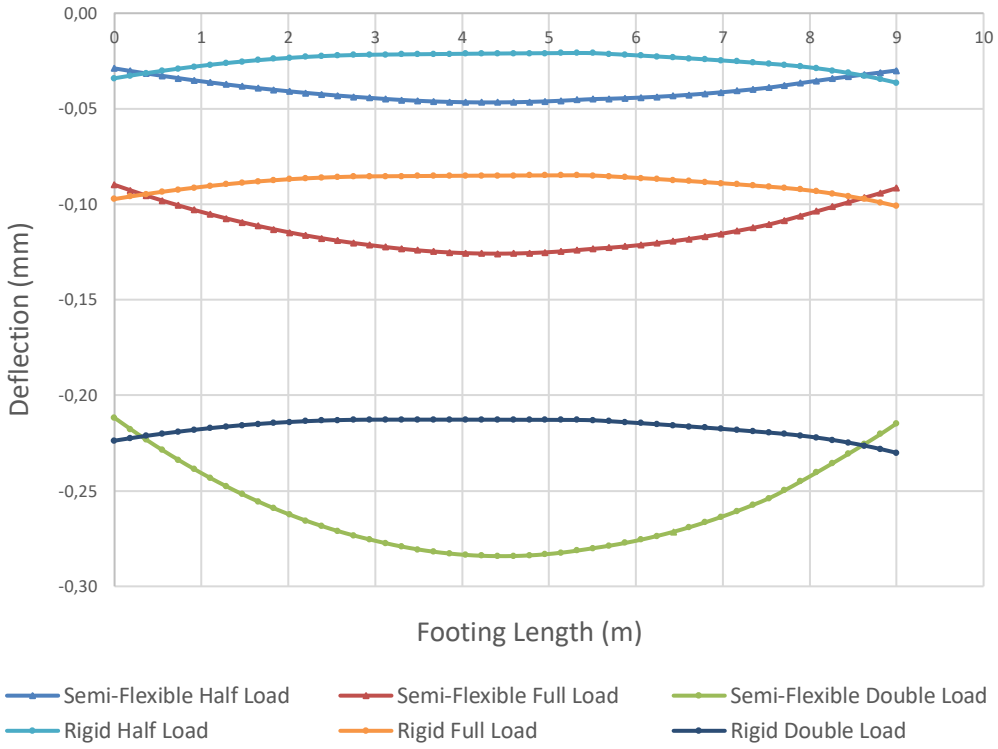

Figure 4.3: Deflection of semi-flexible vs rigid footing loaded on footing geometry

Figure 4.3 illustrates the deflection of the semi-flexible and the rigid footing for three loading magnitudes. It can be seen with the semi-flexible footings that less settlement occurs at the edges of the footing, which will result in a lower contact stress at the edges of the footing than in the middle because the pressure the footing exerted on the rock has become more concentrated at the middle of the footing (higher deflection). It is also observed that the rigid footing settles relatively uniformly in comparison to the semi-flexible footing. Since the difference in footing deflection between the rigid and semi-flexible footing is in the order of 0.3mm for a 2m thick footing, it is almost negligible. Another observation was that the higher the load magnitude applied to the footing, the more flexible the footing behaves on hard rock. Numerical output values are included in Appendix F.2.

The next deformation graph presented in Figure 4.4 is a comparison between the loading on a semi-flexible footing and a rigid footing, with the stress applied over

the area of the pier to assess the effect of the pier's geometry on the behaviour of the foundation.

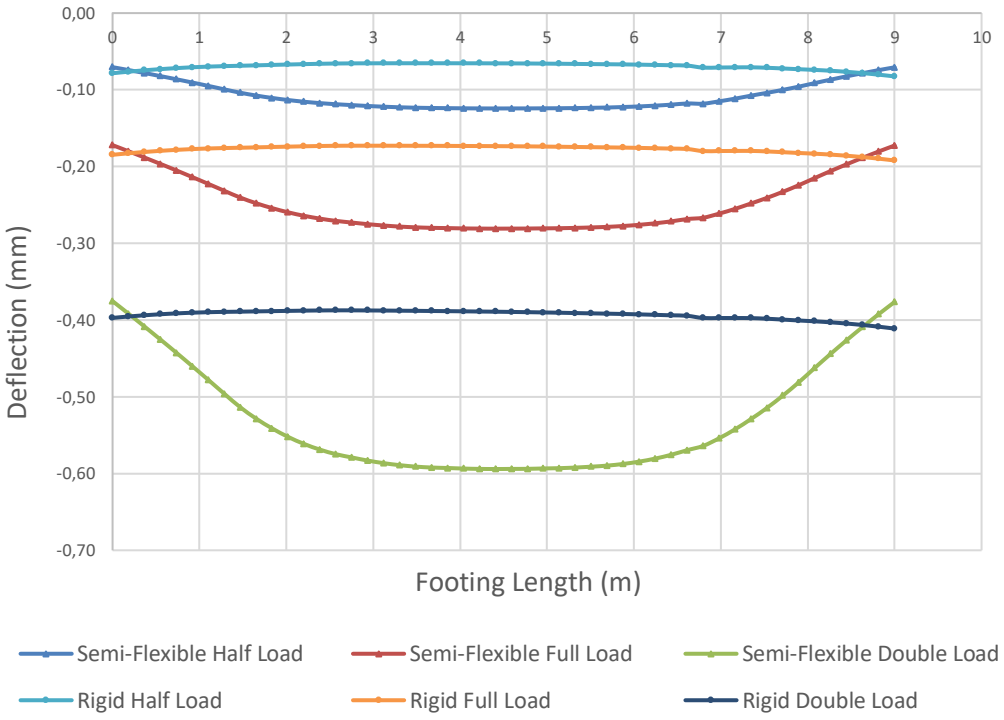

Figure 4.4: Deflection of semi-flexible vs rigid footing loaded on the pier geometry

The same can be observed for the pier geometry in Figure 4.4 as was observed in Figure 4.3 for the footing geometry. The one exception is that the deflection is higher for the semi-flexible footing due to the stress application area being smaller and therefore more concentrated. This illustrates that a higher load concentration and magnitude result in the semi-flexible footing experiencing a higher total deflection, while the rigid footing experiences a higher total settlement but very small distortion. Numerical output values are included in Appendix F.3.

The next deformation graph presented in Figure 4.5 is a comparison between the stress applied over the area of the pier and the stress applied over the area of the footing for the semi-flexible footing.

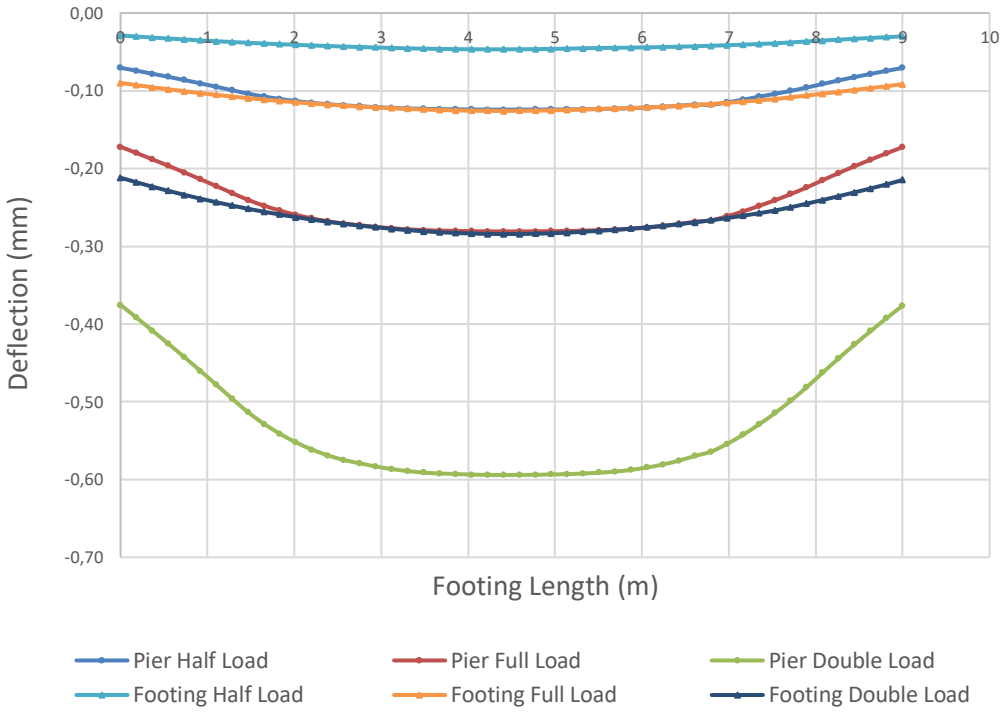

Figure 4.5: Deflection of flexible footing

Figure 4.5 shows that the more concentrated the stress is over an area, the more flexible the foundation behaves for this example. However, the largest deflection case was for the pier with a double load applied to it, which had a deflection of 0.25mm over a 9m span – a very small percentage. Numerical output values are included in Appendix F.4.

The next deformation graph presented in Figure 4.6 is a comparison between the stress applied over the area of the pier and the stress applied over the area of the footing for the rigid footing.

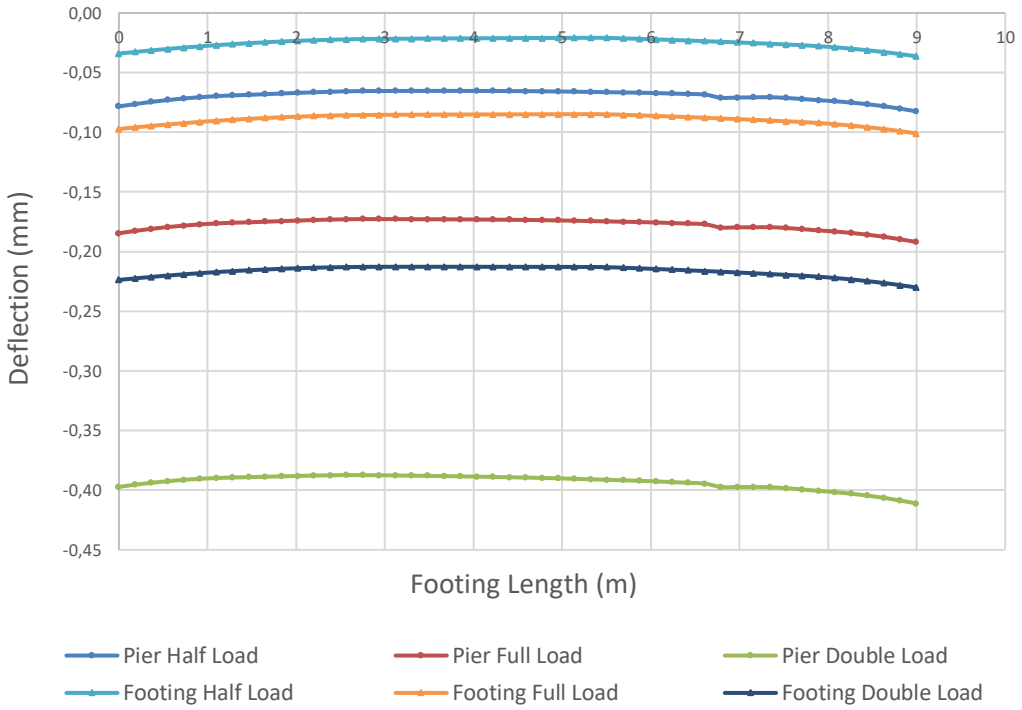

Figure 4.6: Deflection of rigid footing

Figure 4.6 illustrates that neither the load magnitude nor concentration effects the deformation of the rigid footing. However, the rigid footing does behave in a slightly convex shape which shows that there is an effect on the footing, but the effect is negligible. As previously stated, it was observed that the magnitude of the loading and the loading geometry only effects the settlement for a rigid footing. However, the difference in settlement between the full pier load and the full footing load is within 0.1mm and thus considered negligible for this example. Numerical output values are included in Appendix F.5.

Due to the geometry of the column not being square or rectangular, the K_r value described in Section 2.4.1.2 was not valid and the column parameters required needed to be square- or rectangular shaped. However, the K_s value described in Section 2.4.1.1 was used to assess whether the foundation system was rigid or flexible. This concept will be further discussed in Section 4.4.

The methods of loading the footings were also compared. The simplified point load method and the pier geometry method were analysed and compared. As previously stated in Section 4.2, when using the simplified point load method, the footing must be analysed as rigid or else stress concentrations occur. However, when modelling the pier geometry, the footing can also be considered rigid or it can be considered semi-flexible – thus, imitating the behaviour more realistically. Figure 4.7 compares the deflections through the centre of the footing modelled, using the simplified point load method and by modelling the pier with the loading conditions presented in Table 3.1 in Section 3.3. The simplified point load method was modelled using a rigid footing and the pier loading was modelled using both rigid and semi-flexible conditions.

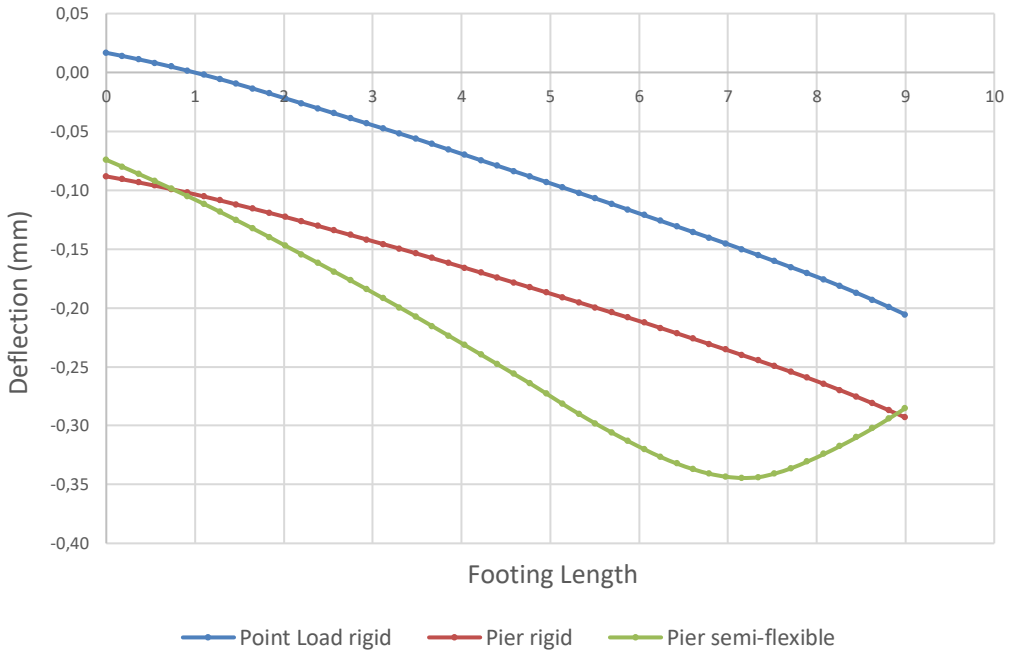

Figure 4.7: Deflections of loading geometries

As expected, the semi flexible foundation loaded on the pier shows deflection at the eccentricity where the point load would have been applied if the simplified point load method was used. Also, as expected, both rigid footings show no deflection. However, the rigid footing, loaded on the pier, has settled more than the rigid

footing loaded using the simplified point load method – thus, showing that using the simplified point load method will yield slightly less conservative results. Due to the deflection difference between the two loaded pier models being 0.1mm over a 2m depth and 9m span, it is safe to assume that the flexible conditions can be used when applying the loading to the pier. Numerical output values are included in Appendix F.6.

It can further be said that if the footing behaves in a flexible manner, springs provided to the structural engineer should rather be derived using displacements on the edges of the pier – instead of at the edges of the foundation since the maximum deflection would be beneath the edges of the pier and not the edges of the footing.

4.4 Rock stiffness

Additionally, the influence of rock stiffness on the deformation of the footing was investigated – as this is theoretically the only parameter that can influence the behaviour as concrete's stiffness cannot be $E = 1 \times 10^6$ GPa in reality. This involved the same vertical stress (full load) being applied to the pier geometry on the semi-flexible footing, while the stiffness of the rock was changed. The rock parameters were summarised in Table 3.4 in Section 3.6. Figure 4.8 compares the displacement at the centre of the footing with the displacement at the edge of the footing at different rock stiffnesses to determine the influence of rock stiffness on the flexibility of the footing.

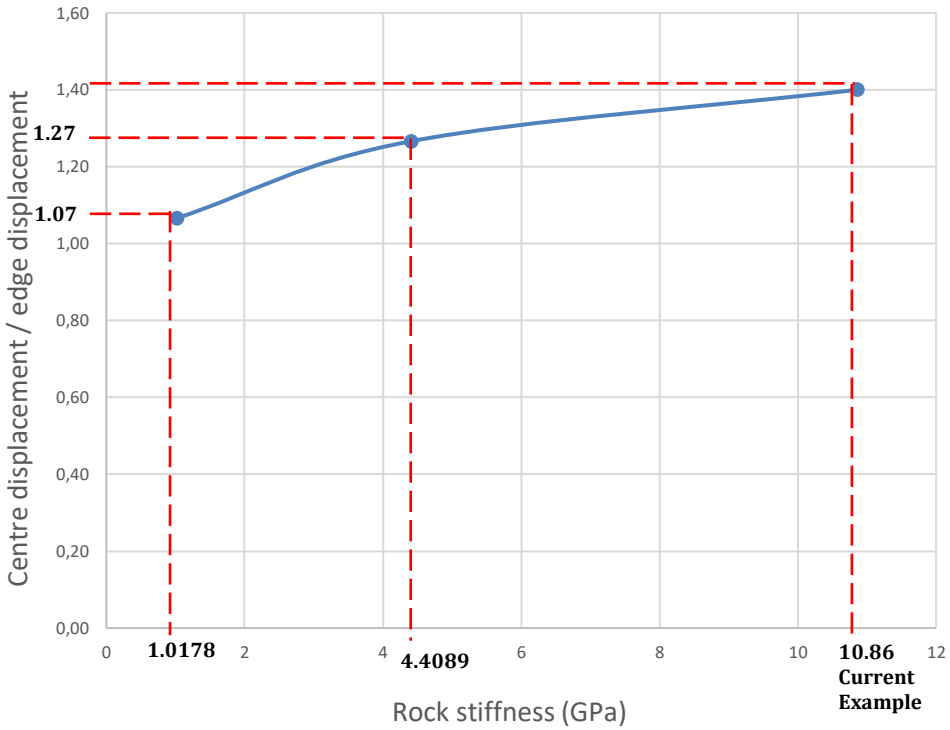

Figure 4.8: Influence of rock stiffness vs footing flexibility

The vertical axis of Figure 4.8 represents a ratio of the maximum deflection of the footing over the minimum deflection of the footing. Figure 4.8 illustrates that the stiffer the rock material, the more flexible the footing behaves.

The South African Bridge Design Code, TMH7 Part 3 (1989), states, however, that when the base is loaded eccentrically while designing bridge foundation, it may be assumed that the contact stress will vary linearly across the base and thus, the base can be assumed to act as a rigid element. This also shows that the simplified method, with an applied 'point load' at an eccentricity, might not be valid and the flexibility of the foundation should be checked before using such method. However, with the knowledge gained from this study, consideration should be given in the designation of steel reinforcement for the footing depending on how stiff the rock is. The stiffer the rock, the more reinforcement should be inserted at the point of maximum deflection.

As previously discussed in Section 4.3, the K_s value was used to assess if the foundation system could be classified as rigid or flexible. Using the rock stiffnesses and flexibility observations in Figure 4.8, the foundation system was assessed using the K_s value. Using a stiffness of 30 GPa for the typical footing and the stiffness of the strong rock (E = 10.86 GPa), K_s = 0.0054, which is classified as semi-flexible according to Table 2.3 in Section 2.4.1.2. Using the same footing stiffness with the weaker rock (E = 4.4089 GPa), K_s = 0.013, which is classified as semi-rigid. Lastly, using the same footing stiffness with the weakest rock (E = 1.0178 GPa), K_s = 0.057, which is also classified as semi-rigid. This method is accurate and can be used to determine foundation system stiffness. However, if more detail into foundation stiffness is required, it is not advised to use this simple hand calculation, but to rather model the footings with a vertical uniform stress applied.

4.5 Solid element versus plate element

The purpose of deciding what element to use for modelling the footing is to save time during computation, to determine structural forces within the element and to obtain the most accurate results from the model. The solid- and plate element models were computed using two loading geometries – the first being the simplified point load method (Figure 3.11), and the second being the model where the pier is taken into consideration (Figure 3.12).

As explained in Section 3.7, the comparison between the rigid solid elements at section 1 (P1), section 2 (P2) and section 3 (P3) on the footing for both load geometry models are displayed in Figure 4.9.

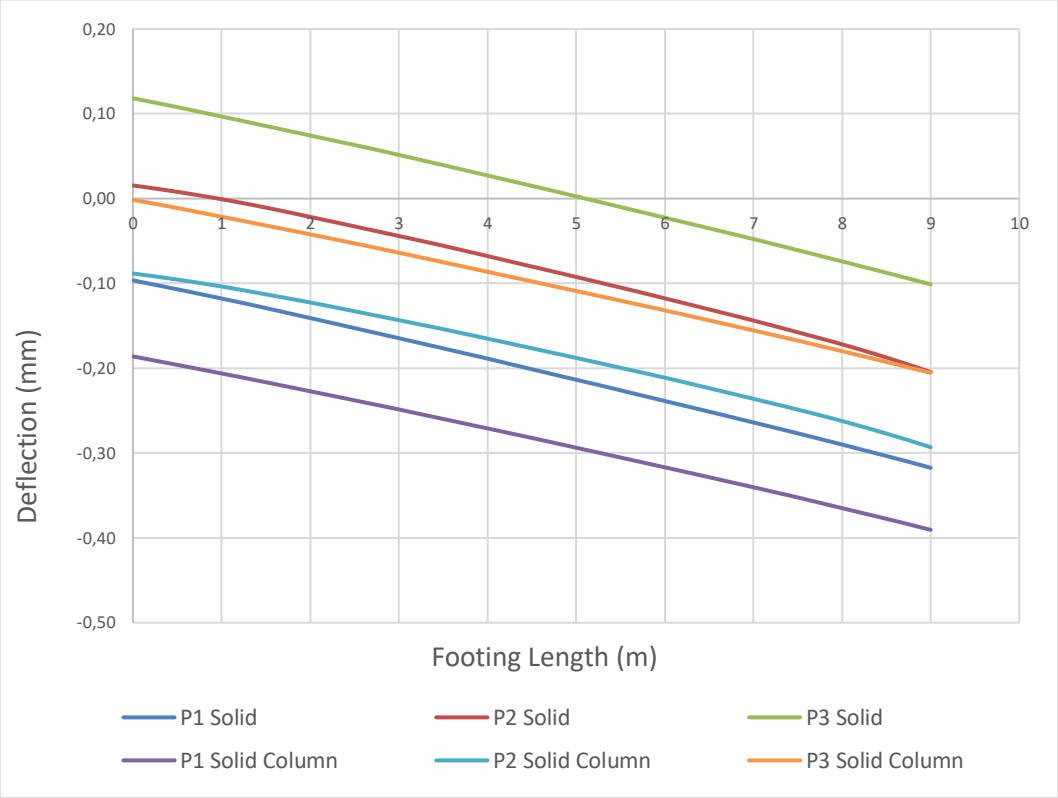

Figure 4.9: Solid element comparison for two load geometries

It is observed that both models do not deflect due to the rigid behaviour of the footings. The model with the pier experienced a higher settlement, whereas the model without the pier experienced more uplift.

As explained in Section 3.7, the comparison between the plate elements at point 1 (P1), point 2 (P2) and point 3 (P3) on the footing for both load geometry models are displayed in Figure 4.10.

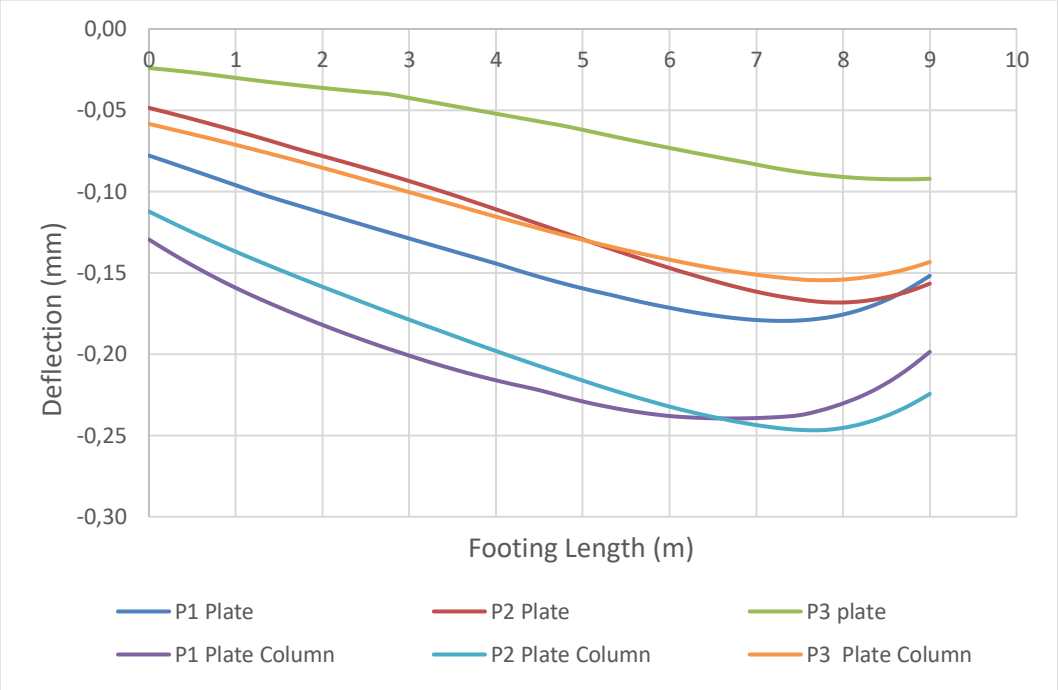

Figure 4.10: Plate element comparison for two load geometries

It is observed that the plate elements show deflection and do not settle uniformly even though it possess a rigid nature. It can be seen that where the plate elements are experiencing more pressure (closer to point 3 because of eccentric loading), there is more deflection. This could be due to the sidewall shear experienced by the plate elements as RS3 would not allow the plate to stand alone, but had to be supported around the edges by the rock. However, just like the solid elements, the model with the pier experienced a higher settlement, which results in similar settlement profiles.

It is observed from Figure 4.9 and Figure 4.10 that both the solid and plate elements have similar settlements in the order of 0.1mm difference. Thus, both elements are suitable for use depending on what outcome is required. It should be noted that the computation for the models containing plate elements were more time strenuous than the models containing the solid elements. The models using solid structural elements computed in under one minute, whereas the models using plate elements were in excess of four minutes. This contradicts the literature as plate elements are

typically used for faster computation, however, the thick plate elements in RS3 take longer to compute. In addition, the models containing the solid elements show more consistency in settlement and deformation in comparison to the plate elements. Therefore, the solid elements not only give more accurate deflection results, but uses less time to compute as well. On the other hand, if structural forces are required, plate elements, unlike solid elements, are able to provide structural forces.

4.6 Comparison of FE models springs

After the foundation system was modelled using RS3 geotechnical FEM and the settlements and lateral movements were obtained, the vertical-, lateral- and rotational springs were derived using the equations derived in Section 3.8. The derived springs were then inserted into the Prokon Frame structural FEM and the nodal settlements were obtained. Thereafter, the outputs were compared to establish if the proposed equations used to derive springs are adequate. The settlements and lateral movements obtained from the RS3 model are presented in Table 4.2.

Table 4.2: Settlements and lateral movements obtained from the RS3 model

RS3 Model	
Vertical displacements (mm)	
Point A	-0,002
Point B	-0,21
Point C	-0,18
Point D	-0,39
Point E	-0,19
Lateral displacements at Point C (mm)	
z-axis	0,01
y-axis	0,01

The springs derived using the settlements and lateral movements obtained from the RS3 model are presented in Table 4.3

Table 4.3: Derived spring values

Springs			
Description	Symbol	Value	Unit
Vertical Spring in X	k_v	116,9	GN/m
Horizontal Spring in Z	k_z	8	GN/m
Horizontal Spring in Y	k_y	69,2	GN/m
Rotational Spring around Z	$k_{\phi z}$	1431,4	GN.m/rad
Rotational Spring around Y	$k_{\phi y}$	2039,4	GN.m/rad

The springs were inserted as nodal supports into the Prokon Frame structural FE model, and the nodal settlements obtained after computation are summarised in Table 4.4.

Table 4.4: Settlements and lateral movements obtained from the Prokon Frame model

Prokon Frame Model	
Vertical displacements (mm)	
Point A	0.02
Point B	-0.19
Point C	-0.18
Point D	-0.37
Point E	-0.17
Lateral displacements at Point C (mm)	
z-axis	0.01
y-axis	0.01

When the settlement values of the models are compared, it is observed that the settlements differ with less than 10% from each other, most of them less than 5%. The exception is that Point A does not differ with less than 10% but if the values are compared, it is calculated that the difference is δ_v = 0.02mm, which is in the order of micro mm. This could be a result of Prokon Frame not giving values to the third or fourth decimal as is done in RS3. However, being within a 10% (Poeppel & Syngros, 2014) difference bracket or differing within a couple of micro mm is

acceptable knowing that the actual displacements will never be 100% the same since spring values were derived using average footing rotations.

4.7 Guideline for geotechnical engineer

This guideline was developed to assist the geotechnical engineer when analysing bridge spread foundations on rock using finite element analysis as a numerical modelling tool. This guideline should be followed by the geotechnical engineer to assist in the iteration process that takes place between the structural and geotechnical engineer.

Step 1: Calculate allowable bearing capacity of the rock and send to the structural engineer to determine footing sizing.

Step 2: Geotechnical engineer receives loadset from the structural engineer.

Step 3: Assess rigidity of the footing. This is done by:

1. Less accurate hand calculated method:
    a. Calculating the K_s value to determine if the foundation system behaves in a rigid or flexible manner according to Equation 23, as described in Section 2.4.1.1.

OR

2. More accurate Finite Element method:
    a. Derive rock parameters by hand or using *RocLab* and use an appropriate constitutive model.
    b. Set the footing stiffness to E = 30GPa or that of the specified concrete strength.

c. Convert the vertical applied load given by the structural engineer to a vertical uniformly distributed stress over the entire footing area using the following equation: $\sigma = \frac{N}{B*L}$
d. Use a solid structural element to model the footing to best imitate reality, however, if structural forces are required within the element, use a plate structural element to model the footing.
e. From the output of the vertical deflection graph, calculate the ratio of centre displacement/edge displacement for the footing. If the ratio is 1.0, the foundation system behaves in a rigid manner. If the ratio is larger or smaller than 1.0, the foundation system behaves in a flexible manner.

If the foundation system behaves in a rigid manner, the simplified point load method can be used (assume *E* = 1x106 GPa) to analyse the foundation as described in Section 3.4.4.1. Thereafter, derive springs according to Section 3.8, using the vertical and lateral displacement results from the edges- and middle of the footing.

OR

If the foundation system behaves in a flexible manner, the entire geometry of the pier should be added to the model (assumed *E* = ±30 GPa) to analyse the foundation. Thereafter, derive springs according to Section 3.8, using vertical and lateral displacement results from the edges of the pier.

Step 4: Provide derived springs to the structural engineer.

The structural engineer will provide new loads to the geotechnical engineer.

Step 5: Repeat Step 3 and 4 until convergence between the structural and geotechnical FE models is achieved. Convergence is reached in two ways:

1. When the changes in the moment and the axial load values (received from the structural engineer) are within 10% difference from the previous loadset (also received from the structural engineer).
2. When the derived spring values are within 10% difference from the spring values derived in the previous iteration.

Chapter 5: Conclusions and Recommendations

5.1 Conclusions

In order to realise the objectives of this research as outlined in Section 1.4 and Section 1.5, different testing procedures and analyses were carried out as described in Section 3. This research aimed to compile a guideline for the geotechnical engineer to optimize the iteration process that takes place between the structural engineer and the geotechnical engineer when modelling the interaction between the structure and the rock for shallow bridge foundations. This was done by determining the settlements using RS3 geotechnical FEM and deriving spring values from the settlements to use in the Prokon Frame structural FEM to achieve convergence with the spring values.

This chapter highlights the main findings in this research:

- Rock is a non-linear material and, therefore, a suitable constitutive model was chosen in order to accurately imitate the rock mass behaviour in a numerical model. The Generalized Hoek-Brown failure criterion was chosen to model the rock. It was chosen based on its wide spread application in industry and accurate results.
- A guideline on how to derive rock mass parameters using the Generalized Hoek-Brown failure criterion was stipulated using the *RocData* software (*RocLab* is more readily available) to determine the FEM material inputs.
- The system stiffness parameter K_s yields accurate results and can be used to classify the foundation system stiffness.
- The effect of rock stiffness on the foundation resulted in the foundation behaving in a more flexible manner, the higher the rock stiffness was. Conversely, the weaker the rock, the more rigid the foundation behaves.

- A simplified method of applying an eccentric loading was proposed and provided accurate results when the footing was assumed to be fully rigid with a stiffness of E = 1e+06 GPa. If the footing is not fully rigid, stress concentrations will occur at the point of load application.
- It was observed and confirmed that rigid footings undergo uniform settlement (when subjected to a uniformly distributed vertical applied load), with no deflection while the contact pressure beneath the footing is not linear.
- It was proved that if a footing is classified as rigid, the simplified point load method can be used to determine settlements, but when the footing is classified as flexible, the entire pier geometry will need to be modelled on a flexible footing (with a stiffness of E = ±30 GPa) to obtain realistic results.
- The difference in footing settlements between a solid structural element and a plate structural element was in the order of 0.1mm when used to model the footing. Thus, depending on the output required, either the solid or plate element can be used. Solid elements show more accurate behaviour of the footing, whereas a plate element can provide the structural forces within the footing that the solid element cannot.
- Spring values were derived from the settlements obtained in the RS3 model in order to use them in Prokon Frame to achieve convergence in the settlement values.
- The springs that were derived from the RS3 geotechnical FEM accurately model the rock material in the Prokon Frame structural FEM, as it was observed that the settlement values from the geotechnical model differ with less than 10% from the structural model.
- A guideline was developed to optimize the iteration process between the geotechnical- and structural engineer in order to assist the geotechnical engineer improve the consistency in the modelling of the interaction between the structure and the rock.

5.2 Recommendations

The following recommendations can be made for future research:

- The guidelines proposed in Section 4.7 should be used by practicing geotechnical engineers when modelling shallow bridge foundations on rock. The research used to develop the guideline will give the geotechnical engineer insight when modelling the interaction between bridge structures and shallow rock foundations.
- This research was limited to shallow bridge foundations, however, many bridge piers are supported by piled foundations. An extension to this research can be pursued by developing a guideline to assist the geotechnical engineer when modelling piled bridge foundations.
- When using any numerical software packages, ensure that help is available or that a seminar is attended to better educate the user on the software.
- There is future value in calibrating the FE models (RS3) against 'real life' situations such as laboratory modelling of shallow bridge foundations on rock or where site monitoring of the foundation settlement has occurred and using the information from the site tests.

List of References

AASHTO. 2002. *Standard specifications for highway bridges*. Seventeent ed. Washington, DC.

Akin, J.E. 2010. *Finite Element Analysis Concepts via SolidWorks*. Houston, Texas: World Scientific.

Algin, H.M. 2007. Practical formula for dimensioning a rectangular footing. *Engineering Structures*. 29(6):1128–1134.

Arnold, A., Laue, J., Espinosa, T. & Springman, S.M. 2010. Centrifuge modelling of the behaviour of flexible raft foundations on clay and sand. In Zurich: Taylor and Francis *International Conference on Physical Modelling in Geotechnics 2010: 28/06/2010-01/07/2010*. 679–684.

Baumann, R.A. & Weisgerber, F.E. 1983. Yield-line analysis of slabs-on-grade. *Journal of Structural Engineering*. 109(7):1553–1568.

Bieniawski, Z.T. 1989. *Engineering rock mass classifications: a complete manual for engineers and geologists in mining, civil, and petroleum engineering*. John Wiley & Sons Inc.

Bowles, J.E. 1996. *Foundation Analysis and Design*. Fifth ed. New York: McGraw-Hill Companies, Inc.

Bozozuk, M. 1978. Bridge abutments move. In Washington DC *Transportation Research Record*. 17–21.

Budavari, S. 1983. Response of the rock mass to excavations underground. *Rock Mechanics in Mining Practice. The South African Institute of Mining and Metallurgy Monograph Series M*. 5:55–76.

Canadian Foundation Engineering Manual. 2006. 4th ed. Richmond, BC, Canada: Canadian Geotechnical Society.

Cen, S. & Shang, Y. 2015. Developments of Mindlin-Reissner Plate Elements. *Mathematical Problems in Engineering*. 2015:1–12.

Chang, K.-H. 2016. Solid Modeling. In 1st ed. Academic Press *E-Design: Computer-Aided Engineering Design*. 124–165.

Chen, Q. & Yin, T. 2019. Should the Use of Rock Quality Designation Be Discontinued in the Rock Mass Rating System? *Rock Mechanics and Rock Engineering*. 52(4):1075–1094.

Chen, W. & Duan, L. 2014. *Bridge Engineering Handbook: Substructure Design*. Second ed. Taylor & Francis Group.

Committee of State Road Authorities. 1989. *TMH 7 Part 3: Code of Practice for the Design of Highway Bridges and Culverts in South Africa*. Pretoria, South Africa: Department of Transport.

Conniff, D.E. & Kiousis, P.D. 2007. Elastoplastic medium for foundation settlements and monotonic soil–structure interaction under combined loadings. *International Journal for Numerical and Analytical Methods in Geomechanics*. 31(March 2007):789–807.

Crowder, J. & Bawden, W. 2004. Review of Post-Peak Parameters and Behaviour of Rock Masses: Current Trends and Research. *Rocnews, fall*. (January 2004):1–14.

Day, P.W. 2018.

Deere, D.U. & Deere, D.W. 1988. The Rock Quality Designation (RQD) Index in Practice. In Louis Kirk ed. Philadelphia: American Society for Testing Materials *Rock Classification Systems for Engineering Purposes*. 91–101.

Edelbro, C. 2004. Evaluation of rock mass strength criteria. Luleå University of Technology.

Goodman, R.E. 1976. *Methods of Geological Engineering in Discontinuous Rocks*. 1st ed. USA: West Publishing Company.

Grover, R.A. 1978. Movements of bridge abutments and settlements of approach pavements in Ohio. In Vol. 678. Washington, DC *Transportation Research Record*. 12–17.

Hoek, E. 1983. Strength of jointed rock masses. *Géotechnique*. 23(3):187–223.

Hoek, E. 1994. Strength of rock and rock masses. *ISRM News Journal*. 2(2):4–16.

Hoek, E. 2001. Rock mass properties for underground mines. *Underground mining methods: engineering fundamentals and international case studies*. 21:1–21.

Hoek, E. & Brown, E.T. 1980. Empirical Strength Criterion for Rock Masses. *Journal of Geotechnical and Geoenvironmental Engineering*. 106(ASCE 15715):1013–1035.

Hoek, E. & Brown, E.T. 1988. The Hoek-Brown Failure Criterion - a 1988 Update. In Toronto: Dept. Civil Engineering, University of Toronto *Proc. 15th Canadian Rock Mech. Symp*. 31–38.

Hoek, E. & Diederichs, M.S. 2006. Empirical estimation of rock mass modulus. *International Journal of Rock Mechanics and Mining Sciences*. 43(2):203–215.

Hoek, E., Wood, D. & Shah, S. 1992. A modified Hoek-Brown failure criterion for jointed rock masses. In Chester, UK: Thomas Telford Publishing *Rock Characterization: ISRM Symposium, Eurock'92, Chester, UK, 14-17 September 1992*. 209–214.

Hoek, E., Kaiser, P.K. & Bawden, W.F. 1995. *Support of underground excavations in hard rock*. Rotterdam, Balkema: CRC Press.

Hoek, E., Marinos, P. & Benissi, M. 1998. Applicability of the geological strength index (GSI) classification for very weak and sheared rock masses. The case of the Athens Schist Formation. *Bulletin of Engineering Geology and the Environment*. 57(2):151–160.

Hoek, E., Carranza, C. & Corkum, B. 2002. Hoek-brown failure criterion – 2002 edition. *Proceedings of the 5th North American Rock Mechanics Symposium dan 17th Tunnelling Association of Canada Conference*. 1(1):267–273.

Hussain, S., Rehman, Z.U., Mohammad, N., Tahir, M., Shahzada, K., Khan, S.W., Salman, M., Khan, M., et al. 2018. Numerical Modeling for Engineering Analysis and Designing of Optimum Support Systems for Headrace Tunnel. *Advances in Civil Engineering*. 2018:10.

Juvencio, E.L., Lopes, F.R. & Nunes, A.L.L.S. 2017. An evaluation of the shaft resistance of piles embedded in gneissic rock. *Soils and Rocks*. 40(1):61–74.

Kuusisto, E. 2017. *SHELLS vs. SOLIDS | Finite Element Analysis Quick Review*. [Online], Available: https://www.linkedin.com/pulse/shells-vs-solids-finite-element-analysis-quick-review-kuusisto-p-e- [2019, October 14].

Lees, A. 2016. *Geotechnical Finite Element Analysis*. First ed. London: ICE Publishing.

Lemmen, H.E., Jacobsz, S.W. & Kearsley, E.P. 2017. The influence of foundation stiffness on the behaviour of surface strip foundations on sand. *Journal of the South African Institution of Civil Engineering*. 59(2):19–27.

Magade, S.B. & Ingle, R.K. 2019. Numerical method for analysis and design of isolated square footing under concentric loading. *International Journal of Advanced Structural Engineering*. 11(1):9–20.

Marinos, P. & Hoek, E. 2001. Estimating the geotechnical properties of heterogeneous rock masses such as Flysch. *Bulletin of engineering geology and the environment*. 60(2):85–92.

Marinos, P.G. & Hoek, E. 2000. GSI: A geologically friendly tool for rock mass strength estimation. *ISRM International Symposium 2000, IS 2000*. 19. [Online], Available: https://www.scopus.com/inward/record.uri?eid=2-s2.0-85053872276&partnerID=40&md5=ef31c2afcd1687017146f793a31b7e91.

Matula, M. & Holzer, R. 1978. Engineering topology of rock masses. In *Proceedings of Felsmekanik Kolloquium, Grundlagen ung Andwendung der Felsmekanik, Karls-ruhe, Germany*. 107–121.

Merritt, F.S. 1976. *Standard Handbook for Civil Engineers*. New York: McGraw-Hill.

van der Merwe, A. 2019.

Meyerhof, G.G. 1953. Some recent foundation research and its application to design. *Struct. Eng.* 31(6):151–167.

Owen, D.R.J. & Hinton, E. 1980. *Finite Elements in Plasticity: Theory and Practice*. Swansea, U.K.: Pineridge Press Limited.

Palmstrom, A. 1995. RMI-a rock mass characterization system for rock engineering purposes. Norway: Oslo University.

Poeppel, A.R. & Syngros, K. 2014. Soil-Foundation-Superstructure Interaction for the Tallest Tower in the World: The Kingdom Tower. In *ASCE 27th Central PA Geotechnical Conference, Hershey, PA*.

Ponnuswamy, S. 2008. *Bridge Engineering*. Second ed. McGraw-Hill Education.

Reddy, J.N. 1999. *Theory and Analysis of Elastic Plates and Shells*. CRC Press.

Rocscience. 2018. *Rock Mass Modulus*. [Online], Available: https://www.rocscience.com/help/rocdata/rocdata/Rock_Mass_Modulus.htm [2019, October 29].

Schneider, H. 1999. *Definition and determination of characteristic soil properties*. Vol. 4. Hamburg, Germany.

Shwetha, K. & Subrahmanya, V.B.P. 2018. Comparison Between Thin Plate And Thick Plate From Navier Solution Using Matlab Software. *International Research Journal of Engineering and Technology*. 5(6):2675–2680.

Singh, B. & Goel, R.K. 2011. *Engineering Rock Mass Classification: Tunneling, Foundations, and Landslides*. Waltham, USA: Butterworth-Heinemann.

Stavridis, L.T. 2010. Plate Theory. In *Structural systems: behaviour and design*. 11–52.

Steele, C.R. & Balch, C.D. 2009. *Introduction to the Theory of Plates Stretching and Bending of Plates - Fundamentals*. Stanford, USA.

Tabsh, S.W. & Al-shawa, A.R. 2005. Effect of Spread Footing Flexibility on Structural Response. *Practice Periodical on Structural Design and Construction*. 10(May):109–114.

Tarbuck, E.J. & Lutgens, F.K. 2005. *Earth: An Introduction to Physical Geology*. Eighth Edition (ed.). USA: Pearson Education Inc.

Tarbuck, E.J. & Lutgens, F.K. 2014. *Earth: An Introduction to Physical Geology*. Eleventh E ed. USA: Pearson Education Inc.

Tessler, A. 1991. A two-node beam element including transverse shear and transverse normal deformations. *International journal for numerical methods in engineering*. 32(5):32.

USACE. 2005. *Stability Analyses of Concrete Structures*. Vol. No. 1110-2. Washington, DC: U.S. Army Corps of Engineers.

Van der Merwe, A. (2019). *Structural engineer's first iteration*.

Walkinshaw, J.L. 1978. Survey of bridge movements in the western United States. In Vol. 678. Washington, DC *Transportation Research Record*. 8–12.

Westergaard, H.M. 1926. Stresses in concrete pavements computed by theoretical analysis. *Public roads*. 7:25.

Wyllie, D.C. 1999. *Foundations on Rock*. Second ed. Vancouver, Canada: E & FN Spon.

Zhan, Y. 2012. Modeling Beams on Elastic Foundations Using Plate Elements in Finite Element Method. *Electronic Journal of Geotechnical Engineering*. 17:2063–2068.

Zhang, X., Chen, Z. & Liu, Y. 2017. Constitutive Models. In Academic Press *The material point method: a continuum-based particle method for extreme loading cases*. 175–219.

Appendix A

A.1 Rock Mass Rating (RMR)

The following six parameters are used to classify rock masses in the RMR system:

1. Uniaxial compressive strength of intact rock material
2. Rock quality designation (RQD)
3. Discontinuity spacing
4. Condition of discontinuities
5. Groundwater conditions
6. Orientation of discontinuities

The ratings of the six parameters are presented in Tables A1 – A6:

Table A.1: Strength of intact rock material (Bieniawski, 1989)

Qualitative description	Compressive strength (Mpa)	Point Load Strength (Mpa)	Rating
Extremely strong	> 250	> 10	15
Very strong	100 - 250	4 - 10	12
Strong	50 -100	2 - 4	7
Fair	25 - 50	1 - 2	4
Weak	5 - 25	Uniaxial compressive strength is preferred	2
Very weak	1 - 5		1
Extremely weak	< 1		0

Intact rock from rock cores should be tested in UCS tests or PLI tests.

Table A.2: Rock Quality Designation (RQD) (Bieniawski, 1989)

Quality	RQD (%)	Rating
Very poor	90 - 100	20
Poor	75 - 90	17
Fair	50 - 75	13
Good	25 - 50	8
Excellent	< 25	5

RQD is discussed in Section 2.2.2.3.

Table A.3: Discontinuity spacing (Bieniawski, 1989)

Description	Spacing (m)	Rating
Very Wide	> 2	20
Wide	0.6 - 2	15
Moderate	0.2 - 0.6	10
Close	0.06 - 0.2	8
Very Close	< 0.06	5

The lowest rating of the discontinuity spacing sets should be considered. The term discontinuity incorporates joints, beddings or foliations, shear zones, faults or other surface of weakness (Edelbro, 2004).

Table A.4: Conditions of discontinuities (Bieniawski, 1989)

Condition of discontinuities	Rating
Very rough surfaces, not continuous, no separation, unweathered wall rock	30
Slightly rough surfaces, separation < 1mm, slightly weathered walls	25
Slightly rough surfaces, separation < 1mm, highly weathered wall	20
Slickensided surfaces OR gouge < 5mm thick OR separation 1 - 5mm, continuous	10
Soft gouge > 5mm thick OR separation > 5mm, continuous	0

The condition of the discontinuities includes roughness, length, weathering of wall rock, separation and infilling material.

Table A.5: Ground water conditions (Bieniawski, 1989)

General conditions	Rating
Completely dry	15
Damp	10
Wet	7
Dripping	4
Flowing	0

Ratings from Tables A1 – A5 are added together to calculate the RMR_{basic}.

Table A.6: Adjustment for discontinuity orientation (Bieniawski, 1989)

Strike and dip orientations of discontinuities	Ratings		
	Tunnels and mines	Foundations	Slopes
Very favourable	-12	-25	-60
Favourable	-10	-15	-50
Fair	-5	-7	-25
Unfavourable	-2	-2	-5
Very unfavourable	0	0	0

The rating adjustment obtained from Table A6 is added to the RMR_{basic} in order to calculate the total RMR.

Appendix B

B.1 Geological Strength Index (GSI)

Table B.1: GSI for characterisation of blocky rock masses based on particle interlocking and discontinuity condition (Hoek et al., 1998)

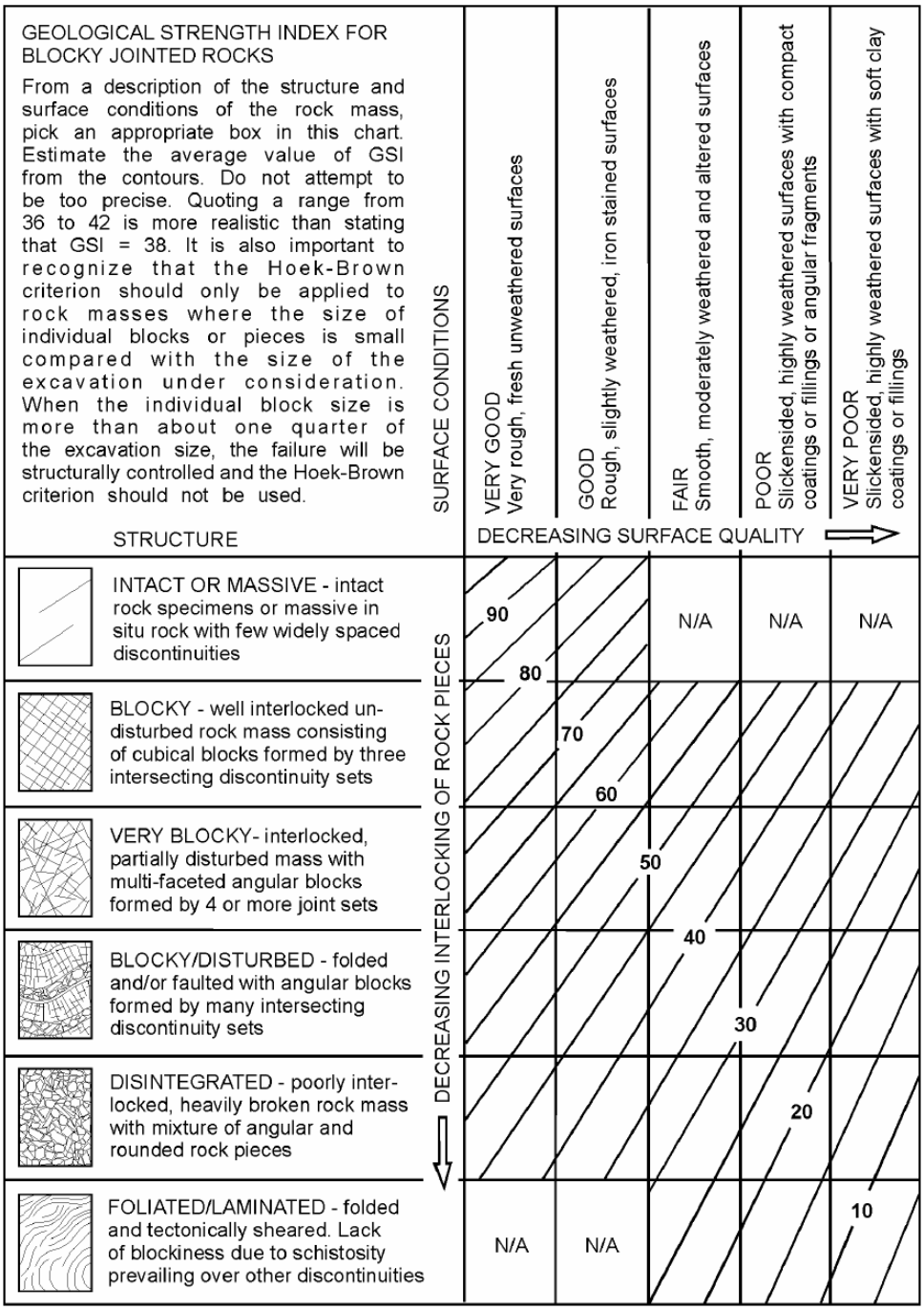

Table B.2: GSI characterisation of shistose metamorphic rock masses based on foliation and discontinuity condition (Hoek, 2001)

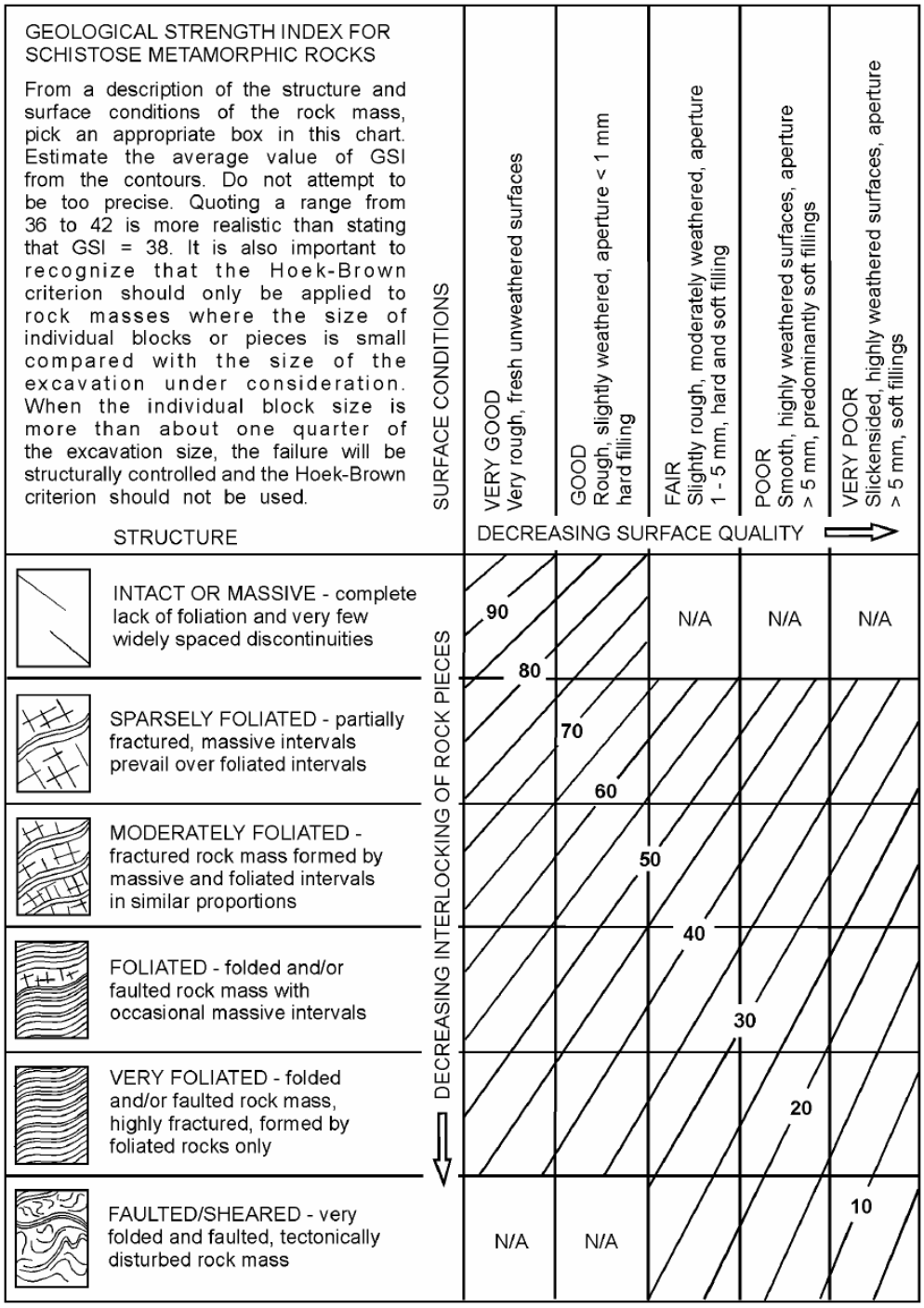

Appendix C

C.1 Generalized Hoek-Brown failure criterion

Table C.1: Field estimates of uniaxial compressive strength (Hoek, 2001)

Grade*	Term	Uniaxial Comp. Strength (MPa)	Point Load Index (MPa)	Field estimate of strength	Examples
R6	Extremely Strong	> 250	>10	Specimen can only be chipped with a geological hammer	Fresh basalt, chert, diabase, gneiss, granite, quartzite
R5	Very strong	100 - 250	4 - 10	Specimen requires many blows of a geological hammer to fracture it	Amphibolite, sandstone, basalt, gabbro, gneiss, granodiorite, peridotite , rhyolite, tuff
R4	Strong	50 - 100	2 - 4	Specimen requires more than one blow of a geological hammer to fracture it	Limestone, marble, sandstone, schist
R3	Medium strong	25 - 50	1 - 2	Cannot be scraped or peeled with a pocket knife, specimen can be fractured with a single blow from a geological hammer	Concete, phyllite, schist, siltstone
R2	Weak	5 - 25	**	Can be peeled with a pocket knife with difficulty, shallow indentation made by firm blow with point of a geological hammer	Chalk, claystone, potash, marl, siltstone, shale, rocksalt,
R1	Very weak	1 - 5	**	Crumbles under firm blows with point of a geological hammer, can be peeled by a pocket knife	Highly weathered or altered rock, shale
R0	Extremely weak	0.25 - 1	**	Indented by thumbnail	Stiff fault gouge

* Grade according to Brown (1981).
** Point load tests on rocks with a uniaxial compressive strength below 25 MPa are likely to yield highly ambiguous results.

Table C.2: Estimate values of the constant mi for intact rock (Hoek, 2001)

Rock type	Class	Group	Texture			
			Coarse	Medium	Fine	Very fine
SEDIMENTARY	Clastic		Conglomerates (21 ± 3) Breccias (19 ± 5)	Sandstones 17 ± 4	Siltstones 7 ± 2 Greywackes (18 ± 3)	Claystones 4 ± 2 Shales (6 ± 2) Marls (7 ± 2)
	Non-Clastic	Carbonates	Crystalline Limestone (12 ± 3)	Sparitic Limestones (10 ± 2)	Micritic Limestones (9 ± 2)	Dolomites (9 ± 3)
		Evaporites		Gypsum 8 ± 2	Anhydrite 12 ± 2	
		Organic				Chalk 7 ± 2
METAMORPHIC	Non Foliated		Marble 9 ± 3	Hornfels (19 ± 4) Metasandstone (19 ± 3)	Quartzites 20 ± 3	
	Slightly foliated		Migmatite (29 ± 3)	Amphibolites 26 ± 6		
	Foliated*		Gneiss 28 ± 5	Schists 12 ± 3	Phyllites (7 ± 3)	Slates 7 ± 4
IGNEOUS	Plutonic	Light	Granite 32 ± 3	Diorite 25 ± 5 Granodiorite (29 ± 3)		
		Dark	Gabbro 27 ± 3 Norite 20 ± 5	Dolerite (16 ± 5)		
	Hypabyssal		Porphyries (20 ± 5)		Diabase (15 ± 5)	Peridotite (25 ± 5)
	Volcanic	Lava		Rhyolite (25 ± 5) Andesite 25 ± 5	Dacite (25 ± 3) Basalt (25 ± 5)	Obsidian (19 ± 3)
		Pyroclastic	Agglomerate (19 ± 3)	Breccia (19 ± 5)	Tuff (13 ± 5)	

* These values are for intact rock specimens tested normal to bedding or foliation. The value of m_i will be significantly different if failure occurs along a weakness plane.

Appendix D

D.1 Rotational spring derivation

The rotational springs used by structural engineers for an internal iteration, before providing loads to the Geotechnical Engineers using only k_s values from Table 2.4, can be derived using force equilibrium. This can be seen in Figure D.1.

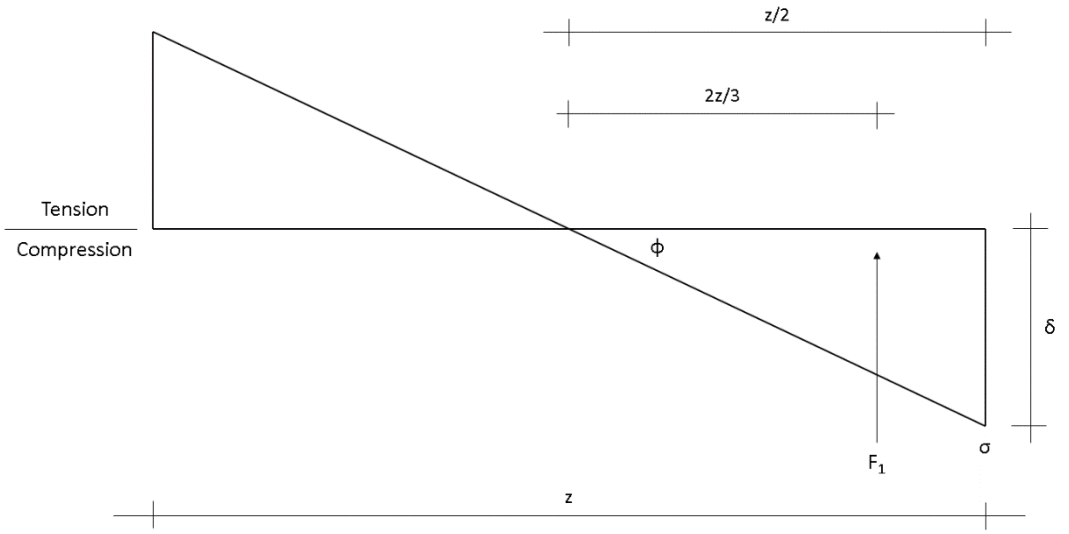

Figure D.1: Rotational spring derivation

Where the deflection in meters is calculated using Equation 28:

$$\delta = \phi\left(\frac{z}{2}\right) \tag{28}$$

With ϕ being the rotation angle in radians and z being the length over which there is rotation in meters.

The force F1 can be calculated using Equation 29.

$$F_1 = \frac{1}{2}\left(\frac{z}{2}\right)(\sigma)$$

$$F_1 = \frac{1}{4}\, z\, \sigma \tag{29}$$

Where σ is the magnitude of the applied stress in kN/m^2. Thereafter the moment can be calculated using Equation 30. The nature of a structural spring is that it cannot go into tension, thus, the half in tension changes to compression.

$$M = 2\,(F_1)\,(\frac{2}{3} \times \frac{z}{2})$$

$$M = \frac{2}{3}\, F_1\, z \tag{30}$$

Equation 29 is substituted into Equation 30.

$$M = \frac{1}{6}\,(\sigma)\,(z^2)$$

The modulus of subgrade reaction in Equation 22, in Section 2.4.1.1, is substituted.

$$M = \frac{1}{6}\, k_s\, \delta\, z^2$$

Thereafter Equation 28 was substituted into the above equation. Thus, the rotational spring stiffness is calculated using Equation 27 in Section 2.6.

$$Rotational\ spring\ stiffness = \frac{1}{12}\, k_s\, \phi\, z^3$$

Appendix E

E.1 Cautious estimate method

The UCS data was obtained from rock cores extracted from boreholes on site. Two UCS values were obtained from different sections of the borehole closest to the footing considered. In order to get a representative value of the UCS data, a cautious estimate was calculated. Firstly, the average of the 2 values was obtained and thereafter the standard deviation. The cautious estimate was calculated by subtracting half the standard deviation σ from the average value μ as shown in Equation 31 (Schneider, 1999). This was done so that the least conservative (inferior) value would be obtained and designed for.

$$Cautious\ estimate = \mu - 0.5\sigma \tag{31}$$

The superior value (i.e. +0.5*σ) will be better to use in determination of the rigidity. With the upper UCS value in the rock core being 48.7 MPa and the lower 39.09 MPa, the average was calculated to be 43.9 MPa and the standard deviation to be 6.8 MPa. Using Equation 31, the cautious estimate of the intact compressive strength σ_{ci} was calculated to be 40.45 MPa.

Appendix F

F.1 Stress concentration output

Distance [m]	Deflection (mm)	
	Flexible Footing	Rigid Footing
0,000	-0,016	-0,043
0,184	-0,024	-0,050
0,367	-0,031	-0,057
0,551	-0,038	-0,064
0,735	-0,045	-0,071
0,918	-0,050	-0,077
1,102	-0,056	-0,082
1,286	-0,061	-0,087
1,469	-0,067	-0,092
1,653	-0,073	-0,097
1,837	-0,079	-0,102
2,020	-0,085	-0,107
2,204	-0,092	-0,111
2,388	-0,098	-0,115
2,571	-0,105	-0,120
2,755	-0,112	-0,124
2,939	-0,120	-0,128
3,122	-0,127	-0,132
3,306	-0,135	-0,136
3,490	-0,145	-0,141
3,673	-0,156	-0,146
3,857	-0,167	-0,151
4,041	-0,180	-0,155
4,224	-0,194	-0,160
4,408	-0,209	-0,165
4,592	-0,225	-0,169
4,776	-0,242	-0,174
4,959	-0,260	-0,179
5,143	-0,282	-0,183
5,327	-0,308	-0,188
5,510	-0,339	-0,193
5,694	-0,377	-0,198
5,878	-0,423	-0,202
6,061	-0,497	-0,207
6,245	-0,614	-0,212
6,429	-0,871	-0,217
6,612	-2,138	-0,226
6,796	-4,368	-0,237
6,980	-1,086	-0,231
7,163	-0,698	-0,235
7,347	-0,549	-0,239
7,531	-0,470	-0,243
7,714	-0,417	-0,247
7,898	-0,379	-0,252
8,082	-0,354	-0,257
8,265	-0,333	-0,262
8,449	-0,312	-0,265
8,633	-0,293	-0,267
8,816	-0,275	-0,269
9,000	-0,257	-0,268

F.2 Deflection of semi-flexible vs rigid footing loaded on footing geometry

Distance [m]	Deflection (mm)					
	Semi-Flexible Half Load	Semi-Flexible Full Load	Semi-Flexible Double Load	Rigid Half Load	Rigid Full Load	Rigid Double Load
0,000	-0,029	-0,090	-0,212	-0,034	-0,097	-0,224
0,184	-0,030	-0,093	-0,218	-0,033	-0,096	-0,222
0,367	-0,032	-0,095	-0,223	-0,031	-0,095	-0,221
0,551	-0,033	-0,098	-0,229	-0,030	-0,093	-0,220
0,735	-0,034	-0,101	-0,234	-0,029	-0,092	-0,219
0,918	-0,035	-0,103	-0,239	-0,028	-0,091	-0,218
1,102	-0,036	-0,105	-0,243	-0,027	-0,090	-0,217
1,286	-0,037	-0,107	-0,248	-0,026	-0,090	-0,216
1,469	-0,038	-0,109	-0,252	-0,025	-0,089	-0,216
1,653	-0,039	-0,111	-0,256	-0,025	-0,088	-0,215
1,837	-0,040	-0,113	-0,259	-0,024	-0,087	-0,214
2,020	-0,041	-0,115	-0,263	-0,023	-0,087	-0,214
2,204	-0,042	-0,116	-0,266	-0,023	-0,086	-0,214
2,388	-0,042	-0,118	-0,268	-0,022	-0,086	-0,213
2,571	-0,043	-0,119	-0,271	-0,022	-0,086	-0,213
2,755	-0,044	-0,120	-0,273	-0,022	-0,086	-0,213
2,939	-0,044	-0,121	-0,275	-0,022	-0,085	-0,213
3,122	-0,045	-0,122	-0,277	-0,022	-0,085	-0,213
3,306	-0,045	-0,123	-0,279	-0,022	-0,085	-0,213
3,490	-0,046	-0,124	-0,281	-0,021	-0,085	-0,213
3,673	-0,046	-0,125	-0,282	-0,021	-0,085	-0,213
3,857	-0,046	-0,125	-0,283	-0,021	-0,085	-0,213
4,041	-0,047	-0,126	-0,284	-0,021	-0,085	-0,213
4,224	-0,047	-0,126	-0,284	-0,021	-0,085	-0,213
4,408	-0,047	-0,126	-0,284	-0,021	-0,085	-0,213
4,592	-0,047	-0,126	-0,284	-0,021	-0,085	-0,213
4,776	-0,046	-0,126	-0,284	-0,021	-0,085	-0,213
4,959	-0,046	-0,125	-0,283	-0,021	-0,085	-0,213
5,143	-0,046	-0,125	-0,282	-0,021	-0,085	-0,213
5,327	-0,045	-0,124	-0,281	-0,021	-0,085	-0,213
5,510	-0,045	-0,123	-0,280	-0,021	-0,085	-0,213
5,694	-0,045	-0,123	-0,279	-0,021	-0,085	-0,214
5,878	-0,044	-0,122	-0,277	-0,022	-0,086	-0,214
6,061	-0,044	-0,121	-0,276	-0,022	-0,086	-0,215
6,245	-0,044	-0,120	-0,274	-0,023	-0,087	-0,215
6,429	-0,043	-0,119	-0,271	-0,023	-0,087	-0,216
6,612	-0,043	-0,118	-0,269	-0,024	-0,088	-0,216
6,796	-0,042	-0,117	-0,267	-0,024	-0,088	-0,217
6,980	-0,041	-0,115	-0,264	-0,025	-0,089	-0,218
7,163	-0,041	-0,114	-0,261	-0,025	-0,090	-0,218
7,347	-0,040	-0,112	-0,257	-0,026	-0,090	-0,219
7,531	-0,039	-0,111	-0,254	-0,026	-0,091	-0,220
7,714	-0,038	-0,108	-0,250	-0,027	-0,091	-0,220
7,898	-0,037	-0,106	-0,245	-0,028	-0,092	-0,221
8,082	-0,035	-0,104	-0,240	-0,029	-0,093	-0,222
8,265	-0,034	-0,101	-0,236	-0,030	-0,094	-0,223
8,449	-0,033	-0,099	-0,231	-0,031	-0,096	-0,225
8,633	-0,032	-0,097	-0,225	-0,033	-0,097	-0,226
8,816	-0,031	-0,094	-0,220	-0,034	-0,099	-0,228
9,000	-0,030	-0,092	-0,215	-0,036	-0,101	-0,230

F.3 Deflection of semi-flexible vs rigid footing loaded on the pier geometry

Distance [m]	Deflection (mm)					
	Semi-Flexible Half Load	Semi-Flexible Full Load	Semi-Flexible Double Load	Rigid Half Load	Rigid Full Load	Rigid Double Load
0,000	-0,070	-0,172	-0,375	-0,078	-0,185	-0,397
0,184	-0,074	-0,180	-0,392	-0,076	-0,183	-0,395
0,367	-0,078	-0,188	-0,408	-0,075	-0,181	-0,394
0,551	-0,082	-0,197	-0,425	-0,073	-0,179	-0,392
0,735	-0,086	-0,205	-0,443	-0,072	-0,178	-0,391
0,918	-0,090	-0,214	-0,460	-0,071	-0,177	-0,390
1,102	-0,095	-0,223	-0,478	-0,070	-0,176	-0,390
1,286	-0,099	-0,232	-0,496	-0,069	-0,176	-0,389
1,469	-0,104	-0,240	-0,514	-0,069	-0,175	-0,389
1,653	-0,107	-0,248	-0,528	-0,068	-0,175	-0,389
1,837	-0,111	-0,254	-0,541	-0,068	-0,174	-0,388
2,020	-0,113	-0,260	-0,552	-0,067	-0,174	-0,388
2,204	-0,115	-0,264	-0,561	-0,066	-0,174	-0,388
2,388	-0,117	-0,268	-0,569	-0,066	-0,173	-0,387
2,571	-0,119	-0,271	-0,575	-0,066	-0,173	-0,387
2,755	-0,120	-0,273	-0,579	-0,066	-0,173	-0,387
2,939	-0,121	-0,275	-0,583	-0,065	-0,173	-0,387
3,122	-0,122	-0,277	-0,586	-0,065	-0,173	-0,388
3,306	-0,123	-0,278	-0,589	-0,065	-0,173	-0,388
3,490	-0,123	-0,279	-0,591	-0,065	-0,173	-0,388
3,673	-0,124	-0,280	-0,592	-0,065	-0,173	-0,388
3,857	-0,124	-0,280	-0,593	-0,065	-0,173	-0,388
4,041	-0,124	-0,281	-0,594	-0,065	-0,173	-0,389
4,224	-0,124	-0,281	-0,594	-0,065	-0,173	-0,389
4,408	-0,124	-0,281	-0,594	-0,065	-0,173	-0,389
4,592	-0,124	-0,281	-0,594	-0,066	-0,174	-0,389
4,776	-0,124	-0,281	-0,594	-0,066	-0,174	-0,390
4,959	-0,124	-0,280	-0,593	-0,066	-0,174	-0,390
5,143	-0,124	-0,280	-0,593	-0,066	-0,174	-0,390
5,327	-0,124	-0,280	-0,592	-0,066	-0,174	-0,391
5,510	-0,123	-0,279	-0,591	-0,066	-0,175	-0,391
5,694	-0,123	-0,279	-0,590	-0,067	-0,175	-0,392
5,878	-0,122	-0,277	-0,587	-0,067	-0,175	-0,392
6,061	-0,122	-0,276	-0,584	-0,067	-0,176	-0,393
6,245	-0,121	-0,274	-0,580	-0,068	-0,176	-0,393
6,429	-0,119	-0,271	-0,576	-0,068	-0,177	-0,394
6,612	-0,118	-0,268	-0,570	-0,068	-0,177	-0,394
6,796	-0,118	-0,267	-0,564	-0,071	-0,180	-0,397
6,980	-0,115	-0,261	-0,554	-0,071	-0,180	-0,397
7,163	-0,111	-0,255	-0,542	-0,071	-0,180	-0,397
7,347	-0,108	-0,248	-0,529	-0,071	-0,180	-0,397
7,531	-0,104	-0,241	-0,514	-0,071	-0,180	-0,398
7,714	-0,100	-0,233	-0,498	-0,072	-0,181	-0,399
7,898	-0,096	-0,224	-0,481	-0,073	-0,182	-0,401
8,082	-0,091	-0,215	-0,462	-0,074	-0,183	-0,402
8,265	-0,087	-0,206	-0,444	-0,075	-0,184	-0,403
8,449	-0,082	-0,197	-0,426	-0,077	-0,186	-0,405
8,633	-0,078	-0,188	-0,409	-0,078	-0,188	-0,406
8,816	-0,074	-0,180	-0,392	-0,080	-0,190	-0,409
9,000	-0,071	-0,173	-0,376	-0,083	-0,192	-0,411

F.4 Deflection of flexible footing

Distance [m]	Deflection (mm)					
	Pier Half Load	Pier Full Load	Pier Double Load	Footing Half Load	Footing Full Load	Footing Double Load
0,000	-0,070	-0,172	-0,375	-0,029	-0,090	-0,212
0,184	-0,074	-0,180	-0,392	-0,030	-0,093	-0,218
0,367	-0,078	-0,188	-0,408	-0,032	-0,095	-0,223
0,551	-0,082	-0,197	-0,425	-0,033	-0,098	-0,229
0,735	-0,086	-0,205	-0,443	-0,034	-0,101	-0,234
0,918	-0,090	-0,214	-0,460	-0,035	-0,103	-0,239
1,102	-0,095	-0,223	-0,478	-0,036	-0,105	-0,243
1,286	-0,099	-0,232	-0,496	-0,037	-0,107	-0,248
1,469	-0,104	-0,240	-0,514	-0,038	-0,109	-0,252
1,653	-0,107	-0,248	-0,528	-0,039	-0,111	-0,256
1,837	-0,111	-0,254	-0,541	-0,040	-0,113	-0,259
2,020	-0,113	-0,260	-0,552	-0,041	-0,115	-0,263
2,204	-0,115	-0,264	-0,561	-0,042	-0,116	-0,266
2,388	-0,117	-0,268	-0,569	-0,042	-0,118	-0,268
2,571	-0,119	-0,271	-0,575	-0,043	-0,119	-0,271
2,755	-0,120	-0,273	-0,579	-0,044	-0,120	-0,273
2,939	-0,121	-0,275	-0,583	-0,044	-0,121	-0,275
3,122	-0,122	-0,277	-0,586	-0,045	-0,122	-0,277
3,306	-0,123	-0,278	-0,589	-0,045	-0,123	-0,279
3,490	-0,123	-0,279	-0,591	-0,046	-0,124	-0,281
3,673	-0,124	-0,280	-0,592	-0,046	-0,125	-0,282
3,857	-0,124	-0,280	-0,593	-0,046	-0,125	-0,283
4,041	-0,124	-0,281	-0,594	-0,047	-0,126	-0,284
4,224	-0,124	-0,281	-0,594	-0,047	-0,126	-0,284
4,408	-0,124	-0,281	-0,594	-0,047	-0,126	-0,284
4,592	-0,124	-0,281	-0,594	-0,047	-0,126	-0,284
4,776	-0,124	-0,281	-0,594	-0,046	-0,126	-0,284
4,959	-0,124	-0,280	-0,593	-0,046	-0,125	-0,283
5,143	-0,124	-0,280	-0,593	-0,046	-0,125	-0,282
5,327	-0,124	-0,280	-0,592	-0,045	-0,124	-0,281
5,510	-0,123	-0,279	-0,591	-0,045	-0,123	-0,280
5,694	-0,123	-0,279	-0,590	-0,045	-0,123	-0,279
5,878	-0,122	-0,277	-0,587	-0,044	-0,122	-0,277
6,061	-0,122	-0,276	-0,584	-0,044	-0,121	-0,276
6,245	-0,121	-0,274	-0,580	-0,044	-0,120	-0,274
6,429	-0,119	-0,271	-0,576	-0,043	-0,119	-0,271
6,612	-0,118	-0,268	-0,570	-0,043	-0,118	-0,269
6,796	-0,118	-0,267	-0,564	-0,042	-0,117	-0,267
6,980	-0,115	-0,261	-0,554	-0,041	-0,115	-0,264
7,163	-0,111	-0,255	-0,542	-0,041	-0,114	-0,261
7,347	-0,108	-0,248	-0,529	-0,040	-0,112	-0,257
7,531	-0,104	-0,241	-0,514	-0,039	-0,111	-0,254
7,714	-0,100	-0,233	-0,498	-0,038	-0,108	-0,250
7,898	-0,096	-0,224	-0,481	-0,037	-0,106	-0,245
8,082	-0,091	-0,215	-0,462	-0,035	-0,104	-0,240
8,265	-0,087	-0,206	-0,444	-0,034	-0,101	-0,236
8,449	-0,082	-0,197	-0,426	-0,033	-0,099	-0,231
8,633	-0,078	-0,188	-0,409	-0,032	-0,097	-0,225
8,816	-0,074	-0,180	-0,392	-0,031	-0,094	-0,220
9,000	-0,071	-0,173	-0,376	-0,030	-0,092	-0,215

F.5 Deflection of rigid footing

Distance [m]	Deflection (mm)					
	Pier Half Load	Pier Full Load	Pier Double Load	Footing Half Load	Footing Full Load	Footing Double Load
0,000	-0,078	-0,185	-0,397	-0,034	-0,097	-0,224
0,184	-0,076	-0,183	-0,395	-0,033	-0,096	-0,222
0,367	-0,075	-0,181	-0,394	-0,031	-0,095	-0,221
0,551	-0,073	-0,179	-0,392	-0,030	-0,093	-0,220
0,735	-0,072	-0,178	-0,391	-0,029	-0,092	-0,219
0,918	-0,071	-0,177	-0,390	-0,028	-0,091	-0,218
1,102	-0,070	-0,176	-0,390	-0,027	-0,090	-0,217
1,286	-0,069	-0,176	-0,389	-0,026	-0,090	-0,216
1,469	-0,069	-0,175	-0,389	-0,025	-0,089	-0,216
1,653	-0,068	-0,175	-0,389	-0,025	-0,088	-0,215
1,837	-0,068	-0,174	-0,388	-0,024	-0,087	-0,214
2,020	-0,067	-0,174	-0,388	-0,023	-0,087	-0,214
2,204	-0,066	-0,174	-0,388	-0,023	-0,086	-0,214
2,388	-0,066	-0,173	-0,387	-0,022	-0,086	-0,213
2,571	-0,066	-0,173	-0,387	-0,022	-0,086	-0,213
2,755	-0,066	-0,173	-0,387	-0,022	-0,086	-0,213
2,939	-0,065	-0,173	-0,387	-0,022	-0,085	-0,213
3,122	-0,065	-0,173	-0,388	-0,022	-0,085	-0,213
3,306	-0,065	-0,173	-0,388	-0,022	-0,085	-0,213
3,490	-0,065	-0,173	-0,388	-0,021	-0,085	-0,213
3,673	-0,065	-0,173	-0,388	-0,021	-0,085	-0,213
3,857	-0,065	-0,173	-0,388	-0,021	-0,085	-0,213
4,041	-0,065	-0,173	-0,389	-0,021	-0,085	-0,213
4,224	-0,065	-0,173	-0,389	-0,021	-0,085	-0,213
4,408	-0,065	-0,173	-0,389	-0,021	-0,085	-0,213
4,592	-0,066	-0,174	-0,389	-0,021	-0,085	-0,213
4,776	-0,066	-0,174	-0,390	-0,021	-0,085	-0,213
4,959	-0,066	-0,174	-0,390	-0,021	-0,085	-0,213
5,143	-0,066	-0,174	-0,390	-0,021	-0,085	-0,213
5,327	-0,066	-0,174	-0,391	-0,021	-0,085	-0,213
5,510	-0,066	-0,175	-0,391	-0,021	-0,085	-0,213
5,694	-0,067	-0,175	-0,392	-0,021	-0,085	-0,214
5,878	-0,067	-0,175	-0,392	-0,022	-0,086	-0,214
6,061	-0,067	-0,176	-0,393	-0,022	-0,086	-0,215
6,245	-0,068	-0,176	-0,393	-0,023	-0,087	-0,215
6,429	-0,068	-0,177	-0,394	-0,023	-0,087	-0,216
6,612	-0,068	-0,177	-0,394	-0,024	-0,088	-0,216
6,796	-0,071	-0,180	-0,397	-0,024	-0,088	-0,217
6,980	-0,071	-0,180	-0,397	-0,025	-0,089	-0,218
7,163	-0,071	-0,180	-0,397	-0,025	-0,090	-0,218
7,347	-0,071	-0,180	-0,397	-0,026	-0,090	-0,219
7,531	-0,071	-0,180	-0,398	-0,026	-0,091	-0,220
7,714	-0,072	-0,181	-0,399	-0,027	-0,091	-0,220
7,898	-0,073	-0,182	-0,401	-0,028	-0,092	-0,221
8,082	-0,074	-0,183	-0,402	-0,029	-0,093	-0,222
8,265	-0,075	-0,184	-0,403	-0,030	-0,094	-0,223
8,449	-0,077	-0,186	-0,405	-0,031	-0,096	-0,225
8,633	-0,078	-0,188	-0,406	-0,033	-0,097	-0,226
8,816	-0,080	-0,190	-0,409	-0,034	-0,099	-0,228
9,000	-0,083	-0,192	-0,411	-0,036	-0,101	-0,230

F.6 Deflections of load geometries

Distance [m]	Deflection (mm)		
	Point Rigid	Pier rigid	Pier Flexible
0,000	0,017	-0,088	-0,074
0,184	0,014	-0,091	-0,080
0,367	0,011	-0,093	-0,086
0,551	0,008	-0,096	-0,092
0,735	0,005	-0,099	-0,099
0,918	0,001	-0,102	-0,105
1,102	-0,002	-0,105	-0,112
1,286	-0,006	-0,109	-0,119
1,469	-0,010	-0,112	-0,126
1,653	-0,014	-0,116	-0,133
1,837	-0,018	-0,119	-0,140
2,020	-0,022	-0,123	-0,147
2,204	-0,026	-0,127	-0,155
2,388	-0,031	-0,130	-0,162
2,571	-0,035	-0,134	-0,169
2,755	-0,039	-0,138	-0,177
2,939	-0,043	-0,142	-0,184
3,122	-0,048	-0,146	-0,192
3,306	-0,052	-0,150	-0,200
3,490	-0,056	-0,154	-0,208
3,673	-0,061	-0,158	-0,216
3,857	-0,066	-0,162	-0,224
4,041	-0,070	-0,166	-0,232
4,224	-0,075	-0,170	-0,240
4,408	-0,079	-0,174	-0,248
4,592	-0,084	-0,178	-0,256
4,776	-0,089	-0,183	-0,264
4,959	-0,093	-0,187	-0,273
5,143	-0,098	-0,191	-0,282
5,327	-0,102	-0,195	-0,290
5,510	-0,107	-0,200	-0,298
5,694	-0,112	-0,204	-0,306
5,878	-0,117	-0,208	-0,313
6,061	-0,121	-0,213	-0,320
6,245	-0,126	-0,217	-0,327
6,429	-0,131	-0,222	-0,332
6,612	-0,136	-0,226	-0,337
6,796	-0,140	-0,231	-0,341
6,980	-0,145	-0,236	-0,343
7,163	-0,150	-0,240	-0,344
7,347	-0,155	-0,245	-0,344
7,531	-0,160	-0,250	-0,341
7,714	-0,166	-0,254	-0,336
7,898	-0,171	-0,259	-0,330
8,082	-0,176	-0,265	-0,324
8,265	-0,182	-0,270	-0,317
8,449	-0,187	-0,275	-0,310
8,633	-0,193	-0,281	-0,302
8,816	-0,199	-0,287	-0,294
9,000	-0,206	-0,293	-0,285